

UC Davis

Research reports

Title

Updates to CalME and Calibration of Cracking Models

Permalink

<https://escholarship.org/uc/item/460234q0>

Authors

Wu, Rongzong
Harvey, John
Lea, Jeremy
[et al.](#)

Publication Date

2021-03-01

DOI

10.7922/G2CR5RNT

Updates to CalME and Calibration of Cracking Models

Authors:

Rongzong Wu, John Harvey, Jeremy Lea,
Angel Mateos, Shuo Yang, and Noe Hernandez

Partnered Pavement Research Center Strategic Plan Element (PPRC SPE) 2.9 (DRISI Task 3215):
CalME Support

PREPARED FOR:

California Department of Transportation
Division of Research, Innovation, and System Information
Office of Materials and Infrastructure

PREPARED BY:

University of California
Pavement Research Center
UC Davis, UC Berkeley




TECHNICAL REPORT DOCUMENTATION PAGE

1. REPORT NUMBER UCPRC-RR-2021-01	2. GOVERNMENT ASSOCIATION NUMBER	3. RECIPIENT'S CATALOG NUMBER
4. TITLE AND SUBTITLE Updates to CalME and Calibration of Cracking Models		5. REPORT PUBLICATION DATE March 2021
		6. PERFORMING ORGANIZATION CODE
7. AUTHOR(S) Rongzong Wu (ORCID 0000-0001-7364-7583), John Harvey (ORCID 0000-0002-8924-6212), Jeremy Lea (ORCID 0000-0003-3445-8661), Angel Mateos (ORCID 0000-0002-3614-2858), Jon Lea (ORCID 0000-0003-0999-469X), Shuo Yang (ORCID 0000-0002-2653-5199), Noe Hernandez		8. PERFORMING ORGANIZATION REPORT NO. UCPRC-RR-2021-01 UCD-ITS-RR-20-97
9. PERFORMING ORGANIZATION NAME AND ADDRESS University of California Pavement Research Center Department of Civil and Environmental Engineering, UC Davis 1 Shields Avenue Davis, CA 95616		10. WORK UNIT NUMBER
		11. CONTRACT OR GRANT NUMBER 65A0628
12. SPONSORING AGENCY AND ADDRESS California Department of Transportation Division of Research, Innovation, and System Information P.O. Box 942873 Sacramento, CA 94273-0001		13. TYPE OF REPORT AND PERIOD COVERED Research report 2017 – 2020
		14. SPONSORING AGENCY CODE
15. SUPPLEMENTAL NOTES DOI:10.7922/G2CR5RNT		
16. ABSTRACT The CalME flexible pavement simulation and design software program has been completely recoded as a web-based application called CalME 3.0. CalME 3.0 retains the same incremental-recursive damage approach and the same forms for damage models and transfer functions as CalME 2.0, which was validated using accelerated pavement testing data from Heavy Vehicle Simulator (HVS) test sections and the WesTrack experiment. The following enhancements and additions are all included in the revised program. First, the old software's fatigue cracking transfer functions for hot mix asphalt (HMA) on aggregate base, cement-stabilized bases, and portland cement concrete have been recalibrated using a new approach for the calibration of mechanistic-empirical pavement design methods; this approach uses "big data" from pavement management systems, explicitly and separately considers between-project and within-project variability, and uses tens to hundreds of times more performance data than are used in conventional calibration methods. Second, the updated program also includes new damage models and transfer functions for in-place recycling materials, including full-depth recycling (FDR) with foamed asphalt plus cement and cement stabilization, and partial-depth recycling (PDR) with emulsified asphalt and foamed asphalt plus cement. Third, the program now has been given the ability to model PDR using cold central plant recycled (CCPR) materials. Fourth, new damage models have been introduced for cement-stabilized bases and cement-stabilized and lime-stabilized subgrade materials to correct problems with the models in CalME 2.0. Fifth, minimum aggregate base thicknesses were developed based on calculations of permanent deformation under construction traffic. Lastly, simplified methods were developed for estimating subgrade stiffnesses (resilient modulus) based on dynamic cone penetrometer (DCP) tests, California bearing ratio (CBR) tests, and R-value tests. It is recommended that CalME 3.0 be implemented for pavement design, that the calibration be updated with new data approximately every 3 to 5 years, that Caltrans traffic databases be checked before they are used again for recalibration, and that use of the recently updated Caltrans DIME database of as-built data be considered for future calibrations.		
17. KEY WORDS CalME, Mechanistic-Empirical Design, calibration, performance data	18. DISTRIBUTION STATEMENT No restrictions. This document is available to the public through the National Technical Information Service, Springfield, VA 22161	
19. SECURITY CLASSIFICATION (of this report) Unclassified	20. NUMBER OF PAGES 101	21. PRICE None

Reproduction of completed page authorized

UCPRC ADDITIONAL INFORMATION

1. DRAFT STAGE Final	2. VERSION NUMBER 1				
3. PARTNERED PAVEMENT RESEARCH CENTER STRATEGIC PLAN ELEMENT NUMBER 2.09	4. DRISI TASK NUMBER 3215				
5. CALTRANS TECHNICAL LEAD AND REVIEWER(S) Raghubar Shrestha	6. FHWA NUMBER CA213215A				
7. PROPOSALS FOR IMPLEMENTATION It is recommended that CalME 3.0 be implemented in design and analysis of pavement performance.					
8. RELATED DOCUMENTS None					
9. LABORATORY ACCREDITATION The UCPRC laboratory is accredited by AASHTO re:source for the tests listed in this report					
R. Wu FIRST AUTHOR	J.T. Harvey TECHNICAL REVIEW	D. Spinner EDITOR	J.T. Harvey PRINCIPAL INVESTIGATOR	R. Shrestha CALTRANS TECH LEAD	T.J. Holland CALTRANS CONTRACT MANAGER

Reproduction of completed page authorized

TABLE OF CONTENTS

LIST OF FIGURES	v
LIST OF TABLES	vi
PROJECT OBJECTIVES.....	vii
EXECUTIVE SUMMARY.....	ix
LIST OF ABBREVIATIONS.....	xviii
1 INTRODUCTION.....	1
1.1 Background	1
1.1.1 State Highway Network	1
1.1.2 Previous Flexible-Surfaced Pavement Design Method.....	2
1.1.3 CalME 1.0 and 2.0.....	2
1.1.4 Calibration and Validation of CalME 1.0 and 2.0.....	6
1.2 CalME 3.0	7
1.2.1 Creation of New Web-based Version.....	7
1.2.2 Updated Standard Materials Library	8
1.2.3 Need for Recalibration and Update of Reliability Approach	9
1.2.4 Comparison of Conventional and New Calibration and Reliability Approach	11
1.2.5 Scope of the Calibration.....	13
2 NEW CALIBRATION METHOD	15
2.1 General Approach for Field Calibration.....	15
2.2 Explanation and Example: Asphalt Concrete Fatigue Damage Model	15
2.3 Transfer Function for Fatigue Cracking.....	17
2.4 Project-Level Performance and Calibration Discussion Example	18
2.4.1 Simple Project Example	18
2.4.2 Monte Carlo Simulation Results and Observations	18
2.4.3 Effects of Different Within-Project-Variability	21
2.4.4 Summary of Project-Level Calibration	22
2.5 Statewide Network-Level Performance and Calibration.....	22
2.5.1 Simple Network Example	22
2.5.2 Monte Carlo Simulation Results and Observations	24
2.5.3 Network-Level Calibration	28
3 PERFORMANCE DATA.....	29
3.1 Introduction	29
3.2 Sub-Networks for Field Calibration	29
3.3 Data Processing.....	30
3.3.1 Determination of Time to 50 Percent Cracking	30
3.3.2 Determination of Observed Shape Parameter <i>β_{observed}</i>	32
3.3.3 Rounding of Asphalt Concrete Surface Layer Thickness	32
3.4 Explanatory Variables in the Data	33
3.5 Data Summary and Basic Trends	33
4 DETAILED CALIBRATION PROCEDURE AND RESULTS	37
4.1 Step-by-Step Procedure.....	37
4.2 General Network Median Input.....	37
4.2.1 Surface Layer Material and Bonding Condition	38
4.2.2 Non-Surface Layer Materials	39
4.3 N-AB: New Flexible Pavements with Aggregate Base.....	40
4.3.1 Sensitivity of CalME Fatigue Cracking Model.....	40
4.3.2 Calibration Cells.....	42
4.3.3 Specific Network Median Input	42

4.3.4	Determination of Critical Damage ω_{50}	43
4.3.5	Initial Selection of Shape Parameter β	44
4.3.6	Determination of Within-Project Variability	45
4.3.7	Determine the Between-Project Variability Factor	46
4.4	Calibration of Existing Transfer Functions for Existing Pavement Types.....	47
4.5	Damage Models and Calibration of Cracking Transfer Functions for In-Place Recycling.....	47
4.5.1	R-PDR-EA: Rehabilitation of Flexible Pavements with PDR-EA.....	49
4.5.2	R-PDR-FA: Rehabilitation of Flexible Pavements with PDR-FA.....	49
4.5.3	R-FDR-FA: Rehabilitation of Flexible Pavements with FDR-FA.....	50
4.5.4	R-FDR-C: Rehabilitation of Flexible Pavements with FDR-C.....	50
4.5.5	Cold Central Plant Recycled (CCPR) Materials	50
4.6	Damage Models and Calibration of Transfer Functions for Pavements with Cemented Bases.....	51
4.6.1	N-CB: New Flexible Pavements with Cemented Base	51
4.6.2	Cement-Stabilized Subgrade and Lime-Stabilized Subgrade.....	51
4.6.3	Damage and Curing Models.....	51
4.6.4	Combining Damage and Curing Models.....	53
4.7	Summary of the Calibration Results	53
5	DESIGN WITH NEW FIELD CALIBRATION.....	55
5.1	Design Inputs	55
5.1.1	Hot Mix Asphalt Materials.....	55
5.1.2	In-Place Recycled Materials.....	56
5.1.3	Cement-Stabilized Materials	57
5.1.4	Other Materials.....	58
5.1.5	Updated Default Subgrade Soil Stiffnesses and Methods for Estimating	58
5.1.6	Minimum Required Aggregate Base Thicknesses	58
5.2	Design Procedure	59
5.3	Comparison with Empirical Design Results	60
6	SUMMARY AND RECOMMENDATIONS.....	63
6.1	Summary	63
6.2	Recommendations	64
	REFERENCES.....	65
	APPENDIX A: PROJECTS USED TO EVALUATE THICKNESS VARIABILITY	68
	APPENDIX B: DEVELOPMENT OF DEFAULT SUBGRADE STIFFNESSES AND METHODS OF TESTING TO ESTIMATE SUBGRADE STIFFNESS.....	69
B.1	Subgrade Stiffness Estimation	69
B.2	Minimum Base Thickness in CalME Design.....	74
B.3	Meta-Analysis to Correlate Empirical Tests with Resilient Modulus.....	75
B.4	References for Development of Subgrade Stiffness Estimation Equations	78

LIST OF FIGURES

Figure 1.1: Time-hardening process for accumulating damage following multiple damage evolution curves, each corresponding to a different level of strain energy experience by the material (4).	4
Figure 1.2: Flowchart of the incremental-recursive performance prediction process used in <i>CalME</i>	5
Figure 1.3: Percent of wheelpath cracked as defined by time to threshold cracking in each sub-section of project.	6
Figure 1.4: Two different within-project variabilities.	10
Figure 1.5: Between-project variability for two projects.	11
Figure 2.1: An example of the transfer function for fatigue damage, $\omega_{50} = 0.1$ and $\beta = -5.0$	17
Figure 2.2: Cracking histories for individual segments as well as the project overall (only showing 100 segments).	19
Figure 2.3: Effect of HMA layer stiffness on pavement fatigue cracking performance.	20
Figure 2.4: Overall average cracking histories for projects with different standard deviations for inputs.	21
Figure 2.5: Cumulative distribution function of the median value of E for projects in the network.	23
Figure 2.6: Cumulative distribution function of the median value of fatigue model parameter A for projects in the network.	23
Figure 2.7: Overall average cracking histories for individual projects in the network and for the project with the median inputs.	24
Figure 2.8: Cracking performance of individual projects and the project with the network median input.	25
Figure 2.9: Effect of network size on the relative error in estimated ω_{50}	26
Figure 2.10: Overall average cracking histories for individual projects in the network with number of load repetitions normalized by N_{50} (i.e., the number of load repetitions to 50% cracking).	26
Figure 2.11: Cumulative distribution function of the normalizing factor.	27
Figure 3.1: A project with extensive observed cracking and an extrapolated t_{50} of 11.3 years.	31
Figure 3.2: A project with zero observed cracking and an extrapolated t_{50} of 20.9 years.	31
Figure 3.3: Empirical cumulative distribution function of asphalt concrete layer thickness for new flexible pavements with aggregate base.	32
Figure 3.4: Distribution of virtual projects across total asphalt concrete surface thickness.	33
Figure 3.5: Distribution of virtual projects across Caltrans pavement climate regions.	34
Figure 3.6: Distribution of virtual projects across 10-year traffic index (TI).	34
Figure 3.7: Variation of average fitted and extrapolated time to 50% cracking with rounded total asphalt concrete surface layer thickness.	35
Figure 3.8: Variation of average fitted and extrapolated time to 50% cracking with Caltrans pavement climate regions.	36
Figure 3.9: Variation of average fitted and extrapolated time to 50% cracking with 10 year traffic index (TI). .	36
Figure 4.1: Sensitivity of <i>CalME</i> fatigue cracking model prediction to various inputs.	41
Figure 4.2 Determination of critical damage ω_{50} (i.e., the damage corresponding to 50% cracking).	43
Figure 4.3: Distribution of observed shape parameter $\beta_{observed}$ for each asphalt concrete surface thickness.	44
Figure 4.4: Distribution of relative performance factor for each asphalt concrete surface thickness.	46
Figure 5.1: Comparison between HMA thickness designs produced by calibrated <i>CalME</i> (assuming same base thickness as the R-value method) and R-value method using <i>CalFP</i>	60
Figure B.1: Required minimum modulus with depth.	71
Figure B.2: Nomograph for estimating soil stiffness from various test methods.	73
Figure B.3: Plots showing published models, median value among the published models (thick gray line), and best fit equation (thick black line).	77

LIST OF TABLES

Table 1.1: Damage or Rutting Models and Transfer Functions for All Materials in CalME 2.0 (5).....	4
Table 3.1: Sub-Networks for the Field Calibration.....	29
Table 3.2: Summary of Calibration Data Available for Different Sub-Networks	30
Table 4.1: List of Mixes Representing Historical Caltrans Asphalt Mixes Used for Calibration.....	39
Table 4.2: List of Non-Surface Materials Representing Historical Caltrans Network Used for Calibration.....	39
Table 4.3: List of Additional Mixes Used for Sensitivity Study.....	40
Table 4.4: Sensitivity Study Factorial for Cracking in New Flexible Pavements with Aggregate Base	41
Table 4.5: Network Median Inputs Specific to the N-AB Network.....	42
Table 4.6: Summary of Asphalt Mixes Used to Estimate Variability of Mix Stiffness and Fatigue Parameter ...	45
Table 4.7: Variabilities of Asphalt Concrete Layer Properties and the Resulting Shape Parameter	46
Table 4.8: Performance Multipliers for Different Design Reliability Levels	47
Table 4.9: Summary of PDR and FDR Field Sections Tested in Summer and Fall of 2020	48
Table 4.10: Summary of Calibration Results for Different Sub-Networks.....	54
Table 5.1: Statewide Median New Asphalt Concrete Materials for Design	56
Table 5.2: Statewide Median In-Place Recycled Materials for Design.....	57
Table 5.3: Statewide Median Cement-Stabilized Materials for Design.....	57
Table 5.4: Default Subgrade Stiffnesses and Minimum Aggregate Base Thicknesses Based on USCS Soil Classification Included in CalME.....	59
Table B.1: Representative Modulus for Various Materials.....	72
Table B.2: Minimum Thickness for Aggregate Base Course from the Chart	74
Table B.3: Minimum Thickness for Aggregate Base Course from the Chart Rounded for Constructability and to the Nearest 0.05 ft.....	74

PROJECT OBJECTIVES

The work documented in this report was completed as part of Partnered Pavement Research Center Strategic Plan Elements 2.9 and 3.38, titled “Support CalME” and “Expand Standard Materials Library and Implement Design Guidance,” respectively. The work directed to be done to support the implementation of *CalME* for SPE 2.9 consisted of the following:

1. Conduct an analysis of the sensitivity of the current version of *CalME* (2.0) to design variables
2. Develop and incorporate models for new materials, treatments, and conditions, as directed by Caltrans
3. Assemble the data needed to calibrate *CalME* for California traffic and climate conditions, materials, and construction practices
4. Calibrate *CalME* for California conditions
5. Prepare documentation for the calibration
6. Assist Caltrans in developing design guidance
7. Develop training materials and assist Caltrans with training

This report summarizes the work of Tasks 1 through 4, and partially completes Tasks 5 and 6. Regarding Task 5, this report documents the approach used for calibration and the detailed results of calibration for one type of pavement in *CalME*. Additional reports will complete the documentation of the calibration of all new materials and treatments and the updating of traffic information to complete Task 5; a user’s guide and site investigation guide currently being finalized will complete Task 6. Training materials were delivered and assistance with training was completed in February 2020. The updating of the new materials in the standard materials library, whose calibration is discussed in this report, was completed as part of SPE 3.38.

EXECUTIVE SUMMARY

Starting in the 1950s, Caltrans used the R-value empirical design method originally developed by Francis Hveem and his colleagues to design new and reconstructed asphalt pavement. The R-value method was last calibrated in the 1960s. In the 1970s, Caltrans started to design asphalt overlays using a deflection-reduction method that was last calibrated in the early 1980s. There have been many changes in materials, construction, and traffic since these methods were introduced and last calibrated.

Realizing the ability of mechanistic-empirical (ME) pavement analysis and design methods to help with addressing these limitations, Caltrans approved an issue memorandum in 2005 titled “Adoption of Mechanistic-Empirical (ME) Pavement Design Method,” which called for the adoption of the ME pavement design methodology to replace existing empirical methods. In response, Caltrans had the University of California Pavement Research Center develop data and models that were incorporated into a computer program called *CalME* (California Mechanistic-Empirical) to enable Caltrans to implement the ME design method for asphalt-surfaced pavements. The initial versions were used for the design of three long-life asphalt projects, which had 40-year design lives and included special provisions for HMA materials using performance-related specifications (PRS).

CalME 2.0, the next version of the program, was released to Caltrans district design offices in September 2014. Both *CalME 1.0* and *2.0* were desktop applications. *CalME 2.0* included relatively mature models for the behavior of the following materials:

- Hot mix asphalt (HMA, including mixes with various PG grades and rubberized asphalt mixes)
- Aggregate base
- Subgrades

CalME 2.0 also included initial models for the following materials:

- Cement-stabilized bases
- Partial-depth recycling with asphalt emulsion plus cement stabilization
- Full-depth recycling with
 - No stabilization
 - Foamed asphalt plus cement stabilization
- Cement- and lime-stabilized subgrades

CalME 2.0 was primarily intended for use on projects using performance-related specifications (PRS) for the HMA materials. The PRS included minimum limits for flexural stiffness and flexural beam fatigue, and maximum limits for permanent deformation using repeated simple shear testing, which was later replaced with repeated load triaxial testing. Because *CalME* was originally intended for use with PRS, the reliability approach in *CalME* 2.0 did not consider the variability between HMA materials from different sources; instead it only looked at the within-project variability for a given HMA material by considering the variabilities of the stiffness, fatigue, and permanent deformation properties around the PRS prescribed limit.

Traditional ME methods that use Miner's Law (hypothesis of linear accumulation of damage) only use the initial undamaged responses of the pavement to temperature and load, and assume the development of the entire damage process to the end failure state. One of the objectives for the development of *CalME* was to allow its response calculations (i.e., the models that predict damage based on critical strains, stresses, and deformations) to be calibrated initially using instrumentation and monitoring data from accelerated pavement testing (APT), such as the data collected from Heavy Vehicle Simulator (HVS) test sections, as well as test track and field section data. The incremental-recursive approach used in *CalME* means that the entire damage process measured by APT section instruments can be used for calibration of response and damage models from the first load through the end of the project, with many data points in between. The incremental-recursive approach also permits use of deflection and other response data to track the damage and aging processes on test tracks and field sections for calibration of the damage process, even when failure has not yet manifested itself on the pavement surface, provided that measurements are regularly taken after construction.

The response, damage, and distress models in *CalME* 2.0 for bottom-up fatigue cracking, reflective cracking, and rutting were initially calibrated using HVS tests on 24 flexible pavement sections tested between 1995 and 2006. The damage and distress models were then recalibrated using accelerated pavement testing data from the Federal Highway Administration's WesTrack project. WesTrack used tractor-trailer trucks that were loaded to legal axle load limits, operating at 45 mph (72 km/hr) on a closed-circuit track under ambient conditions, whereas the HVS testing had controlled temperatures and a wheel moving at about 4.5 mph (7 km/hr). The results from the 26 original sections of the WesTrack project, which were trafficked from 1996 to 1998, were used to calibrate the transfer functions relating damage to cracking and rutting. The initial calibration for crushing and bottom-up fatigue cracking of cemented stabilized base and subgrade materials was based on HVS data from the Danish Road Institute. The incremental-recursive approach in *CalME* allowed calibration of the entire damage process on the WesTrack sections using time histories of backcalculated HMA stiffnesses.

Additional review of the rutting and reflective cracking models in *CalME* 2.0 came from comparisons of modeled and measured results using APT results from Alabama, Minnesota, and Spain.

From 2016 to 2018, the UCPRC developed a completely recoded, web-based version of *CalME* (*CalME* 3.0) for Caltrans. While the basic logic remained the same, the underlying databases were redesigned, and the code was optimized. Test results from sampled materials across the statewide network over the preceding six years—including extensive sampling of HMA materials since the introduction of Superpave mix designs by Caltrans in 2014—were introduced into the standard materials library that *CalME* designers select from.

After approximately six years during which only a few major projects requiring extensive pavement design were built, the defeat of Proposition 8 in November 2018, which would have repealed the funding for pavement rehabilitation, reconstruction, and land additions from Senate Bill 1 (2017), quickly increased the demand for longer-life pavement designs (20 years for rehabilitation and reconstruction on lower traffic volume routes, and 40 years on high traffic volume routes) and designs for heavy traffic. In early 2019, Caltrans requested that *CalME* 3.0 be recalibrated and its results re-checked for validity and reliability. The calibration of the responses (strains, stresses, deformations) and damage models were well calibrated from the previous HVS and test track calibrations. The objective was to calibrate the transfer functions relating damage to distress on the surface. The rutting transfer functions were also considered well calibrated and were less of a concern on the Caltrans network than cracking; therefore, the fatigue cracking of asphalt mixes, stabilized bases, and subgrades was the focus of the calibration.

The UCPRC proposed that the calibration be done using a new approach that would take advantage of Caltrans investments in its pavement management system (PMS) databases for as-builts and its many years of condition survey data. In addition to the intense Caltrans efforts on improving those data, the UCPRC had improved the usefulness of that data for performance modeling for the PMS through quality checking and by matching as-built records to condition time histories. More than 10 years of extensive review of the data had produced a very large database for development of performance models for the Caltrans pavement management system. This database was available for *CalME* 3.0 calibration, as well as for calibration of the *Pavement ME* program from AASHTO, which is used to design jointed plain concrete pavement. The new calibration approach permits the use of tens to thousands of more performance observations and lane-miles of data than conventional ME calibration approaches.

In early 2019, it was also identified that *CalME* 3.0 designs for 40-year flexible pavement designs with high truck traffic were resulting in much thinner HMA layers than those produced using the empirical Hveem R-value method. In earlier work on *CalME* 1.0/2.0, the UCPRC had identified two types of contributions to variability:

within-project variability and *between-project variability*. Differences between the performance-related properties of materials produced by different suppliers are the primary source of between-project variability. But differences in median construction quality provided by different contractors also contribute to between-project variability. Within-project variability comes from variations of the natural subgrade and the variability of materials production and construction using the given set of materials a contractor brings to a single project. Within-project variability considers the rate of development of distress extent within a single project as time and cumulative traffic-loading progress. It was quickly determined that not including between-project variability was the cause of the unreasonably thin designs. Sensitivity analysis showed that the between-project variability of HMA stiffness and fatigue properties seen in the standard materials library of mixes sampled across the statewide network was the largest contributor to pavement cracking performance simulated in *CalME*. Using *CalME* on projects without including PRS to control performance-related mix properties was ignoring a large source of unreliability in the designs.

Without PRS, asphalt mixes only need to pass performance-related binder specifications and volumetric mix design requirements that do not fully address rutting, stiffness, and fatigue characteristics. Specific stiffness, fatigue performance, and rutting performance-related properties of the mix that will be delivered to the project for construction are unknown to a designer. Although use of *CalME* with the assumption of relatively low between-project variability would be acceptable if PRS were used, it was clear from the analysis that between-project variability needs to be included in *CalME* for use on non-PRS projects.

In addition to investigation of HMA, the following new materials were also added to *CalME* 3.0 and calibrated, or updated and recalibrated if they were already in *CalME*, with available information from Caltrans PMS data, accelerated pavement testing data, new field testing done in the summer and fall of 2020, and/or the literature:

- Full-depth recycling, with the following types of stabilization:
 - Cement stabilization (FDR-C)
 - Foamed asphalt and cement stabilization (FDR-FA)
 - No stabilization (FDR-N), treated as a type of aggregate base
- Partial-depth recycling, with the following types of stabilization
 - Foamed asphalt and cement stabilization (PDR-FA)
 - Asphalt emulsion stabilization (PDR-EA)
- Cold Central Plant Recycling
 - CCPR with cement stabilization (CCPR-C)
 - CCPR with foamed asphalt and cement stabilization (CCPR-FA)
 - CCPR with asphalt emulsion stabilization (CCPR-EA)

The modeling approach for these materials was changed or updated in *CalME* 3.0 from the one in *CalME* 2.0:

- Cement-stabilized bases:
 - Lean concrete base (LCB)
 - Cement-treated base (CTB)
- Stabilized subgrades:
 - Cement-stabilized subgrade (CSS)
 - Lime-stabilized subgrade (LSS)
- Full-depth recycling, with the following types of stabilization:
 - Foamed asphalt and cement stabilization (FDR-FA)
 - No stabilization (FDR-N), treated as a type of aggregate base

The new calibration approach developed by the UCPRC to calibrate *CalME* 3.0 aims to improve calibration and the reliability approach used in ME design by doing the following:

- Using all the good quality distress performance data and as-built data in the Caltrans PMS databases collected since 1978 and quality checked over the last 10 years; this provides orders of magnitude more performance data for calibration, with the data organized by project.
- Using median properties to match median performance and using the variability of observed median performance to determine between-project variability, after using *CalME* to account for the effects of climate, pavement cross section, and traffic.
- Backcalculating within-project variability by matching the shape of observed performance time history.

It was assumed that calibration using the very large amounts of performance data available in the PMS and representative mix data for that time period would provide a more comprehensive calibration than using detailed performance data along with sampling and testing of materials from a few projects, as is done in the traditional calibration approach. In addition, the new approach explicitly separates within-project and between-project variability in the calibration, and in the design method. This allows for use of appropriately different between-project reliability factors for PRS and non-PRS projects.

The inputs to *CalME* include structure (layer materials and thicknesses), traffic (spectrum and volume), and climate (climate zone). The layer materials and bonding conditions are not recorded in the PMS and must be estimated for the field calibration. The new calibration method does not require detailed knowledge of any specific project when conducting a statewide network-level calibration. Instead, network median inputs are determined for the explanatory variables, namely materials properties, which reflect the characteristics of the network. This approach required development of a statewide median material for each material type based on the distributions

of properties for those materials from statewide testing. The weighted average performance of a set of mixes from the UCPRC databases was used to represent statewide median inputs for the time periods present in the cracking and rutting performance data since 1978 to reflect changes in materials and construction over the time period during which the performance data were collected.

All the materials from statewide testing are available in *CalME* 3.0; however, for non-PRS design, only the statewide median materials are available. Now that the calibration is completed, comparisons with sections with detailed sampling and testing can provide additional validation.

The cracking performance data collected from across the state highway network since 1978 were divided into what are referred to elsewhere in this report as “sub-networks,” based on pavement structure group and structure type, as shown in the following table.

Structure Group	Structure Type	Total Number of Virtual Projects	Total Lane Miles of Virtual Projects	Observation Period
New flexible pavement	With aggregate base	8,350	1,063	1978-2014
New flexible pavement	With cement base (cement-treated base or lean concrete base)	1,366	161	1978-2014
Rehabilitation with new HMA	New HMA over old flexible pavement	253,841	34,702	1978-2014
Rehabilitation with new HMA	New HMA over old rigid pavement	7,877	1,401	1978-2014
Rehabilitation with partial-depth in-place recycled layer	With engineering emulsion as the stabilizing agent	6,717	892	1978-2018
Rehabilitation with full-depth in-place recycled layer	With foam asphalt as the stabilizing agent	1,431	174	1978-2018
Rehabilitation with full-depth in-place recycled layer	With cement as the stabilizing agent	19	6	1978-2020

Field calibrations were conducted separately for each pavement group/type sub-network following this procedure:

1. Identify and assemble information. This involves organizing the pavement management system data into virtual projects. This creates the linkage between as-built and other project information (date of construction, treatment type, layer thickness, traffic, climate, and other explanatory variables) with performance data. Data processing is also conducted in this step.
2. Sensitivity analysis of the *CalME* model. Review performance sensitivity to identify the most sensitive explanatory variables by running *CalME*.
3. Separate calibration data into calibration cells. Each cell is a distinct combination of recorded explanatory variables.

4. Perform calibration for each calibration cell independently. Focus calibrations on those cells that have more performance data.
 - Determine the statewide network median input (NMI) for each material (same NMI was used for materials across all sub-networks) by reviewing historical data.
 - Determine the median time to 50% cracking in the performance data for each calibration cell.
 - Run *CalME* using NMI to determine the calculated damage at the estimated time to reach 50% cracking, which is used to calibrate one of the two transfer function coefficients: damage at 50% cracking.
 - Review the distribution in the performance data of the second cracking transfer function parameter, the shape parameter β , for the current cell.
 - Select a subset of explanatory variables that will be allowed to have variance in the Monte Carlo simulation to account for observed within-project variability, and check that Monte Carlo simulation of those variables along with the shape factor match observed within-project variability.
 - Calculate the normalizing factor C_n for each virtual project, and determine the between-project factor for desired design reliability level.
5. Summarize the calibration results from the individual cells and develop global calibrations whenever reasonable.

The general calibration approach is described in Chapter 2 of this report. Chapter 3 summarizes the performance data. Chapter 4 presents the details of the calibration of new asphalt-surfaced pavements with aggregate base as an example of the process used on each sub-set of the network, and summarizes the addition of new materials and updates to existing materials. Chapter 5 describes updated default subgrade soil stiffnesses included in *CalME* 3.0 and the development of required minimum aggregate base thicknesses based on subgrade soil type that are included in *CalME* 3.0. Chapter 5 also shows a comparison of *CalME* 3.0 HMA minimum thicknesses versus those from the R-value empirical method versus truck traffic levels. The appendices include a list of the projects used to evaluate HMA thickness variability in construction and discussions of the development of the default subgrade stiffnesses and estimation of subgrade stiffness from empirical tests.

In summary:

- The *CalME* flexible pavement simulation and design software has been completely recoded as a web-based application called *CalME* 3.0. *CalME* 3.0 retains the same incremental-recursive damage approach and the same forms for damage models and transfer functions as *CalME* 2.0, which were validated previously using accelerated pavement testing data from Heavy Vehicle Simulator test sections and the WesTrack full-scale traffic closed-circuit track experiment.

- Fatigue cracking transfer functions for HMA on aggregate base, cement-stabilized bases, and portland cement concrete have been recalibrated using a new approach for the calibration of mechanistic-empirical pavement design methods. The method explicitly and separately considers between-project and within-project variability.
- The new approach in *CalME* 3.0 permits use of “big data” from pavement management systems by assuming median properties for materials, and calibrating for different structures, material types, traffic levels, and climates. This approach offers better integration with pavement management systems and performance-related specifications. *CalME* 3.0 assumes statewide median materials properties, although in the future it will also be possible to characterize regional median materials.
 - The calibration of the fatigue cracking transfer functions, using tens to hundreds of times more data than are used in conventional calibration methods, was successful.
 - A limitation for the calibration was the scarcity of field sections for some materials, primarily full-depth recycling with cement stabilization (FDR-C), partial-depth recycling with foamed asphalt plus cement (PDR-FA), different types of cold central plant recycling (CCPR), and cement-stabilized and lime-stabilized subgrades.
 - There were also some concerns regarding unexpected trends in cracking performance versus estimated lane-based traffic in the performance data from the PMS, which is thought to be attributable to problems with lane distribution factors for truck traffic.
- New damage models and transfer functions have been introduced for in-place recycling materials, including full-depth recycling (FDR) with foamed asphalt plus cement and cement stabilization, and partial-depth recycling (PDR) with emulsified asphalt and foamed asphalt plus cement. The ability to model PDR using cold central plant recycled (CCPR) materials has also been added. New damage models have been introduced for cement-stabilized bases and cement-stabilized and lime-stabilized subgrade materials to correct problems with the models in *CalME* 2.0.
- Minimum aggregate base thicknesses were developed for use in *CalME* 3.0 based on calculations of permanent deformation under construction traffic. Simplified methods were developed for estimating subgrade stiffnesses (resilient modulus) based on dynamic cone penetrometer (DCP) tests, California bearing ratio (CBR) tests, and R-value tests based on an extensive literature review and regression of relationships found in the literature. These methods are intended to supplement measurements of resilient modulus as part of site materials characterization.

The following recommendations address gaps and challenges identified in the calibration of *CalME* 3.0 and in the addition of new materials and models.

- The calibration should be updated with new data approximately every 3 to 5 years with a focus on new materials that had limited performance data in previous calibrations.
- Because they have implications for future designs, traffic estimates made by earlier methods should be examined in a review of Caltrans traffic data.
- An investigation should be conducted into the use of the Caltrans DIME database for calibrations since the database has the capability to capture as-built construction data that can provide better information regarding materials types, thicknesses, and, potentially, performance-related test results.

LIST OF ABBREVIATIONS

AB	Aggregate base
BPV	Between-project variability
CalME	California Mechanistic-Empirical
CBR	California bearing ratio
CCPR	Cold Central Plant Recycled
CDF	Cumulative distribution function
CSS	Cement-stabilized subgrades
CTB	Cement treated base
DCP	Dynamic Cone Penetrometer
DPI	DCP Penetration Index
FDR	Full-depth recycled
HMA	Hot mix asphalt
HVS	Heavy Vehicle Simulator
IPR	In-place recycled
IR	Incremental-recursive
LCB	Lean concrete base
LSS	Lime-stabilized subgrade
ME	Mechanistic-Empirical
MEPDG	Mechanistic-Empirical Pavement Design Guide
NMI	Network median input
PDR	Partial-depth recycled
PMS	Pavement management system
PRS	Performance related specifications
RPF	Relative performance factor
SC	South coast
SDF	Standard deviation factor
SML	Standard Materials Library
SSG	Soil Stiffness Gauge
TI	Traffic index
USCS	Unified Soil Classification
WPV	Within-project variability

SI* (MODERN METRIC) CONVERSION FACTORS

APPROXIMATE CONVERSIONS TO SI UNITS

Symbol	When You Know	Multiply By	To Find	Symbol
LENGTH				
in	inches	25.4	Millimeters	mm
ft	feet	0.305	Meters	m
yd	yards	0.914	Meters	m
mi	miles	1.61	Kilometers	Km
AREA				
in ²	square inches	645.2	Square millimeters	mm ²
ft ²	square feet	0.093	Square meters	m ²
yd ²	square yard	0.836	Square meters	m ²
ac	acres	0.405	Hectares	ha
mi ²	square miles	2.59	Square kilometers	km ²
VOLUME				
fl oz	fluid ounces	29.57	Milliliters	mL
gal	gallons	3.785	Liters	L
ft ³	cubic feet	0.028	cubic meters	m ³
yd ³	cubic yards	0.765	cubic meters	m ³
NOTE: volumes greater than 1000 L shall be shown in m ³				
MASS				
oz	ounces	28.35	Grams	g
lb	pounds	0.454	Kilograms	kg
T	short tons (2000 lb)	0.907	megagrams (or "metric ton")	Mg (or "t")
TEMPERATURE (exact degrees)				
°F	Fahrenheit	5 (F-32)/9 or (F-32)/1.8	Celsius	°C
ILLUMINATION				
fc	foot-candles	10.76	Lux	lx
fl	foot-Lamberts	3.426	candela/m ²	cd/m ²
FORCE and PRESSURE or STRESS				
lbf	poundforce	4.45	Newtons	N
lbf/in ²	poundforce per square inch	6.89	Kilopascals	kPa
APPROXIMATE CONVERSIONS FROM SI UNITS				
Symbol	When You Know	Multiply By	To Find	Symbol
LENGTH				
mm	millimeters	0.039	Inches	in
m	meters	3.28	Feet	ft
m	meters	1.09	Yards	yd
km	kilometers	0.621	Miles	mi
AREA				
mm ²	square millimeters	0.0016	square inches	in ²
m ²	square meters	10.764	square feet	ft ²
m ²	square meters	1.195	square yards	yd ²
ha	Hectares	2.47	Acres	ac
km ²	square kilometers	0.386	square miles	mi ²
VOLUME				
mL	Milliliters	0.034	fluid ounces	fl oz
L	liters	0.264	Gallons	gal
m ³	cubic meters	35.314	cubic feet	ft ³
m ³	cubic meters	1.307	cubic yards	yd ³
MASS				
g	grams	0.035	Ounces	oz
kg	kilograms	2.202	Pounds	lb
Mg (or "t")	megagrams (or "metric ton")	1.103	short tons (2000 lb)	T
TEMPERATURE (exact degrees)				
°C	Celsius	1.8C+32	Fahrenheit	°F
ILLUMINATION				
lx	lux	0.0929	foot-candles	fc
cd/m ²	candela/m ²	0.2919	foot-Lamberts	fl
FORCE and PRESSURE or STRESS				
N	newtons	0.225	Poundforce	lbf
kPa	kilopascals	0.145	poundforce per square inch	lbf/in ²

1 INTRODUCTION

1.1 Background

1.1.1 State Highway Network

The California Department of Transportation (Caltrans) owns and operates a network of approximately 50,000 lane-miles. Approximately 25 percent of the network has a concrete surface and the remaining 75 percent is surfaced with asphalt (*I*). The types of asphalt-surfaced—also called “flexible surfaced” by Caltrans—pavement structures include:

- Conventional flexible: hot mix asphalt (HMA) on aggregate base (AB)
- Composite: HMA on concrete (PCC)
- Semi-rigid: HMA on either lean concrete base or cement-treated base Type A
- Full-depth recycled (FDR), including:
 - HMA on cement-stabilized in-place recycled base (FDR-C)
 - HMA on in-place recycled base stabilized with foamed asphalt and cement (FDR-FA)
 - HMA on in-place recycled base stabilized with lime (FDR-L)
 - HMA on non-stabilized in-place recycled base (FDR-N)
- Partial-depth recycled (PDR), including:
 - HMA on foamed asphalt and cement-stabilized partial-depth recycled HMA (PDR-FA)
 - HMA on asphalt emulsion-stabilized partial-depth recycled HMA (PDR-EA)
- Cold central plant recycling (CCPR) alternatives for mixing recycled materials within the construction site that would otherwise be processed in-place as FDR or PDR
- Full-depth HMA on subgrade
- Asphalt-surfaced pavements built on cement- or lime-stabilized subgrades (CSS and LSS)

HMA materials include conventional and polymer-modified dense-graded HMA, and gap-graded rubberized hot mix asphalt (RHMA-G). Other types of asphaltic materials are used on the surface of the HMA or RHMA-G, including different kinds of open-graded mixes or seal coats which are both considered non-structural.

Pavement design work involving asphalt-surfaced pavement includes rehabilitation and reconstruction of existing asphalt-surfaced and concrete-surfaced pavements, lane additions, widening, and new pavement on new alignments.

1.1.2 Previous Flexible-Surfaced Pavement Design Method

Starting in the 1950s, Caltrans used the R-value empirical design method originally developed by Francis Hveem and his colleagues to design new and reconstructed asphalt pavement. The R-value method was last calibrated in the 1960s. In the 1970s Caltrans started to use a deflection-reduction method for design of asphalt overlays, which was last calibrated in the early 1980s. While groundbreaking at the time of their development, these design methods are extremely limited in their ability to consider current issues of importance to Caltrans for design and analysis, such as pavement preservation overlays; longer design lives for new pavement, reconstruction and rehabilitation; new materials; the variety of asphalt; new specifications for cemented and granular materials; recycled materials (in-place and plant recycled asphalt, concrete and granular materials and rubberized asphalt); construction compaction; the variety and condition of existing pavement structures; reflective cracking in asphalt pavements; climate regions; increases in tire inflation pressures and axle loads; traffic speed; variability of materials and construction practices; and uncertainty regarding future traffic growth.

Calibration of the R-value method is not well documented. During its development, traffic levels were less than about 10 million ESALs, and according to oral history the method was last checked against accelerated pavement testing data from the AASHO Road Test (1958-60), a few years after completion of that study, which was conducted in central Illinois.

Traffic levels have grown tremendously since the last calibration of the R-value method. The R-value design equations have been extrapolated beyond the traffic levels for which they were calibrated, up to 84.7 million ESALs. In addition to extrapolation from the original data used to develop it, the R-value method also has within it some unknown degree of “reliability.” Fifty percent reliability traditionally means that there is a 50 percent probability that a pavement will fail prior to its design life and a 50 percent probability it will fail after. A reliability of 90 percent would mean that there is only a 10 percent probability that it would fail before its design life. The basic concept of reliability, which was not widely implemented until about 10 years after the R-value method was developed, was not incorporated into the method, even though it has been included in more recent design methods. However, the meaning of reliability, consideration of the sources of variability of pavement design lives, and how to implement reliability in a statistically meaningful way is an area of ongoing development.

1.1.3 CalME 1.0 and 2.0

Realizing the ability of mechanistic-empirical (ME) pavement analysis and design methods to help with addressing these limitations, Caltrans approved an issue memorandum in 2005 titled “Adoption of Mechanistic-Empirical (ME) Pavement Design Method,” which called for the adoption of ME pavement design methodology to replace existing empirical methods. In response, Caltrans had the University of California Pavement Research

Center develop a computer program called *CalME* (California Mechanistic-Empirical) to enable Caltrans to implement the ME design method. The initial versions were used for the design of three long-life asphalt projects, which had 40-year design lives and included special provisions for HMA materials using performance-related specifications (PRS). *CalME 2.0*, the next version of the program, was released to Caltrans district design offices in September 2014. Both *CalME 1.0* and *2.0* were desktop applications.

Caltrans planning for the transition to ME design included the following considerations that are addressed in this report:

- The need for ongoing improvement of models as better information is developed
- Use of ME design with performance-related testing and specifications
- The need for ongoing feedback from the Caltrans pavement management system (PMS) to verify and update the method, which has not been done for most empirical and ME methods around the world (2).

ME design is an iterative process in which trial pavement designs are adjusted repeatedly either manually or automatically based on predicted performance until an optimal design is reached. A key component of any ME design system is a module that predicts the performance of a given pavement design. The module includes two parts: mechanistic damage models and empirical transfer functions that relate distress to damage. In *CalME*, *damage* is defined as loss of stiffness and permanent deformation. Cracking distresses are correlated with loss of stiffness damage from fatigue, and rutting distresses are correlated with permanent deformation damage. In *CalME*, damage is assumed to be irreversible between successive increments, following the principle of time hardening as shown in Figure 1.1, which shows how damage is accumulated over three time increments each with a different loading condition (3).

This module and the pavement damage and distresses included in it can vary from one ME design system to another, depending on the specific project. In *CalME 2.0*, the module's predicted distresses included fatigue cracking, reflective cracking, rutting, and smoothness. Material types and their associated distresses are shown in Table 1.1.

CalME uses an incremental-recursive performance prediction process. Figure 1.2 shows a flowchart of this process and it illustrates both the "incremental" and the "recursive" parts of the module. Specifically, "incremental" refers to the part of the process where damage to pavement layers and the associated manifestation of distress based on damage are predicted for each time increment, and "recursive" refers to the part where layer stiffnesses are updated after each increment of time/traffic loading accounting for damage and aging in the previous increment before the response calculations are performed in the next time increment (6). Damage is updated following the time-hardening principle shown in Figure 1.1.

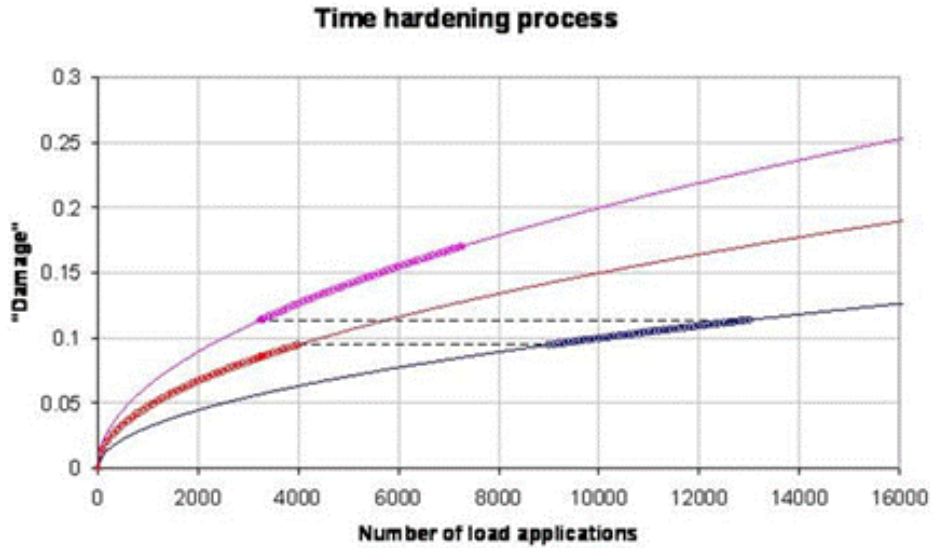


Figure 1.1. Time-hardening process for accumulating damage following multiple damage evolution curves, each corresponding to a different level of strain energy experience by the material (4).

Table 1.1: Damage or Rutting Models and Transfer Functions for All Materials in CalME 2.0 (5)

Material	Stiffness Loss or Permanent Deformation Damage Models	Transfer Function
Hot mix asphalt (various mixes), rubberized hot mix asphalt mixes, polymer-modified mixes	Stiffness loss from fatigue: Bottom-up fatigue for all layers or bottom-up load related reflective cracking fatigue on cracked HMA and PCC Permanent deformation: all layers within 100 mm of surface	Fatigue damage to surface cracking Permanent deformation to surface rutting
Cement treated base materials	Bottom-up fatigue	
Lightly cemented materials	Crushing	
Unbound granular materials	Rutting for each layer	Permanent deformation to surface rutting
Full-depth recycling as pulverization, foamed asphalt/cement bound	Fatigue, rutting	Permanent deformation to surface rutting
Subgrade	Rutting	Permanent deformation to surface rutting
Hot-in-place recycling, cold-in- place recycling	Rutting, fatigue	
Cement and lime-stabilized subgrade	Fatigue, crushing	

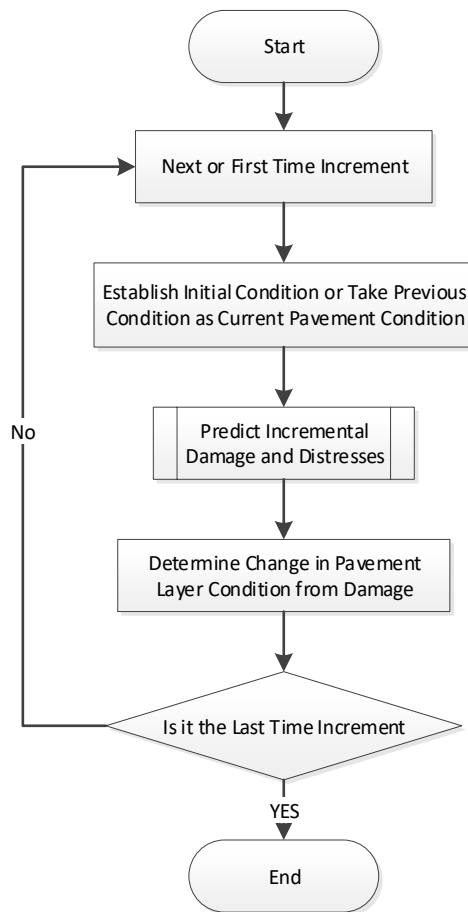


Figure 1.2: Flowchart of the incremental-recursive performance prediction process used in *CalME*.

CalME 2.0 uses Monte Carlo simulation for evaluating the statistical reliability of a given pavement design accounting for within-project variability. Essentially, to account for construction variability, *CalME* generated a set of random pavement structures that together provided a representative sample of the as-built structures for a given pavement design. In addition, a designer could elect to include the uncertainties associated with predicting future climate conditions.

CalME 2.0 was primarily intended for use on projects using performance-related specifications (PRS) for the HMA materials. The PRS included minimum limits for flexural stiffness and flexural beam fatigue, and maximum limits for permanent deformation using repeated simple shear testing, which was later replaced with repeated load triaxial testing. Because *CalME* was originally intended for use with PRS, the reliability approach in *CalME 2.0* did not consider the variability between HMA materials from different sources; instead it only looked at the within-project variability for a given HMA material by considering the variabilities of the stiffness, fatigue, and permanent deformation properties around the PRS prescribed limit. For other materials, typical variabilities around average values of stiffness, rutting, and fatigue properties (as applicable) from statewide field testing were considered. Typical variability of thicknesses for all materials were taken from the literature (5).

In *CalME* 2.0, the random variation of stiffness, thickness and materials fatigue, and permanent deformation properties from the Monte Carlo simulation is transformed into variations in damage, and then from damage into performance in terms of distress by the respective functions. Permanent deformation and damage are predicted for a single point and the variations of these values are considered to be within-section variations. For rutting, Monte Carlo simulation produces the mean and standard deviation of rut depth. Crack propagation is defined in terms of time to some threshold extent of cracking in terms of crack length per surface area of the wheelpath in sub-sections within the project. The number of sub-sections is defined by the number of simulations included in the Monte Carlo simulation. For example, as shown in Figure 1.3, ten Monte Carlo simulations were run, and the years to different percentages of cracking in the wheelpaths is defined by the time to reach 1 m/m² of cracking in each of ten sub-sections of the project (5).

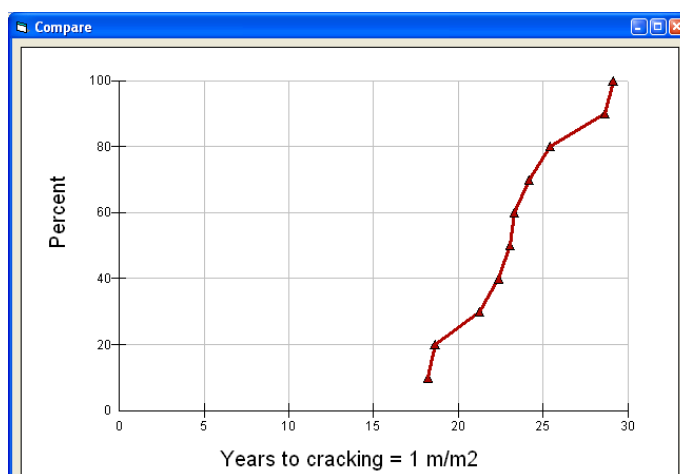


Figure 1.3: Percent of wheelpath cracked as defined by time to threshold cracking in each sub-section of project.

1.1.4 Calibration and Validation of *CalME* 1.0 and 2.0

One of the objectives for the development of *CalME* was to allow its response calculations (i.e., the models that predict damage based on critical strains, stresses and deformations) to be calibrated initially using instrumentation and monitoring data from accelerated pavement tests, such as the data collected from Heavy Vehicle Simulator (HVS) test sections, as well as test track and field section data. The incremental-recursive approach used in *CalME* means that the entire damage process measured by HVS test section instruments can be used for calibration of response and damage models from the first load through the end of the project, with many data points in between. In contrast, ME methods that use Miner’s Law (hypothesis of linear accumulation of damage) only use the initial undamaged responses of the pavement to temperature and load, and assume the development of the entire damage process to the end failure state (5).

The incremental-recursive approach also permits use of deflection and other response data to track the damage and aging processes on test tracks and field sections for calibration of the damage process, even when failure has not yet manifested itself on the pavement surface, provided that measurements are regularly taken after construction. In contrast, ME methods using Miner's Law must use biased data sets for their calibration because sections that have been damaged but have not yet manifested distress at their surface are essentially excluded from the calibration data set or must be considered as undamaged in the data set (5).

The *CalME* response, damage, and distress models for bottom-up fatigue cracking, reflective cracking, and rutting were initially calibrated using HVS tests on 24 flexible pavement sections (4,7,8,9,10,11). The HVS is a linear accelerated pavement testing (APT) device used with test sections that are 3.3 ft wide×26.4 ft long (1×8 m). The HVS also has controlled temperature and a slow-moving load. Loading above legal axle load limits is included as part of the accelerated loading process.

The damage and distress models were then recalibrated using accelerated pavement testing data from the National Cooperative Highway Research Program WesTrack project (12,13). WesTrack used tractor-trailer trucks that were loaded to legal axle load limits, operating at 45 mph (72 km/hr) on a closed-circuit track under ambient conditions. The results from the 26 original sections of the WesTrack project, which was trafficked from 1996 to 1998, were used to calibrate the transfer functions relating damage to cracking and rutting. The initial calibration for crushing and bottom-up fatigue cracking of lightly cemented materials was based on HVS data from the Danish Road Institute (14). The incremental-recursive approach in *CalME* allowed calibration of the entire damage process on the WesTrack sections using time histories of backcalculated HMA stiffnesses.

Additional review of the rutting and reflective cracking models in *CalME* came from comparisons of modeled and measured results using APT results from the National Center for Asphalt Technology (15), MnROAD (16), and the Centro de Estudios y Experimentación de Obras Públicas (CEDEX) in Spain (17), and in cooperation with the University of Minnesota (18,19).

CalME 2.0 was used to design three PRS AC long-life projects on Interstates 5 and 80 in Northern California between 2012 and 2014 (20,21), and another on Interstate 5 in Sacramento in 2018.

1.2 CalME 3.0

1.2.1 Creation of New Web-based Version

From 2016 to 2018, the UCPRC developed a completely recoded, web-based version of *CalME* for Caltrans. While the basic logic remained the same, the underlying databases were redesigned and the code was optimized.

Test results from sampled materials across the statewide network over the preceding years—including extensive sampling of HMA materials since the introduction of Superpave mix designs by Caltrans in 2014—were introduced into the standard materials library that *CalME* designers select from. The most recent report on the standard materials library also includes information about the *CalME* models for cracking (6).

1.2.2 Updated Standard Materials Library

New materials added to *CalME* 3.0 and calibrated, or updated and recalibrated if they were already in *CalME*, with available information include the following:

- Full-depth recycling, with the following types of stabilization:
 - Cement stabilization (FDR-C)
 - Foamed asphalt and cement stabilization (FDR-FA)
 - No stabilization (FDR-N), treated as a type of aggregate base
- Partial-depth recycling, with the following types of stabilization
 - Foamed asphalt and cement stabilization (PDR-FA)
 - Asphalt emulsion stabilization (PDR-EA)
- Cold Central Plant Recycling
 - CCPR with cement stabilization (CCPR-C)
 - CCPR with foamed asphalt and cement stabilization (CCPR-FA)
 - CCPR with asphalt emulsion stabilization (CCPR-EA)

The modeling approach for these existing materials also changed from the one in *CalME* 2.0:

- Cement-stabilized bases:
 - Lean concrete base (LCB)
 - Cement-treated base (CTB)
- Stabilized subgrades:
 - Cement-stabilized subgrade (CSS)
 - Lime-stabilized subgrade (LSS)

The recalibration and introduction of an updated reliability approach in *CalME* 3.0 required development of a statewide median material for each material type based on the distributions of properties for those materials from statewide testing. All the materials from statewide testing are available in *CalME* 3.0, however, for non-PRS design only the statewide median materials are available.

1.2.3 Need for Recalibration and Update of Reliability Approach

After approximately six years during which only a few major projects requiring extensive pavement design were built, the defeat of Proposition 8 in November 2018, which would have repealed the funding for pavement repair and capacity from Senate Bill 1 (2017), quickly increased the demand for longer life pavement designs (more than 20 years, typically 40 years) and designs for heavy traffic. In early 2019, Caltrans requested that *CalME* 3.0 be recalibrated and its results rechecked for validity and reliability.

The UCPRC proposed that the calibration be done using a new approach that would take advantage of Caltrans investments in its pavement management system databases for as-builts and its many years of condition survey data. The UCPRC improved the usefulness of that data extensively for performance modeling for the PMS through quality checking and by matching as-built records to condition time histories. More than 10 years of extensive review of the data had produced a very large database for development of empirical-mechanistic performance models for the Caltrans pavement management system. This database was available for *CalME* calibration, as well as for calibration of the Pavement ME program from AASHTO, which is used for design of jointed plain concrete pavement.

In early 2019, it was also identified that *CalME* designs for 40-year flexible pavement designs with high truck traffic were resulting in much thinner HMA layers than those produced using the empirical Hveem R-value method, which Caltrans has kept in use and made minor adjustments to periodically since it was introduced in the 1950s. It was quickly determined that not including between-project variability was the cause of the unreasonably thin designs. The between-project variability of HMA stiffness and fatigue properties seen in the standard materials library of mixes sampled across the network was the largest contributor to pavement cracking performance simulated in *CalME*. Using *CalME* on projects without including PRS to control performance-related mix properties was ignoring a large source of unreliability in the designs.

As noted previously, in earlier work on *CalME* 1.0/2.0, the UCPRC identified two types of contributions to variability: *within-project variability* and *between-project variability*. Differences in performance-related properties between materials produced by different suppliers are the primary source of between-project variability. Differences in median construction quality between different contractors would also contribute to between-project variability.

Within-project variability comes from variations of the natural subgrade and the variability of materials production and construction using the given set of materials that a contractor brings to a single project. Within-project variability considers the rate of development of distress extent within a project as time and traffic progress. If there was no variability of materials properties in a project due to the natural subgrade and no variability in

materials production and construction of the other layers, then theoretically the entire project would fail at exactly the same time. For example, the entire project would go from zero to 100 percent of the wheelpath cracked at the same time. Of course, this does not happen in practice.

Here is an example of within-project variability. Suppose there were two contractors, A and B, working with the same materials on the same project, as shown in Figure 1.4. If both have the same median construction quality but Contractor A's construction quality variability is higher than Contractor B's, then the project would reach a typical cracking failure extent threshold extent (such as 25 percent of the wheelpath cracked) earlier if Contractor A built the project than if Contractor B built it. In this case, the within-project variability of the subgrade is included in the within-project variability shown for both contractors.

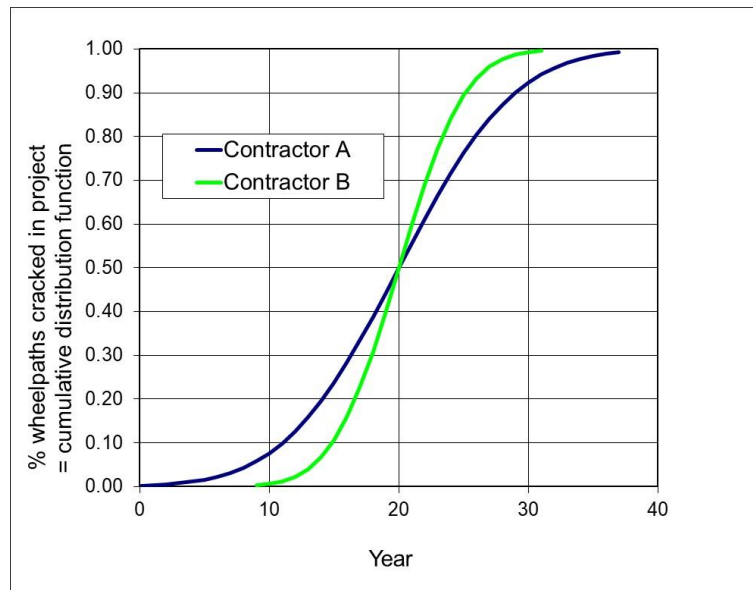


Figure 1.4: Two different within-project variabilities.

Between-project variability addresses the uncertainty regarding the materials that a contractor would bring to a project in a low-bid environment, and to potential differences in median construction quality between contractors. Figure 1.5 shows a situation where Contractor A and Contractor B have the same within-project variability, but Contractor A brings an HMA material with a combination of stiffness and fatigue properties that results in less cracking than if Contractor B won the project.

Without PRS, asphalt materials only need to pass performance-related binder specifications and volumetric mix design requirements that do not fully address fatigue characteristics. Specific stiffness, fatigue performance, and rutting performance-related properties of the mix that will be delivered to the project for construction are unknown to a designer. Use of the calibration of *CalME* with 50 percent between-project reliability was acceptable if the

PRS were used to ensure that materials with the same or better properties were delivered to the project. It was clear from the analysis that between-project variability needed to be included in *CalME* for use on non-PRS projects.

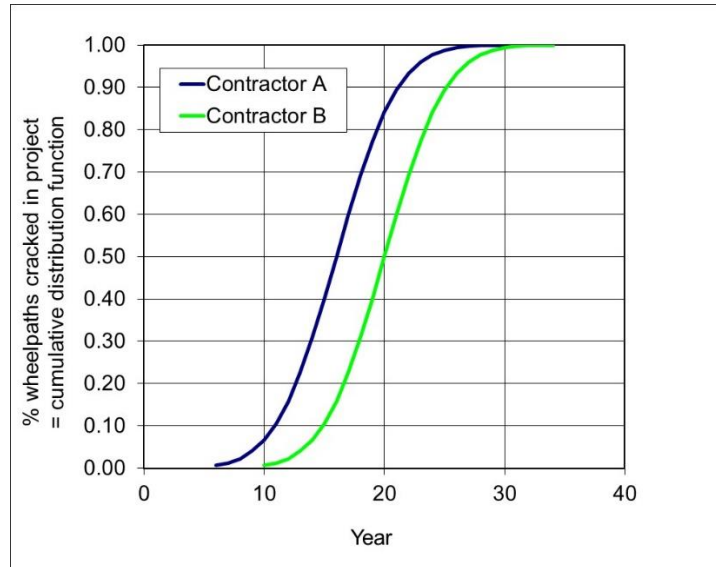


Figure 1.5: Between-project variability for two projects.

1.2.4 Comparison of Conventional and New Calibration and Reliability Approach

The conventional approach to calibrating an ME method, which has been used since calibration of the Shell Method and Asphalt Institute Method in the 1970s and early 1980s, through calibration of the Mechanistic-Empirical Pavement Design Guide (22) consists of the following:

- Identify short sections of pavement
 - Preferably most of the pavements have some failure on them, otherwise the time to failure would be uncertain because it hasn't occurred yet.
 - The sections need to have a construction time history.
- Collect the materials properties on the test sections.
- Backcast the traffic and materials properties to the time of construction.
- Simulate the performance using measured materials properties using Miner's Law, which has the following issues:
 - The response engine calculating critical stresses, strains, and deformations is unverified.
 - The damage evolution and predicted state of damage on the section is also unverifiable because use of Miner's Law forces the shape of the damage evolution curve.
 - Only the end state of distress is used for calibration.

- Find calibration coefficients for the calculated damage-to-distress transfer function to minimize the errors between observed and measured distress.
- Use the variability around the minimized error transfer function for reliability.

The conventional approach has several limitations:

- It requires expensive and time-consuming sampling and testing of materials properties for each section, resulting in a small number of sections being available for calibration.
- It ignores the fact that a design-bid-build (low-bid) designer does not know the performance-related properties of the materials the contractor will bring to the job; this results in a blurred understanding of the sources of variability and their consideration in the design reliability approach.

The new calibration approach developed by the UCPRC to calibrate *CalME* 3.0 aims to improve calibration and the reliability approach used in ME design by doing the following:

- Use all the good quality distress performance data and as-built data in the Caltrans PMS databases collected since 1978 and quality checked over the last 10 years; this provides orders of magnitude more performance data for calibration, with the data organized by project.
- Use median properties to match median performance, and use the variability of observed median performance to determine between-project variability, after using *CalME* to account for the effects of climate, pavement cross section, and traffic.
 - The weighted average performance of a set of mixes from the UCPRC databases was used to represent the time periods present in the cracking and rutting performance data since 1978.
- Backcalculate within-project variability by matching the shape of observed performance time history.

It was assumed that calibration using the very large amounts of data available in the PMS performance data and representative mix data for that time period would provide a more comprehensive calibration than just using detailed sampling and testing of materials from a few projects. Once the calibration is completed, comparisons with sections with detailed sampling and testing can provide additional validation.

The new approach also explicitly separates within-project and between-project variability in the calibration, and in the design method. This allows for use of appropriately different between-project reliability factors for PRS and non-PRS projects. The need for explicit consideration of between-project reliability and the inherent problem of calibrating using measured materials properties in a design-bid-build approach is expressed in the following excerpt from the MEPDG report:

From MEPDG report Section 3.3.2 OVERVIEW OF FLEXIBLE PAVEMENT DESIGN PROCESS

3.3.2.1 Design Inputs Trial Design Inputs and Site Conditions

A major difficulty in obtaining adequate design inputs is that the desired project specific information is not generally available at the design stage and must often be estimated several years in advance of construction. The actual materials used in a project may not 3.3.4 even be known until a few weeks before construction begins. The designer should obtain as much data as possible on in-situ material properties, traffic, and other inputs for use in design to obtain a realistic design. The designers should also conduct a sensitivity analysis to identify key factors that affect pavement performance. Based on sensitivity analysis results, provisions could be made in the contract documents for stringent control of the quality of key material properties (e.g., asphalt concrete stiffness), or the design could be modified to make the pavement performance less sensitive to the input in question. (22)

The inclusion of between-project reliability in *CalME* 3.0 overcomes the need for the sensitivity analysis in the project design process called for in the MEPDG report to assess the range of potential materials that might be delivered to the project—which depends on who wins the design-bid-build contract.

1.2.5 Scope of the Calibration

Experience on the Caltrans network indicated that rutting of the HMA was the most common and largest contributor to rutting. The HMA rutting models in *CalME*—which were calibrated using HVS and WesTrack data, with some additional validation from other test tracks—were considered to be reasonably well calibrated.

Rutting of the granular base and subgrade layers, which is controlled by structural design, is typically not the critical design criterion for asphalt-surfaced pavements for longer design lives in California. Rutting of the underlying layers was typically observed to occur where drainage was poor or after extensive cracking of the surface allowed water to enter those layers. The rutting models for unbound layers—which were calibrated using HVS and WesTrack data—were therefore also considered sufficiently calibrated. In addition, rutting data were only available for the 2010 and 2011 automated pavement conditions surveys in the PMS.

The primary focus for the *CalME* 3.0 calibration was on developing transfer functions for fatigue and reflective cracking of the HMA layers, damage models and transfer functions for new materials (specifically, in-place recycling alternatives), and transfer functions (but not the damage models) for materials that had not been previously well calibrated (specifically, cement-stabilized base and cement- and lime-stabilized subgrade layers).

2 NEW CALIBRATION METHOD

2.1 General Approach for Field Calibration

The calibration approach for *CalME* 3.0 was developed with the assumption that all projects follow the given ME model under consideration. With this assumption, Monte Carlo experiments of *CalME* simulations were used to develop pavement performance distributions and then to develop transfer function parameters that related the simulated performance distributions to the observed distributions of project performance.

The calibration of the asphalt concrete fatigue transfer functions is presented here as an example for all the other transfer function calibrations. Although this report provides an overview of the performance data used for those other calibrations, the details of the other transfer functions' calibrations appear in other reports that are being prepared.

2.2 Explanation and Example: Asphalt Concrete Fatigue Damage Model

Fatigue damage in asphaltic materials is caused by the repeated application of tensile strains due to both traffic loading and daily temperature cycles. In *CalME*, only traffic-related fatigue damage is considered.

Fatigue damage affects the stiffness master curve of asphaltic materials. Specifically, the equation between mix stiffness and reduced time for asphaltic material with fatigue damage becomes:

$$\log E = \delta + \frac{\alpha \times (1 - \omega_E)}{1 + \exp(\beta + \gamma \log(tr))} \quad (1)$$

where ω_E is the stiffness damage caused by fatigue cracking, which is in turn calculated from the following equation:

$$\omega_E = \min[1.0, \omega] \quad (2)$$

$$\omega = \left(\frac{MN}{MN_p} \right)^{\alpha_f} \quad (3)$$

where: MN is the number of load applications in millions,

MN_p is the allowable number of load repetitions in millions,

α_f is a material-dependent model parameter.

MN_p is calculated in turn using the following equation:

$$MN_p = A \times \left(\frac{\varepsilon}{\varepsilon_{ref}} \right)^\beta \times \left(\frac{E}{E_{ref}} \right)^{\beta/2} \quad (4)$$

where: ε = bending strain at the bottom of the asphalt layer in $\mu\varepsilon$, negative for tensile,

ε_{ref} = -200 microstrain is the reference bending tensile strain,

E_{ref} = 3,000 MPa (435 ksi) is the reference stiffness, and

A and β are material constants.

Equations (1) to (4) only describe how damage is determined when bending strain and AC layer stiffness remain constant, which is typically not the case. For damage accumulation throughout the design life of a pavement, *CalME* adopts an incremental-recursive (IR) procedure. As described previously, “Incremental” refers to the fact that *CalME* simulates pavement performance one increment at a time. The default duration of each increment is 30 days, but a user may set the duration as short as one day. “Recursive” refers to the fact that *CalME* uses the output from one increment recursively as the input to the next increment.

During a simulation of pavement performance, the strain and stiffness on the right-hand side of Equation (4) may change from increment to increment. In addition, there are different loading conditions (wheel load level and loading temperature, etc.) within each increment. Essentially, there are multiple damage evolution functions in effect both within and between simulation increments. The accumulation of damage within each increment follows Miner’s Law:

$$\Delta\omega_i = \sum_j \Delta\omega_{ij} \quad (5)$$

where subscripts i and $i - 1$ indicate simulation increments, and subscript j indicates loading conditions. $\Delta\omega_{ij}$ is the incremental damage caused by the j -th loading condition for the i -th increment and it is calculated as:

$$\Delta\omega_{ij} = \left[\frac{MN_{e,ij} + \Delta MN_{ij}}{MN_p(\varepsilon_{ij}, E_{i-1})} \right]^{\alpha_f} - \omega_{i-1} \quad (6)$$

where MN_e is the effective number of load applications required with the present parameters, to produce the damage at the beginning of the increment i denoted as ω_{i-1} :

$$MN_{e,ij} = \omega_{i-1}^{\frac{1}{\alpha}} \cdot MN_p(\varepsilon_{ij}, E_{i-1}) \quad (7)$$

The time-hardening process shown in Figure 1.1 demonstrates how damage is accumulated over three time-increments, each with only one loading condition within each increment. This same process can be used to simulate fatigue damage in laboratory fatigue tests. In fact, the model parameters α_f , A , and β are determined for each material in *CalME* by fitting fatigue test data following the fatigue damage model.

2.3 Transfer Function for Fatigue Cracking

Once the fatigue damage is determined, the percent of wheelpath cracked, denoted as *CRK*, can be calculated using the following equation:

$$CRK = \frac{100}{1 + \left(\frac{\omega}{\omega_{50}}\right)^\beta} \quad (8)$$

where ω_{50} and β are model parameters to be determined through field calibration, and each may depend on additional factors such as pavement structure type, climate condition, HMA layer thickness. ω_{50} also represents the fatigue damage corresponding to 50 percent wheelpath cracking based on the form of the equation. Figure 2.1 illustrates the correlation between fatigue damage and percent wheelpath cracking. This equation is the transfer function for the fatigue cracking model used in *CalME*. Note that this equation is essentially a recast of earlier versions proposed for *CalME*.

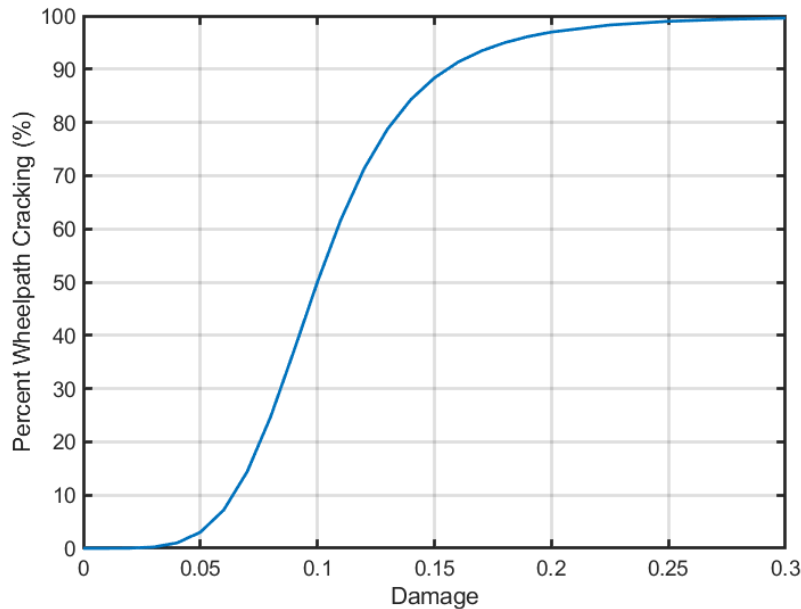


Figure 2.1: An example of the transfer function for fatigue damage, $\omega_{50} = 0.1$ and $\beta = -5.0$.

2.4 Project-Level Performance and Calibration Discussion Example

The first step in developing a field calibration procedure is to run Monte Carlo simulations at the project level and examine the effects of the transfer function parameters on pavement performance. The steps for an example project are shown in this section using a simple example to demonstrate the process.

2.4.1 Simple Project Example

For this example, the pavement in the project is assumed to have three layers with 120 mm (0.4 ft) HMA over 300 mm (1.0 ft) of AB over subgrade. The AB and subgrade layers have constant stiffnesses of 300 MPa (43.5 ksi) and 50 MPa (7.3 ksi), respectively. The HMA layer is viscoelastic, but the loading temperature and loading frequency are assumed to be constant at 20°C (68°F) and 10 Hz. The HMA material is assumed to be the “2020 Standard HMA Type A Mix with PG 64-XX Binder and up to 15% RAP for non-PRS Projects” from the *CalME* standard materials library.¹

The within-project variabilities for the project come from two sources: the stiffness of HMA layer denoted as E , and the fatigue model parameter A for the HMA layer. Both E and A follow lognormal distributions. Specifically, E has a mean value of 3,000 MPa (435 ksi) and a standard deviation of 600 MPa (87 ksi) (i.e., $E \sim LN(3000, 600)$), where $LN(P_1, P_2)$ indicates a random variable following lognormal distribution with mean P_1 and standard deviation P_2). Parameter A has a mean value of 150 and a standard deviation of 60 (i.e., $A \sim LN(150, 60)$).

To conduct a Monte Carlo experiment, a project is divided into many segments, and each segment has a constant pair of values for (E, A) determined by random sampling. The performance of each segment is associated with a *CalME* simulation in the Monte Carlo experiment.

2.4.2 Monte Carlo Simulation Results and Observations

Figure 2.2 shows the cracking histories for different segments within a project as well as the overall average and median. As expected, some segments reach 100 percent cracking very quickly while other segments last much longer. Each of the individual curves is a transformed version of the transfer function because the fatigue damage is a monotonic function of the number of load repetitions applied. The large difference between different segments illustrates the effect of within-project variability (WPV) (i.e., the variability of $[E, A]$) for this particular project).

¹ For this simplified example, traffic is applied with standard equivalent single axles (i.e., 80 kN [18 kips] single axles with dual tires). The strain at the bottom of the HMA layer only depends on the HMA layer stiffness and is calculated using a regression equation developed from the *CalME 3.0* response engine, *OpenPave*, which uses *CalME*'s axle load spectra data to calculate pavement response.

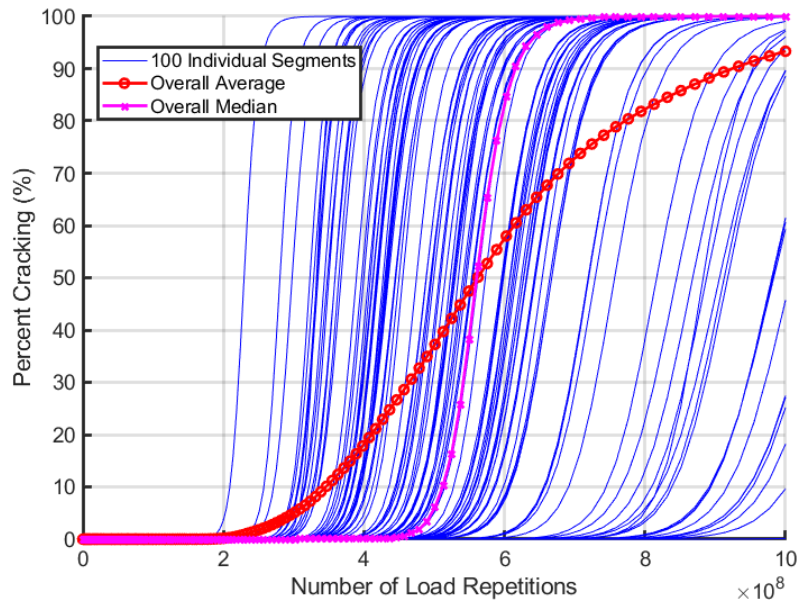


Figure 2.2: Cracking histories for individual segments as well as the project overall (only showing 100 segments).

The overall average shown in Figure 2.2 is the performance data typically collected in pavement condition surveys. Figure 2.2 indicates that the shape of the cracking history curve for individual segments is very different from the shape of the overall average curve: the overall average curve is much flatter than the curves for individual segments. This is because the shape for an individual segment depends on the transfer function alone while the shape of the overall average also reflects the amount of WPV.

Figure 2.2 also shows the overall median performance, which was determined by finding the median of percent cracking among all segments at any given time. Unlike the overall average, the overall median has the same shape as the individual segments. This is because pavement performance is a monotonic function of different inputs. This general trend is hereafter referred to as the *monotonic property* of pavement systems.

For example, it is easy to see that increasing fatigue model parameter A always leads to longer pavement cracking life if all other inputs are equal. However, the effect of stiffness E is less straightforward since it is the product of $E \cdot \epsilon$ (i.e., work) that drives the damage, and damaged stiffness is again dependent on initial stiffness. As an example, the effect of HMA stiffness on pavement performance, indicated by the number of load repetitions to 50 percent cracking, is shown in Figure 2.3. For the simplified example under discussion, the figure shows that a stiffer HMA layer generally leads to shorter cracking life. Note that this trend is typically reversed when the HMA thickness is increased.

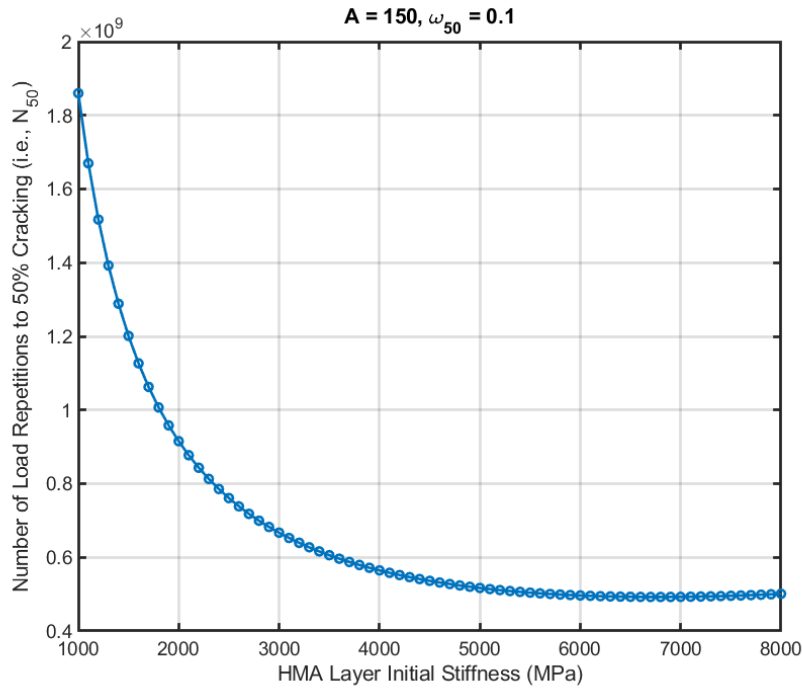


Figure 2.3: Effect of HMA layer stiffness on pavement fatigue cracking performance.

The observation that overall median performance has the same shape as individual segment performance suggests that the overall median can be used to recover the transfer function. This can be mathematically proven for the HMA fatigue model under discussion herein and is also generally true for all ME models if the monotonic property holds. However, the overall median curve is less practical to observe than the overall average, if it is possible to observe it at all, because dividing a project into segments can be a subjective process. Therefore, it is still necessary to use the overall average curve for field calibration. This turns out to be possible, as is explained below.

Figure 2.2 also shows a striking feature: the overall average and overall median reach 50 percent at the same time. This is not a coincidence. Specifically, this is because the overall average is essentially the cumulative distribution function (CDF) of cracking life for the project. The number of load repetitions to 50 percent cracking on the overall average curve therefore is the median cracking life of the project, which only depends on the median of (E, A) because of the monotonic property. Since the overall average converges to the overall median as the variability decreases to zero, the overall median is technically a special case of the overall average and therefore must go through the same point at 50 percent cracking.

2.4.3 Effects of Different Within-Project-Variability

This is further demonstrated in Figure 2.4, which shows the overall average cracking histories for five simulated projects that have the same mean value for (E, A) but different standard deviations. All the overall averages pass through the same point at 50 percent cracking with minor deviations that can be attributed to the random nature of Monte Carlo simulations. By extension, t_{50} (the number of repetitions to 50 percent cracking is hereafter designated as N_{50} and the time to reach N_{50} is designated as t_{50}) only depends on the median of (E, A) for a given project as soon as the traffic history is determined. t_{50} is more practical than N_{50} because pavement performance history is typically recorded over time rather than traffic count.

Figure 2.4 also illustrates the effect of WPV on the expected pavement performance. The shape of the overall average cracking curves change with the amount of WPV. The higher the WPV, the more spread out the pavement performance is, as indicated by the flatter slope of the mid portion of the overall average cracking curves.

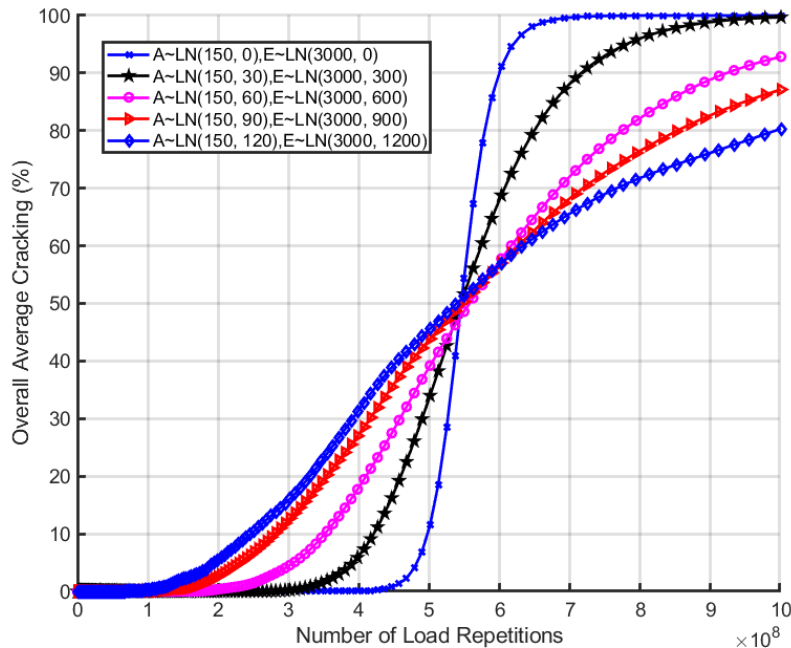


Figure 2.4. Overall average cracking histories for projects with different standard deviations for inputs.

2.4.4 Summary of Project-Level Calibration

In summary, the time to reach 50 percent cracking (i.e., t_{50}) only depends on the median values of ME inputs, while the shape of the overall average cracking history curve reflects the amount of WPV, which is a function of the variability of the ME inputs). If the statistical distributions of all the ME inputs for a given project are known, the transfer function can be identified through the following steps:

1. The damage corresponding to t_{50} , denoted as ω_{50} in Equation (8), can be calculated using the project median ME inputs.
2. The shape parameter of the transfer function, denoted as β in Equation (8), can be backcalculated by running Monte Carlo simulations and finding the best match between simulated overall average cracking curve and the observed one.

Note that this procedure only works if the project-level ME inputs are known.

2.5 Statewide Network-Level Performance and Calibration

At the statewide network-level, the Monte Carlo simulations are conducted using the same project simplifications as in the project-level simulations.

2.5.1 Simple Network Example

At the network level, the median values of (E, A) for individual projects are likely to follow their own layer of random distribution, especially if the network is large enough. In this section, the expected network-level performance is again illustrated by running Monte Carlo simulations for the asphalt concrete fatigue cracking model for a simple example network. Specifically, the following assumptions are used to produce a simple network performance example:

- The median value of E for projects in the network is randomly chosen between 3,000 and 7,000 MPa (435 and 1,015 ksi) at 500 MPa (73 ksi) intervals (i.e., nine values in total).
- The coefficient of the standard deviation of E in each project is fixed at 0.2 for all projects.
- The median value of A is randomly chosen between 75 and 300 (0.5 and 2.0 times a median on log scale of 150) for all projects in the network, uniformly distributed in log space with eight intervals in between (i.e., nine values in total).
- The coefficient of standard deviation of A in each project is fixed at 0.4 for all projects.

Note that these numbers were selected to illustrate the network performance and calibration approach. The findings derived from this example hold in general, although the values themselves are for illustration only. The cumulative distribution functions for E and A are shown in Figure 2.5 and Figure 2.6 respectively.

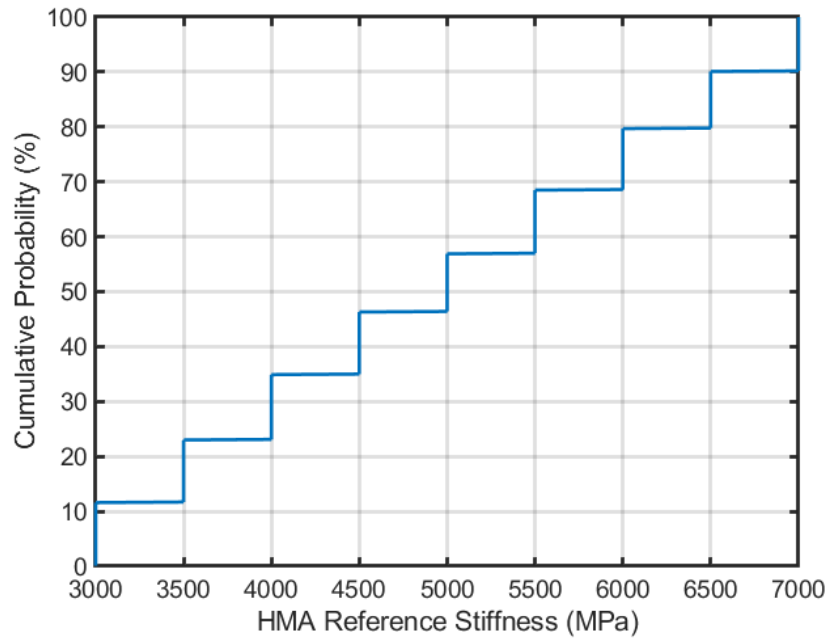


Figure 2.5: Cumulative distribution function of the median value of E for projects in the network.

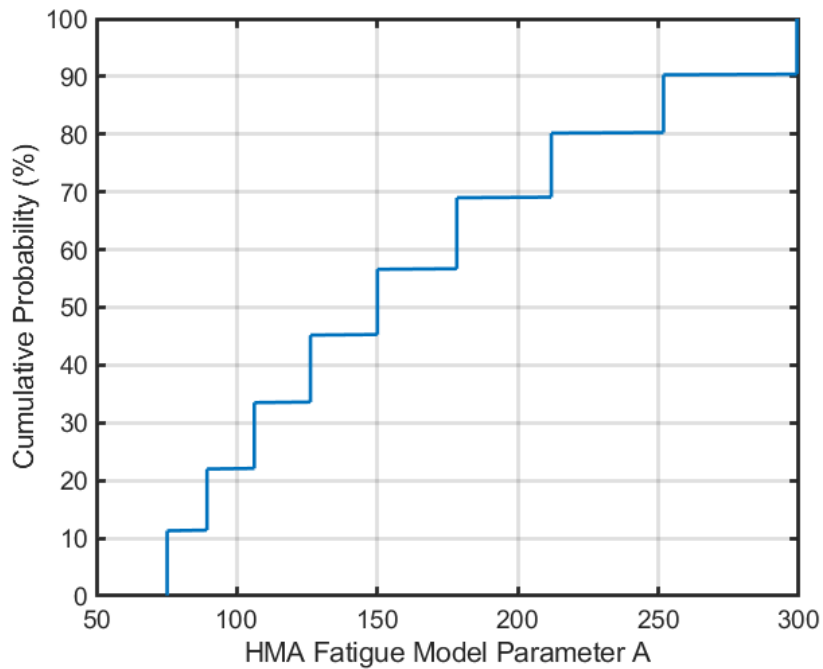


Figure 2.6: Cumulative distribution function of the median value of fatigue model parameter A for projects in the network.

2.5.2 Monte Carlo Simulation Results and Observations

Figure 2.7 shows the simulated overall average cracking histories for individual projects in the network along with the one for a project with the network median inputs (NMI), which in this case is 5,000 MPa (725 ksi) for E and 150 for A . Note that the individual value of E and A in NMI may be different from the corresponding network median because the NMI is determined with the combinations ranked by the corresponding pavement performance.

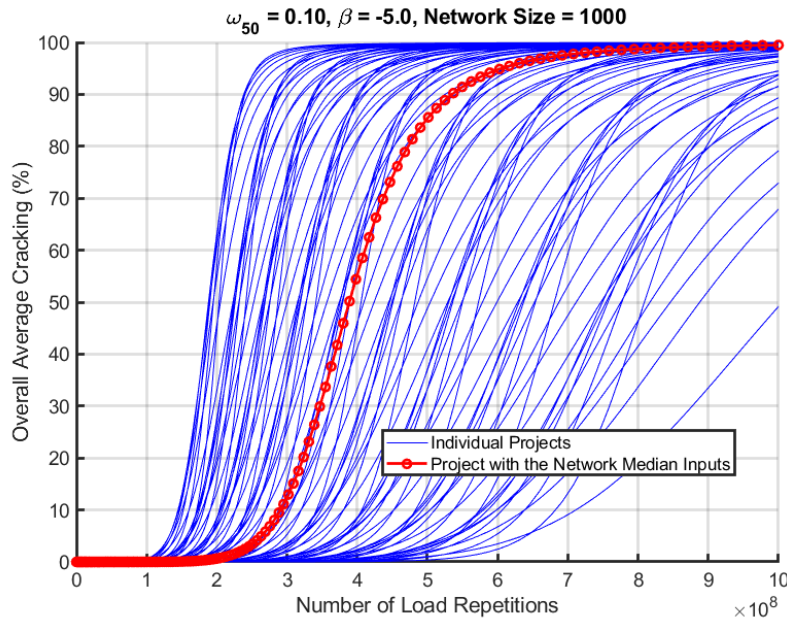


Figure 2.7: Overall average cracking histories for individual projects in the network and for the project with the median inputs.

For every project in Figure 2.7, there is a corresponding N_{50} that reflects the median value of (E, A) for the given project. As expected and as illustrated in the figure, the performance of the project with NMI is somewhere in the middle among all projects in the network. In fact, the N_{50} of the project with NMI is the same as the network median N_{50} with minor differences likely due to rounding errors in Monte Carlo simulations. This is illustrated in Figure 2.8, which shows that the N_{50} for the project with NMI is the same as the median (i.e., 50th percentile) of N_{50} for all the individual projects in the network.

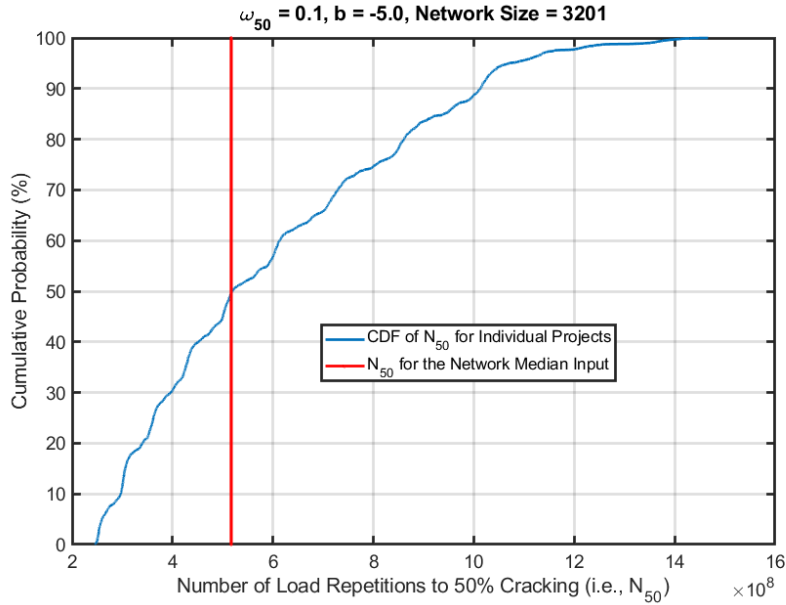


Figure 2.8: Cracking performance of individual projects and the project with the network median input.

When simulating the network performance for this example, ω_{50} was set to 0.10. This value needs to be estimated without knowing the actual value of (E, A) for each individual project. The following are known, however:

- N_{50} of each individual project
- NMI of the given network

It is hypothesized that the fatigue damage in the HMA layer for the project with NMI is equal to the true ω_{50} after applying load repetitions equal to the median N_{50} of the network. To test this hypothesis, multiple rounds of network-level Monte Carlo simulations were run with different network sizes, and ω_{50} was estimated following the hypothesis. The relative error in estimated ω_{50} is shown in Figure 2.9. As shown in the figure, the error in estimated ω_{50} ranges from 1 to 6 percent and generally, but not always, decreases with the increase in network size. It is therefore concluded that this hypothesis is true and provides a reasonable way to estimate ω_{50} from network-level data.

Figure 2.10 shows the normalized version of Figure 2.7, with the number of load repetitions divided by the corresponding N_{50} for each project. Figure 2.10 also includes a curve representing a project with no WPV, which as expected, is steeper than the curves for individual projects. As discussed in the previous section, the slope of the middle portion of each normalized curve reflects the amount of WPV for that project. Examining the distribution of the slopes allows one to evaluate the distribution of WPV for the network.

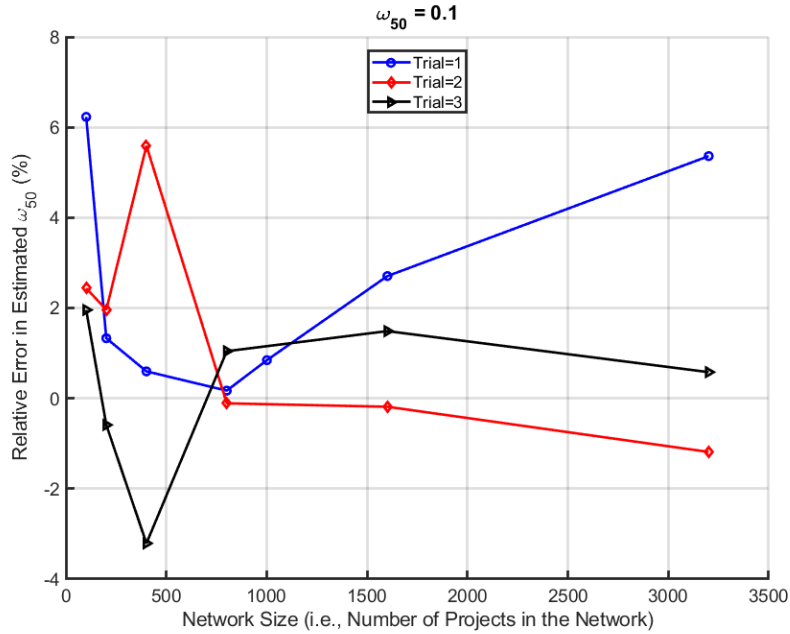


Figure 2.9: Effect of network size on the relative error in estimated ω_{50} .

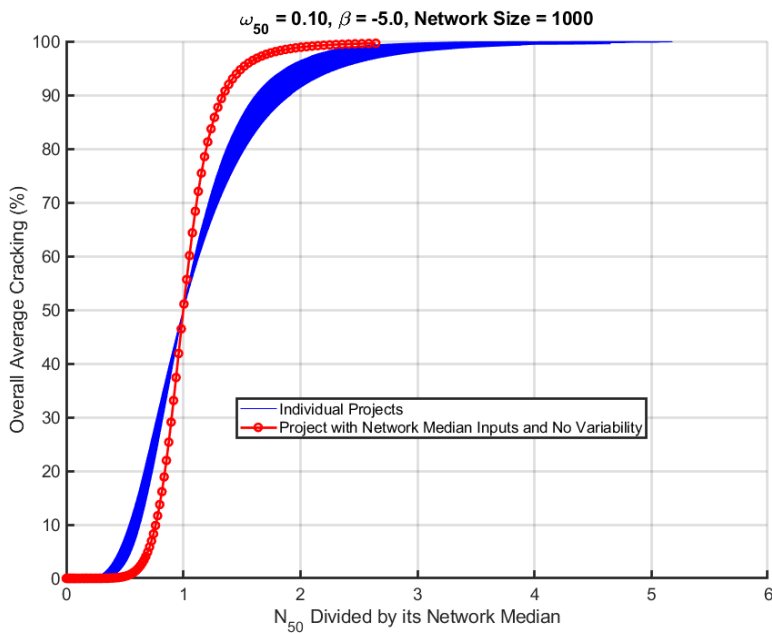


Figure 2.10: Overall average cracking histories for individual projects in the network with number of load repetitions normalized by N_{50} (i.e., the number of load repetitions to 50% cracking).

The variability between different projects (i.e., the between-project variability, BPV) regarding the ME inputs in the network can be evaluated by reviewing the distribution of the following normalizing factor:

$$c_n = \frac{N_{50}}{\tilde{N}_{50}} \quad (9)$$

where \tilde{N}_{50} is the network median of N_{50} . Note that in actual calibration t_{50} is more practical than N_{50} , so the alternative definition should be used when considering a smaller set of data for which the traffic volume is roughly the same:

$$c_n = \frac{t_{50}}{\tilde{t}_{50}} \quad (10)$$

Figure 2.11 shows the CDF function of c_n for this simulated network. For easier reference, C_n is hereafter referred to as the relative performance factor (RPF). As expected, the 50th percentile of c_n is exactly 1.0. This chart provides a way to account for the BPV if one were to use NMI to design pavements. For example, the 5th percentile of c_n is approximately 0.5 according to Figure 2.11. This means that one can achieve 95 percent reliability regarding BPV by multiplying the N_{50} predicted using NMI by 0.5 as the pavement design N_{50} .

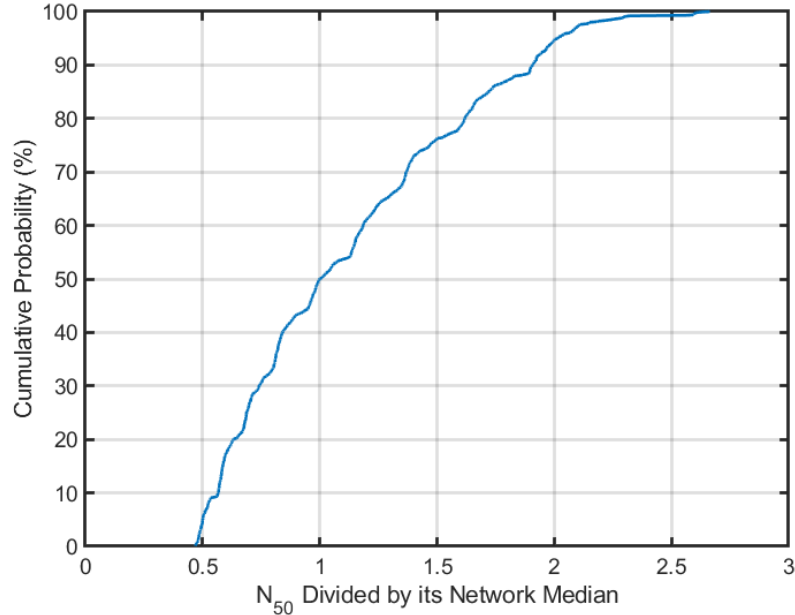


Figure 2.11: Cumulative distribution function of the normalizing factor.

In summary, the project performance predicted by the ME model using the network median ME inputs should have an N_{50} value matching the observed network median N_{50} . The distribution of c_n can be used to account for BPV for the desired level of design reliability.

2.5.3 Network-Level Calibration

Based on the observations from the example network-level Monte Carlo simulations, the transfer function can be identified with the following steps using the network-level data:

1. Review ME inputs for the statewide network and determine the NMI, and the typical standard deviations.
2. Determine t_{50} and mid portion slope of the observed cracking history curve for each project within the network.
3. Determine the observed network median t_{50} using the results from Step 2.
4. Simulate the pavement with NMI but without any WPV, determine the damage in the HMA layer corresponding to the network median t_{50} determined in Step 3. This is the estimated (i.e., calibrated) ω_{50} for the transfer function.
5. Review the slopes determined in Step 2 and select the proper percentile of the slope for use in design considering the desired reliability level. Lower slope corresponds to higher reliability.
6. The β parameter of the transfer function can be backcalculated by running Monte Carlo simulations sampling from the distributions of a selected set of explanatory variables and matching the slope determined in Step 5.
7. Calculate the normalizing factor c_n , then find the percentiles corresponding to different desired reliability levels for design. These percentiles can be used as multipliers on estimated design life to account for different design reliability.

The highway network may need to be sub-divided into calibration cells based on structure type (new pavements, HMA overlay over old cracked flexible pavements, etc.), HMA layer thickness, traffic level, climate zone, etc. The procedure outline above can then be applied to each of the calibration cells. The calibration results can then be grouped and simplified for use in the actual design.

3 PERFORMANCE DATA

3.1 Introduction

The fatigue cracking transfer function identified through field calibration is in essence an empirical correlation between the fatigue damage predicted by the ME model and the probability of surface cracking. To ensure the high accuracy of such empirical correlations, it is necessary to divide a highway network into sub-networks in which the pavement structures are similar and, in turn, have similar failure mechanisms.

3.2 Sub-Networks for Field Calibration

The list of sub-networks for the field calibration is shown in Table 3.1. As shown in the table, the division is mostly based on the structure type.

Table 3.1: Sub-Networks for the Field Calibration

No.	Structure Group	Structure Type	Abbreviation
1.1	New flexible pavement	With aggregate base	N-AB
1.2	New flexible pavement	With cement base (cement-treated base or lean concrete base)	N-CB
2.1	Rehabilitation with new HMA	New HMA over old flexible pavement	R-FP
2.2	Rehabilitation with new HMA	New HMA over old rigid pavement	R-RP
3.1	Rehabilitation with partial-depth in-place recycled layer	With engineering emulsion as the stabilizing agent	R-PDR-EA
4.1	Rehabilitation with full-depth in-place recycled layer	With foam asphalt as the stabilizing agent	R-FDR-FA
4.2	Rehabilitation with full-depth in-place recycled layer	With cement as the stabilizing agent	R-FDR-C

Before the performance data extracted from the Caltrans pavement management system (PMS) software program *PaveM* can be used for the field calibration, the pavements the data covers must be divided into short lane-by-lane segments with uniform construction histories, traffic, and climate. This results in approximately uniform explanatory variables for the associated performance time histories. Each of these segments with its associated performance time history will serve as a basic unit for field calibration and are hereafter referred to as “virtual projects.” Note that multiple virtual projects can occupy the same space but they must be from different time periods. A brief summary of the amount of data available for each of the sub-networks is listed in Table 3.2.

Table 3.2: Summary of Calibration Data Available for Different Sub-Networks

Sub-Network Abbreviation	Total Number of Virtual Projects	Total Lane Miles of Virtual Projects	Observation Period
N-AB	8,350	1,063	1978-2014
N-CB	1,366	161	1978-2014
R-FP	253,841	34,702	1978-2014
R-RP	7,877	1,401	1978-2014
R-PDR-EA	6,717	892	1978-2018
R-FDR-FA	1,431	174	1978-2018
R-FDR-C	19	6	1978-2020

3.3 Data Processing

The following discussion of data processing and trends for new flexible pavements with aggregate base is intended to demonstrate the processes also used for other materials.

3.3.1 Determination of Time to 50 Percent Cracking

As mentioned in Chapter 2, one of the key performance metrics is the time to 50 percent cracking. Usually, pavements have undergone some maintenance or rehabilitation before reaching such a high extent of distress. It is therefore necessary to introduce a procedure to provide a reasonable estimate of the time to 50 percent cracking (i.e., t_{50}). After some trial and error, it was found that t_{50} of virtual projects can be determined reasonably well, fitting and extrapolating the observations for each virtual project using the following rules:

1. The correlation between time in years and percent wheelpath cracked has the same functional form as the transfer function (see Equation (8)).
2. The observed time history needs to be constrained with two data points: 0% cracking at year zero and 99 percent cracking at year 50.

The constraint at year 50 is arbitrary but is believed to be reasonable. A flexible pavement is not expected to last more than 50 years. Figure 3.1 and Figure 3.2 show two examples of the extrapolation: one with extensive observed cracking and the other showing no cracking during any observations of its performance.

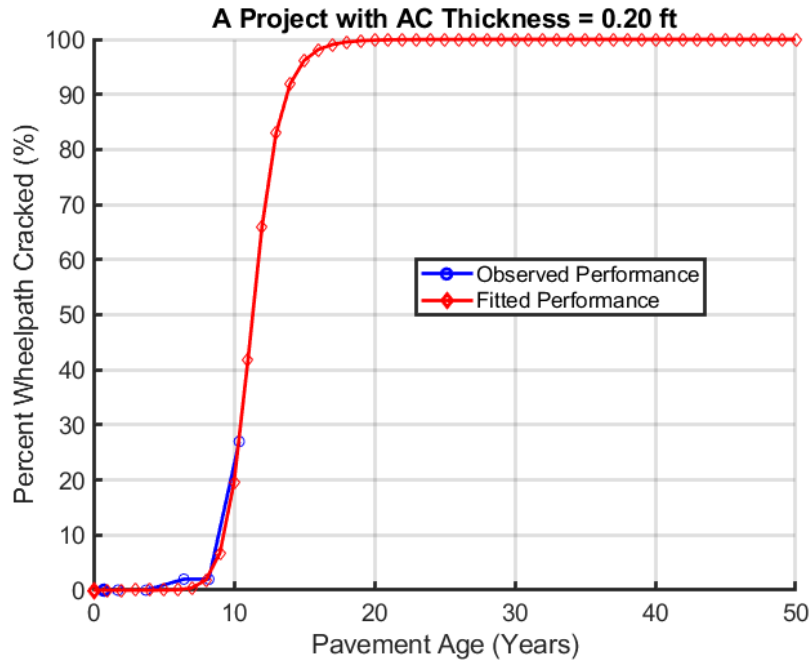


Figure 3.1: A project with extensive observed cracking and an extrapolated t_{50} of 11.3 years.

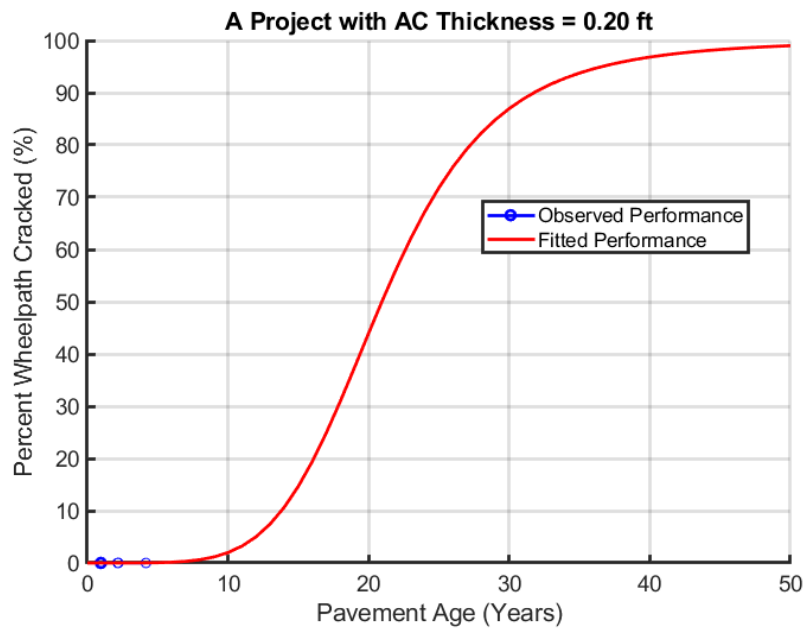


Figure 3.2: A project with zero observed cracking and an extrapolated t_{50} of 20.9 years.

3.3.2 Determination of Observed Shape Parameter $\beta_{observed}$

As mentioned in the previous section, the transfer function (see Equation (8)) is used to fit the actual crack development history. As a result, the shape parameter β is also determined for each virtual project and is denoted as $\beta_{observed}$. The distribution of $\beta_{observed}$ will be used to determine the true β value of the transfer function.

3.3.3 Rounding of Asphalt Concrete Surface Layer Thickness

The recorded constructed asphalt concrete layer thickness in the performance database varies almost continuously, as shown by the cumulative distribution function in Figure 3.3 for flexible pavements with aggregate base. For field calibration purposes, asphalt concrete surface layer thicknesses are rounded to the nearest 0.10 ft (30 mm). This increases the amount of data available for each distinct thickness group. “Asphalt concrete surface” hereafter refers to the new asphalt layers built in a given construction event, which is the total thickness of all asphalt layers for new pavements and reconstruction, and the thickness of the new asphalt layers for overlays.

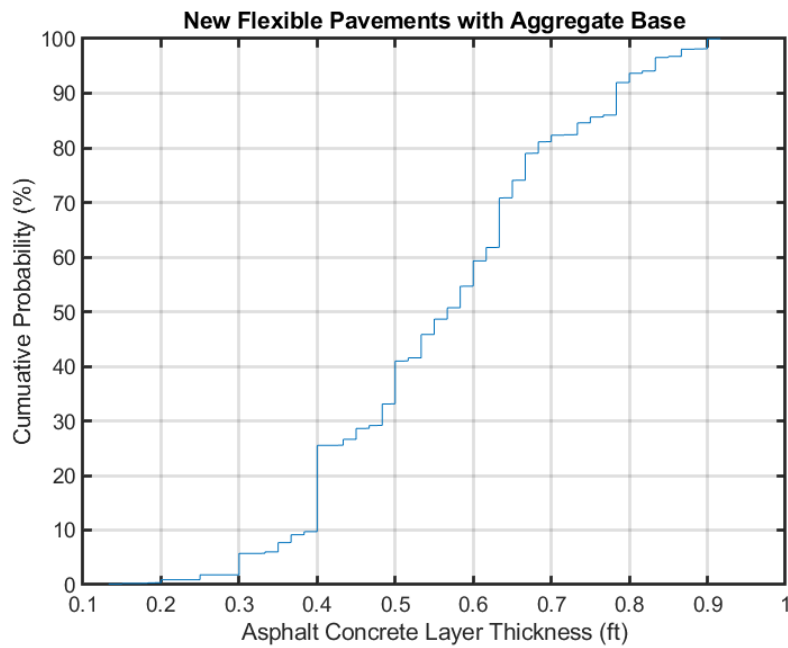


Figure 3.3: Empirical cumulative distribution function of asphalt concrete layer thickness for new flexible pavements with aggregate base.

3.4 Explanatory Variables in the Data

Pavement performance may be sensitive to, and hence may be explained by, variables such as layer thickness, truck traffic, climate region, and material quality. These variables are referred to as explanatory variables. Not all explanatory variables are recorded in the Caltrans PMS database. The following are some of the limitations:

- For new flexible pavements: there are no data for the subgrade.
- For rehabilitation projects: there are no data for the existing structure other than the milling depth.
- There are no records for the mechanical properties (such as fatigue resistance of HMA layer, stiffness of the aggregate base layer) of the materials used.

During field calibration, the effects of recorded explanatory variables are accounted for using *CalME* models. The effects of the remaining explanatory variables are accounted for through the within- and between-project variabilities.

3.5 Data Summary and Basic Trends

As noted earlier, this section’s sample examination of the data for the N-AB sub-network (new flexible pavements with aggregate base) has been undertaken to provide a perspective on the nature and quality of the PMS data available.

As expected and as shown in Figure 3.4 to Figure 3.6, the PMS data are not uniformly distributed across various explanatory variables such as total asphalt concrete surface thickness, climate, and traffic volume.

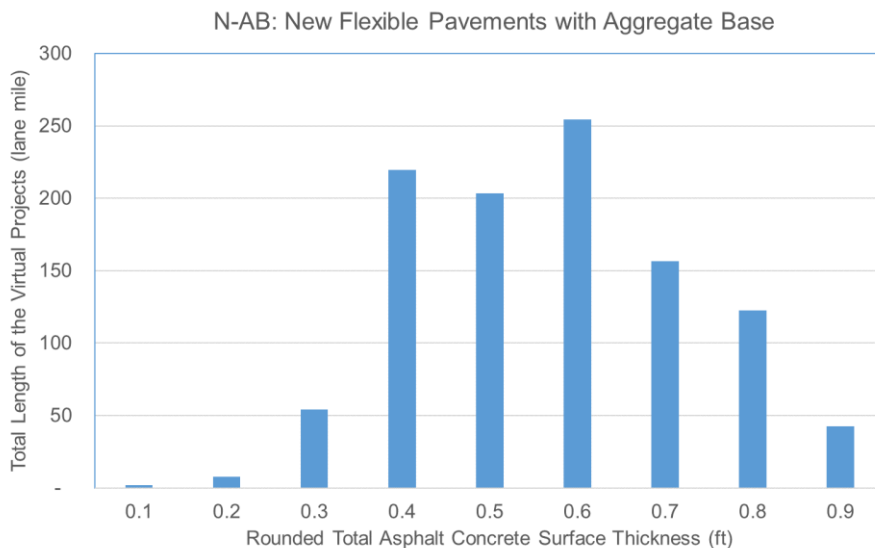


Figure 3.4: Distribution of virtual projects across total asphalt concrete surface thickness.

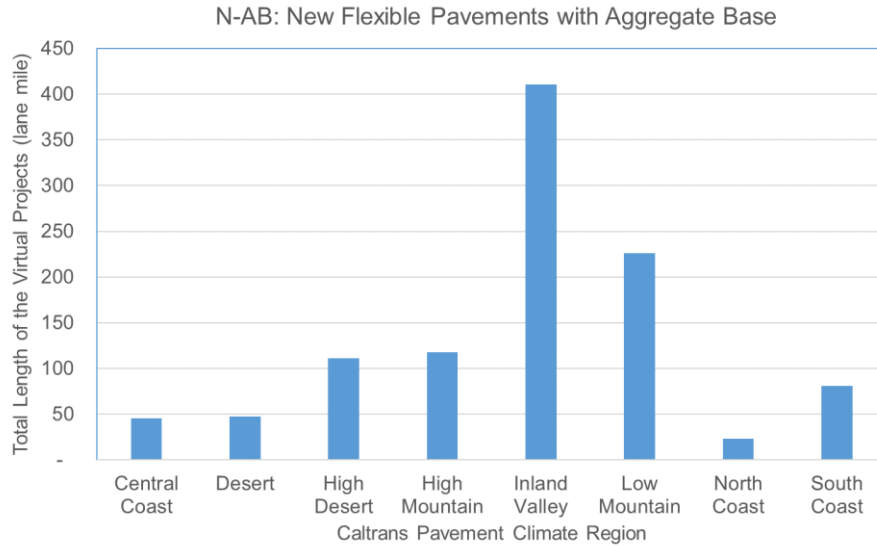


Figure 3.5: Distribution of virtual projects across Caltrans pavement climate regions.

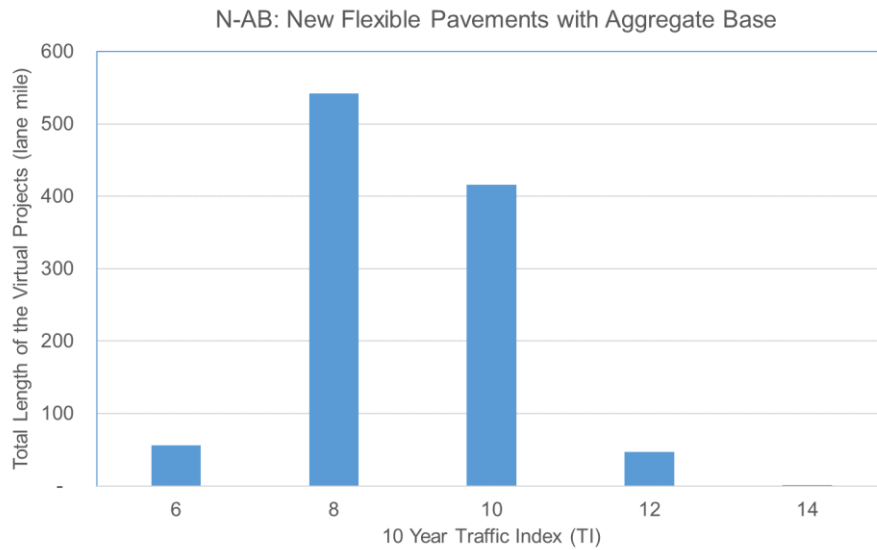


Figure 3.6: Distribution of virtual projects across 10-year traffic index (TI).

Figure 3.7 to Figure 3.9 show the average pavement cracking performance trends with respect to total asphalt concrete surface layer thickness, Caltrans climate region, and traffic index, respectively. The following discussion regarding these figures must consider that the performance data that they are built from are not uniformly distributed across each thickness, region, and traffic index. The figures show fitted and extrapolated years to 50 percent of the wheelpath being cracked. Nearly all of these new pavements were designed to last 20 years using the R-value method. The critical distress controlling pavement life, fatigue cracking or rutting, and the distress

severities and extents defining failure are not identified in the R-value method. If the design method is correctly accounting for each of the explanatory variables, the average time to 50 percent wheelpath cracking should be about 20 years, with the average indicating 50 percent reliability.

It can be seen in all the figures that the designs are on average not reaching 20 years of life. This may be an indication that many pavements are underdesigned in some manner and may also reflect the aggressiveness of the extrapolation approach described previously. It can be seen in Figure 3.7 that in general, pavements last longer as thickness increases for thicknesses above 0.3 ft (note that there are very few observations of new HMA thickness less than 0.4 ft). It must be noted that the R-value method includes tradeoffs of HMA thickness versus AB thickness, and it is uncertain how many of the designs for projects in the database used the minimum allowable HMA thickness and how many used thicknesses greater than the minimum. The averages shown in Figure 3.8 indicate some differences in cracking performance between climate regions. The R-value method does not account for climate region. It can be seen in Figure 3.9 that R-value designs seem to have shorter lives as traffic volume increases above a ten-year traffic index of 10 (approximately 3 million ESALs). If the empirical design method was correctly accounting for the traffic, there should be no trend in the averages. It must be remembered that the information shown in Figure 3.7 to Figure 3.9 is not normalized accounting for the intended design lives of projects (CAPM, 10-year rehabilitation, 20-year rehabilitation), traffic levels, or any other variables that are not shown in each figure. They were intended to provide a very early indication of sensitivity and approximate cracking lives in the calibration data set. A sensitivity analysis for *CalME* 3.0 simulations for a factorial of input variables is shown in Section 4.3.1.

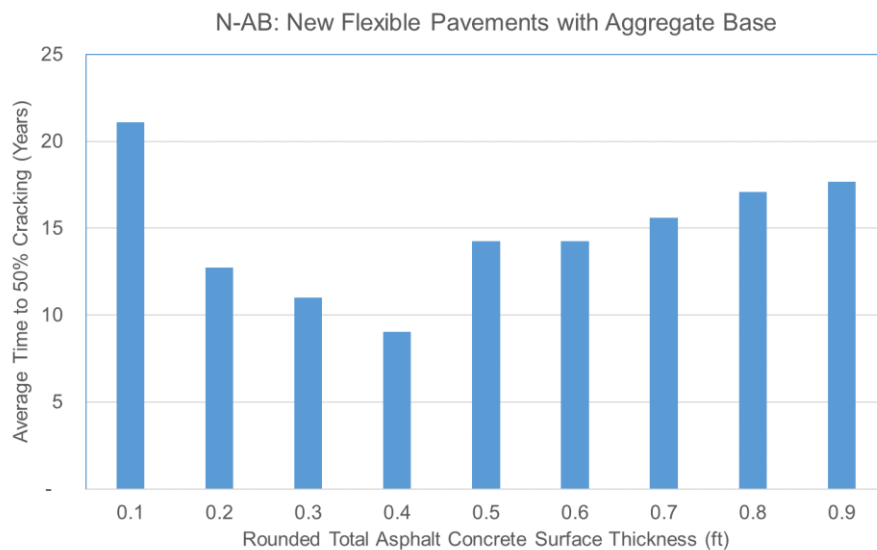


Figure 3.7: Variation of average fitted and extrapolated time to 50% cracking with rounded total asphalt concrete surface layer thickness.

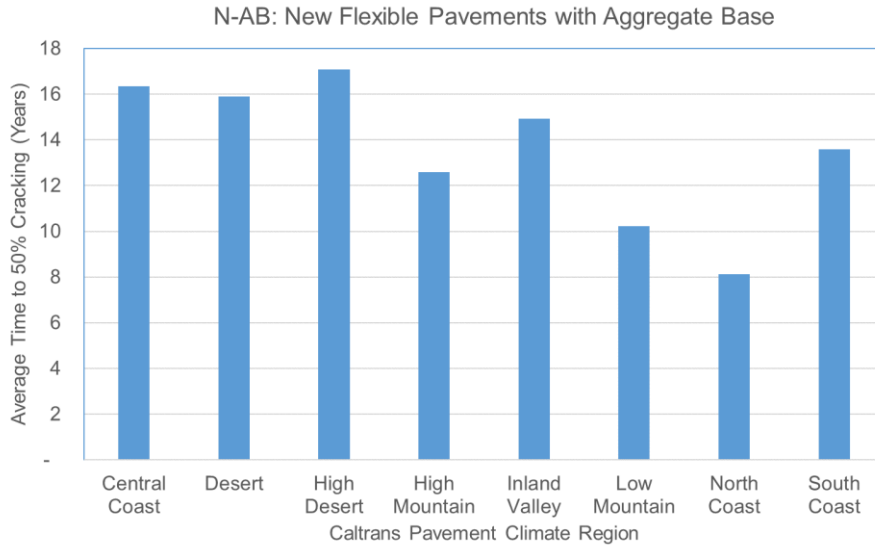


Figure 3.8: Variation of average fitted and extrapolated time to 50% cracking with Caltrans pavement climate regions.

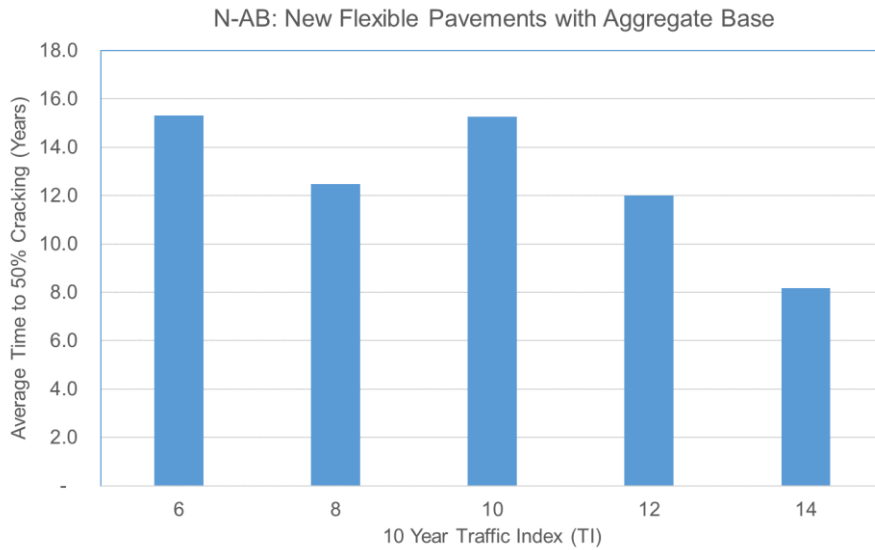


Figure 3.9: Variation of average fitted and extrapolated time to 50% cracking with 10 year traffic index (TI).

4 DETAILED CALIBRATION PROCEDURE AND RESULTS

4.1 Step-by-Step Procedure

The method described in Section 2.5.3 was followed when conducting the field calibration for *CalME* 3.0 and the step-by-step procedure appears below. Note that field calibrations were conducted separately for each pavement group/type sub-network described in Chapter 3.

1. Identify and assemble information. This involves organizing the pavement management system data into virtual projects (see Section 3.2 for definition). This creates the linkage between as-built and other project information (date of construction, treatment type, layer thickness, traffic, climate, and other explanatory variables) with performance data. The data processing as outlined in Section 3.3 is also conducted in this step.
2. Sensitivity analysis of the *CalME* model. Review performance sensitivity to identify the most sensitive explanatory variables by running *CalME*.
3. Separate calibration data into calibration cells. Each cell is a distinct combination of recorded explanatory variables.
4. Perform calibration for each calibration cell independently. Focus calibrations on those cells that have more performance data.
 - Determine the statewide network median input (NMI) for each material (same NMI was used for materials across all sub-networks) by reviewing historical data.
 - Determine the median time to 50% cracking, denoted as \tilde{t}_{50} , for the current cell.
 - Run *CalME* using NMI to determine the damage at \tilde{t}_{50} : this is the calibrated ω_{50} for the current cell.
 - Review the distribution of the shape parameter β of actual crack propagation for the current cell.
 - Select a subset of explanatory variables that will be allowed to have variance in the Monte Carlo simulation to account for the amount of observed within-project variability following the procedure described in Section 2.5.3.
 - Calculate the normalizing factor C_n for each virtual project using Equation (10), and determine the between-project factor for desired design reliability level as described in Section 2.5.2.
5. Summarize the calibration results from the individual cells and develop global calibrations whenever reasonable.

4.2 General Network Median Input

As explained earlier, the new calibration method does not require detailed knowledge of any specific project when conducting statewide network-level calibration. Instead, one needs to estimate the network median input for these unknown explanatory variables, which reflect the characteristics of the network.

The inputs to *CalME* includes structure (layer materials, thicknesses, and bonding conditions), traffic (spectrum and volume), and climate (climate zone). The layer materials and bonding conditions are not recorded in the PMS and must be estimated for the field calibration.

4.2.1 Surface Layer Material and Bonding Condition

The type of asphalt concrete surface materials on the Caltrans highway network have changed over the last 30 years as Caltrans has implemented changes in mix design procedures and changes in the use of mixes with rubberized binder, among other things. The following is a summary of Caltrans practice regarding asphalt concrete materials that was incorporated into the simulations of projects constructed in different time periods:

- For the period before 2000: The QC/QA specification for hot mix asphalt was not yet implemented. Data showed that average air-void contents were about 11 percent, and that a high percentage of multi-lift paving had poor bonding because there were no tack coat requirements in the Standard Specifications (23).
- For the period of 2000 to 2015: The QC/QA specification was implemented, and tack coat was required in the Standard Specifications. Data showed that the average air-void content was reduced to about 7 percent (23). The hot mix asphalt lifts were found to be mostly well-bonded. The mandate to increase rubber usage also led to rubberized mix being placed on most surfaces. However, RHMA-G surfacing was limited to 0.20 ft (60 mm) thickness, so there is usually HMA underneath.
- From 2015 to the present: Caltrans adopted the Superpave method for mix design, which generally increased binder contents and increased fatigue performance (24).

The UCPRC has characterized mixes representing each of these time periods. It was decided to use a weighted average performance of these historical mixes to represent the asphalt layer behavior as part of the NMI of the Caltrans network. In particular, the following specific proportions were used based on a rough estimate of historical Caltrans practices and the distribution of project construction dates in the calibration data:

- Before 2000:
 - 50% of the mixes had low binder content and 50% of the mixes had medium binder content.
 - 70% of the projects had bonded asphalt concrete lifts, while 30% had some unbonded lifts.
- After 2000:
 - The surface layer was always RHMA-G, and there was an HMA layer underneath if the total asphalt concrete layer thickness was more than 0.20 ft (60 mm).
 - 90% of the projects had bonded asphalt concrete lifts and 10% had some unbonded lifts.
- The number of projects before and after year 2000 each consists of 50 percent of the total projects.

Table 4.1: List of Mixes Representing Historical Caltrans Asphalt Mixes Used for Calibration

Mix ID	Description	Time Period
WT_17FMH	The mix used in WesTrack Section 17, fine gradation, medium asphalt content (5.4%), high air voids (12%), PG 64-22 binder, crushed alluvial, no RAP, Superpave mix design	Before 2000
WT_03FLH1	The mix used in WesTrack Section 3, fine gradation, low asphalt content, high air voids, PG 64-22 binder, low binder content (4.7%), high air-void content (12%), rushed alluvial, no RAP, Superpave mix design	Before 2000
SP1_J_Hveem	A RHMA-G mix produced in District 4, with blasted basalt aggregate following Hveem mix design, PG 64-16 base binder, 1/2" mix, no RAP, 8% binder content, 6% air-void content, Hveem mix design	After 2000 (RHMA surface)
SP1_A_Hveem	An HMA Type A mix produced in District 3, with PG 64-16 binder, 3/4" alluvial aggregate, no RAP, 5% binder content, 6% air-void content, Hveem mix design	After 2000 (HMA below RHMA)

4.2.2 Non-Surface Layer Materials

The term *non-surface layer materials* refers to those materials below the asphalt concrete layers such as aggregate base, cement-treated base, and subgrade. No mechanical properties of these materials are recorded in the PMS database. The materials selected to represent non-surface layers in the historical Caltrans network for calibration of the overall models for fatigue cracking of the asphalt layers are listed in Table 4.2.

Table 4.2: List of Non-Surface Materials Representing Historical Caltrans Network Used for Calibration

Material Type	Abbreviation	Description	Reference Stiffness MPa (ksi)
Aggregate base	AB	Aggregate Base-Class 2, stiffness based on backcalculation of field project deflection data	310 (45.0)
Subgrade	SG	Clayey sand (SC), stiffness based on R-value correlation. R-value = 23	95 (13.8)
Lean concrete base or cement-treated base	CB	Lean concrete base and CTB-Class A have similar performance, fatigue based on calibrated MEPDG model, stiffness based on backcalculation of field project deflection data	6,000 (870.0)
Old HMA	OHMA	Based on samples of old HMA layers in multiple locations with ages between 5 and 55 years, stiff but has low fatigue resistance	9,108 (1,320.7)
Old PCC	OPCC	Typical PCC	35,000 (5,075.0)
PDR-EA*	PDR-EA	Partial-depth recycled material stabilized with engineering emulsion, fatigue performance based on lab testing of field samples, stiffness based on backcalculation of field project deflection data	1,500 (217.5)
FDR-FA*	FDR-FA	Full-depth recycled material stabilized with foam asphalt, fatigue performance based on HVS test results, stiffness based on HVS and backcalculation of field project deflection data	2,500 (362.5)
FDR-C*	FDR-C	Full-depth recycled material stabilized with cement, fatigue performance based on HVS test results, stiffness based on HVS and backcalculation of field project deflection data	7,500 (1,087.5)

* Historical materials used for calibration of new asphalt pavement and rehabilitation models. These materials were updated to reflect more recent practice after calibration of the overall models was completed, and the updated stiffnesses are shown in Table 5.2.

4.3 N-AB: New Flexible Pavements with Aggregate Base

This section presents the details of the new approach using new asphalt pavement with aggregate base (N-AB) as an example. Similar procedures were used for all other sub-networks.

4.3.1 Sensitivity of CalME Fatigue Cracking Model

To evaluate the sensitivity of the *CalME* fatigue cracking model to various inputs, a batch of *CalME* runs were made using the full factorial of the following variables:

- Surface type: material type of asphalt concrete surface, see mixes listed in Table 4.1 and Table 4.3. The mixes were selected to represent a large range of performance regardless of when they were produced.
- Asphalt concrete thickness: combined thickness of the structural asphalt concrete layers including HMA and RHMA-G
- Traffic volume: traffic index (TI) for 10 years
- Bonding condition between different asphalt concrete lifts: either bonded or unbonded
- Base thickness: thickness of the aggregate base layer
- Subgrade type: unified soil classification of the subgrade
- Climate zone: climate designation based on the Caltrans pavement climate region map

The batch run factorials are listed in Table 4.4.

Table 4.3: List of Additional Mixes Used for Sensitivity Study

Mix ID	Description	Time Period
WT_16FLH2	HMA mix with PG 64-22 binder, fine gradation, low binder content (4.7%), high air-void content (12%), Fine Crushed Alluvial from Dayton Nevada, no RAP, Superpave mix design	Before 2000
RHMA_R21	RHMA-G mix with PG 64-16 base binder, 1/2" crush river gravel, no RAP, 7.5% binder content, 9% air-void content, Hveem mix design	Between 2000 and 2015
RHMA_GR	RHMA-G mix with PG 64-16 base binder, 1/2" blasted basalt from Vallejo, no RAP, 8.3% binder content, 6% air-void content Superpave mix design	After 2015
HMA_GR	HMA mix with PG 64-22 binder (PG+X Mix J), 3/4" crushed river gravel from Sacramento, 15% RAP, 5.3% binder content, 7% air-void content, Superpave mix design	After 2015
SP1_A_SP	HMA Type A mix with PG 64-16 binder, 3/4" alluvial from Sacramento, no RAP, 5.5% binder content, 6% air-void content, Superpave mix design	After 2015

The sensitivity plot for these inputs is shown in Figure 4.1, which indicates the effects of various inputs on the cracking performance, one at a time. Overall, it suggests that the explanatory variables for this structure type include surface type, traffic volume, asphalt-bound-layer bonding condition, and asphalt concrete thickness. Relatively speaking, the cracking performance is not sensitive enough to base thickness, subgrade type, or climate zone to consider in the calibration of the transfer function, although these variables do need to be considered in project-level design.

Table 4.4: Sensitivity Study Factorial for Cracking in New Flexible Pavements with Aggregate Base

Variable	Abbreviation	Levels
Surface type	<i>Surface type</i>	All mixes listed in Table 4.1 and Table 4.3 except mix SP1_J_Hveem
Asphalt concrete thickness	<i>acthickness</i>	0.4 ft (120 mm), 0.6 ft (180 mm), 0.9 ft (270 mm)
Traffic volume	<i>ti10</i>	6, 8, 10, 12
Asphalt bound layer bonding condition	<i>bonding</i>	bonded, unbonded
Base thickness	<i>basethickness</i>	Thin (0.5 ft), medium (1.0 ft), thick (1.5 ft)
Subgrade type	<i>subgradetype</i>	CH, SC, GP
Climate zone	<i>climatezone</i>	CC (Central Coast), D (Desert), HD (High Desert), HM (High Mountain), IV (Inland Valley), LM (Low Mountain), NC (North Coast), SC (South Coast), SM (South Mountain)

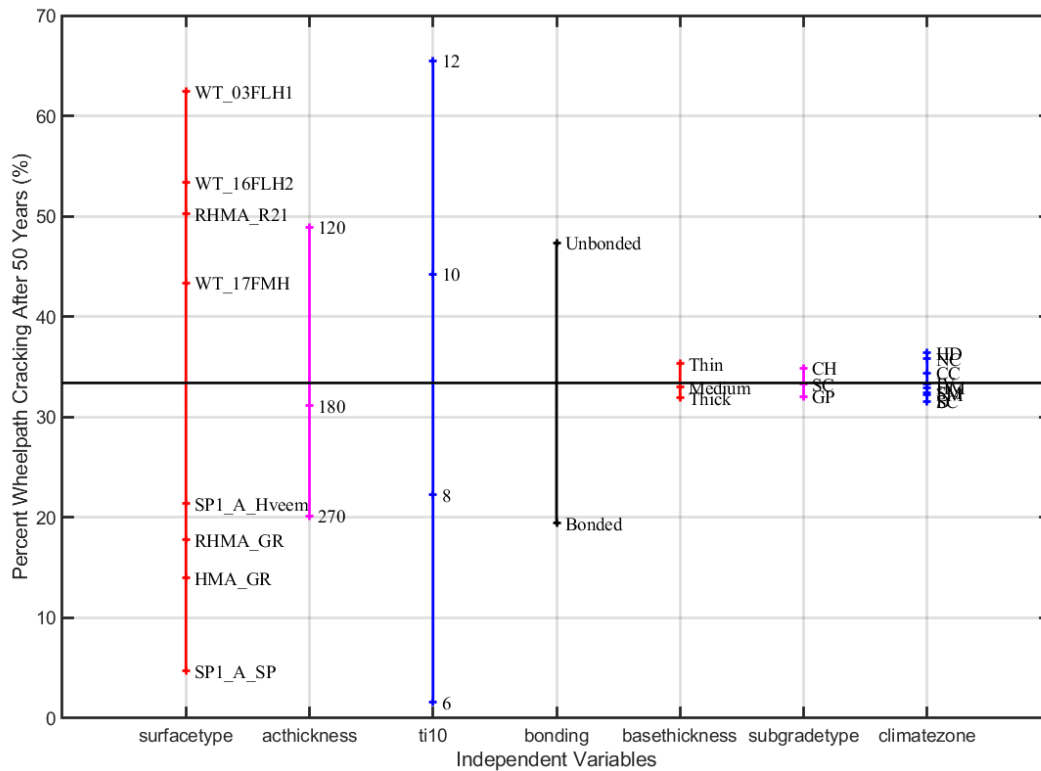


Figure 4.1: Sensitivity of CalME fatigue cracking model prediction to various inputs.

4.3.2 Calibration Cells

Based on the sensitivity study, the PMS data were divided into calibration cells based on *acthickness* and *ti10*. In other words, for each unique combination of *acthickness* and *ti10*, a series of *CalME* runs was conducted for the different combinations of *surfacetype* and *bonding* identified for the different historical periods. This allowed calculation of the median network damage following the weighted average approach outlined in Section 4.2.1. For each calibration cell, the network median inputs (NMI) needed to be determined. The value for the general NMI is described in Section 4.2. The inputs specific to the N-AB network are discussed below.

4.3.3 Specific Network Median Input

As mentioned in Section 4.2, *CalME* inputs include structure (layer materials and thicknesses), traffic (spectrum and volume), and climate (climate zone). The NMI for materials and bonding conditions are described in Section 4.2. This section describes the NMI for layer thickness, traffic, and climate. Note that these inputs are specific to each calibration cell. The structure used for this sub-network includes the following layers:

- Up to two layers of asphalt concrete surface materials
- Aggregate base (AB)
- Subgrade (SG)

Note that there is no subbase layer. Based on the fact that *CalME* predictions are not sensitive to AB layer thickness, to simplify the *CalME* simulations a decision was made to not include the subbase, and to treat the aggregate subbase (ASB) as AB. The thicknesses of HMA surface layers and traffic volume depend on the calibration cell. The other components of the NMI are listed in Table 4.5. Although an actual climate region can be used for each individual virtual project, it was decided to use the Inland Valley to reduce the number of *CalME* runs since *CalME* simulation results were not found to be very sensitive to climate region.

Table 4.5: Network Median Inputs Specific to the N-AB Network

Variable	Network Median Input
Aggregate base thickness	1.0 ft (300 mm)
Climate region	Inland Valley
Traffic load spectrum	Group2

4.3.4 Determination of Critical Damage ω_{50}

Once the damage history for each calibration cell was calculated using *CalME*, the critical damage ω_{50} was calculated for each individual virtual project by finding the calculated damage corresponding to its t_{50} . The plan was to then review the correlation between ω_{50} and traffic volume as well as surface layer thickness to identify any trends. However, this approach was found to lead to high sensitivity between ω_{50} and traffic volume. It was therefore decided to use the recorded *ti10* value only as a guide.

Specifically, the *ti10* value for each of the virtual projects was assumed to be unknown and therefore it could have been any of the values recorded in the PMS database. In other words, the initial step was to pool the PMS data for the same surface layer thickness without considering traffic volume. This allowed identification of a trend line for the correlation between calibrated ω_{50} and *acthickness* by adjusting the traffic volume for each *acthickness*. The hope was that the distribution of the resulting traffic volume would match that of the recorded values. This process is further illustrated in Figure 4.2.

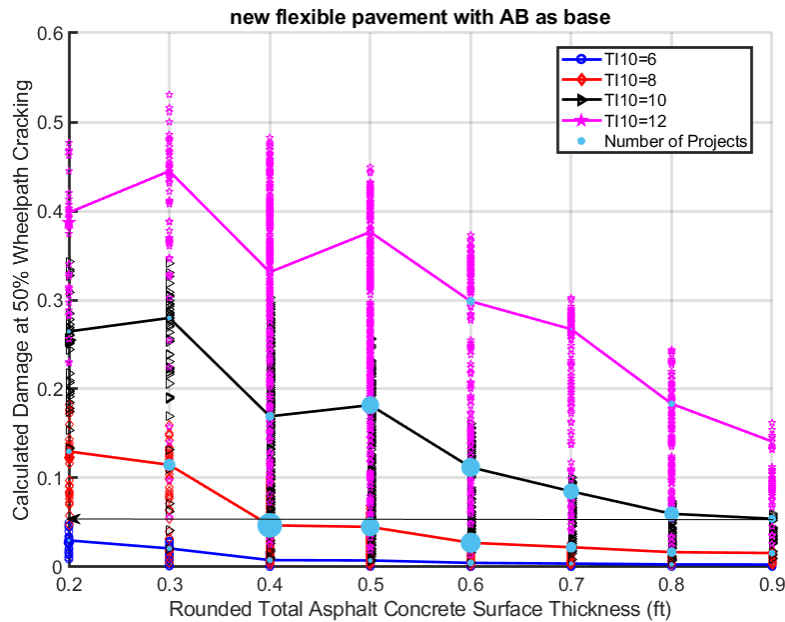


Figure 4.2 Determination of critical damage ω_{50} (i.e., the damage corresponding to 50% cracking).

As shown in Figure 4.2, the values of ω_{50} were determined for each *acthickness* and each assumed *ti10*. The size of the large solid circles indicates the amount of data with recorded *ti10* that matches the assumed value. If the recorded *ti10* values were accurate, the ω_{50} for each *acthickness* with the largest solid circles should be used. Since it was known that there are a number of assumptions in traffic measurements and assignment of traffic to different lanes in the historical traffic data, *ti10* values were believed to only be approximately accurate. Therefore,

the calibrated ω_{50} was only required to approximately pass through the solid circles. For this particular calibration, a constant value of 0.06 was selected for ω_{50} , as indicated by the arrow in the plot, because it was approximately near the center of gravity of the circles.

4.3.5 Initial Selection of Shape Parameter β

The distribution of the observed shape parameters for this calibration of new asphalt pavement with aggregate base is shown in Figure 4.3, in which the cumulative distribution functions are grouped by total asphalt concrete layer thickness. The shape parameter β is determined by reviewing the distribution of the observed shape parameter $\beta_{observed}$, as explained in Section 3.3.2. As shown in Section 2.4.2, β is negative and should have a higher absolute value than the $\beta_{observed}$ so that the contribution to WPV of the variability of the most significant mechanistic design inputs can also be considered in the Monte Carlo simulation. If WPV is only accounted for by calibrating the shape parameter β for an entire project to a single value, then project-specific variability cannot be accounted for properly in a Monte Carlo simulation. Based on Figure 4.3, the most extreme values of the observed shape parameter $\beta_{observed}$ is approximately -30. This value was selected for the transfer function (i.e., Equation (8)) as a starting point to assess the contributions of the variability of mechanistic inputs to WPV.

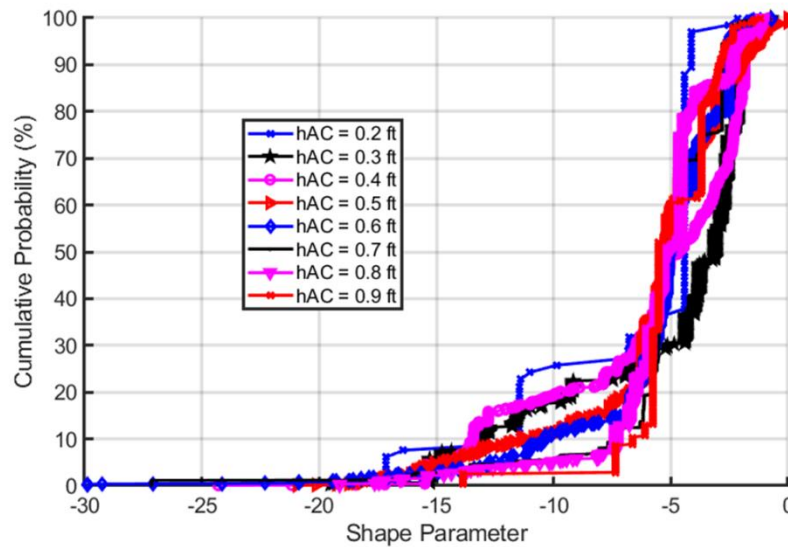


Figure 4.3: Distribution of observed shape parameter $\beta_{observed}$ for each asphalt concrete surface thickness.

4.3.6 Determination of Within-Project Variability

As shown in Figure 4.3, the median value of the observed shape parameter $\beta_{observed}$ is about -5.0. The next step was to evaluate whether the use of the estimated median distributions of important mechanistic variables would result in the observed within-project variability (WPV) (i.e., the same result as using a fixed $\beta_{observed}$ of about -5.0).

In *CalME*, WPV with respect to wheelpath cracking performance is accounted for by sampling from the distributions of these three sets of variables for each layer:

- Thicknesses
- Stiffnesses
- Fatigue resistance

These variables were selected because their variance is known to have a large effect on WPV. Distributions for each of these were available from previous research. A parametric study further showed that the cracking performance predicted by *CalME* is most sensitive to the properties of the asphalt concrete surface layer. It was therefore decided to only vary the properties of the asphalt concrete layers when checking whether the observed equivalent median shape parameter from simulations matched the observed shape parameter.

The typical variance of total asphalt layer thickness came from data collected from cores and ground-penetrating radar stored in the Caltrans *iGPR* tool. Fourteen different projects built between 2000 and 2010 were analyzed, totaling 33 miles total length of paving. The conclusion was that the thickness variability found in the these projects matched those identified from the literature when developing *CalME* 2.0.

The typical variance of HMA stiffness and the fatigue damage equation parameter *A* was determined for each mix type and PG grade from laboratory flexural fatigue testing of 35 total HMA and RHMA-G mixes. Small changes were made to the mix stiffness and fatigue variability factors in *CalME* 2.0 based on this reevaluation. The mix types considered are shown in Table 4.6.

Table 4.6: Summary of Asphalt Mixes Used to Estimate Variability of Mix Stiffness and Fatigue Parameter

Mix Type	Field Mix Field Compact	Field Mix Lab Compact	Lab Mix Lab Compact	Field Mix Plant Compact	Total
RHMA-G	3	4	6	1	14
HMA	6	5	10	0	21

A batch of Monte Carlo simulations was run with different combinations of asphalt layer thickness, stiffness, and fatigue parameter variabilities close to the values estimated as described above to evaluate whether the resulting equivalent shape factors were similar to the median observed shape parameter. Three combinations were found to result in observed shape parameters that are close to -5.0, as can be seen in Table 4.7. Based on these results, the first set was selected for use in the calibration WPV because these values are closest to those observed in the evaluation of thickness and asphalt properties described above.

Table 4.7: Variabilities of Asphalt Concrete Layer Properties and the Resulting Shape Parameter

No.	Thickness COV	Stiffness SDF*	SDF* for Fatigue Parameter A	Resulting Shape Parameter β
1	0.07	1.20	1.35	-5.11
2	0.10	1.20	1.05	-5.17
3	0.10	1.20	1.25	-4.95

* SDF of a variable x is defined as the $e^{cov(\ln(x))}$

4.3.7 Determine the Between-Project Variability Factor

The cumulative distribution functions of relative performance factor (RPF) defined in Equation (10) for the N-CB sub-network is shown in Figure 4.4. As explained in Section 2.5.2, this chart can be used to determine the factors needed to account for between-project variability.

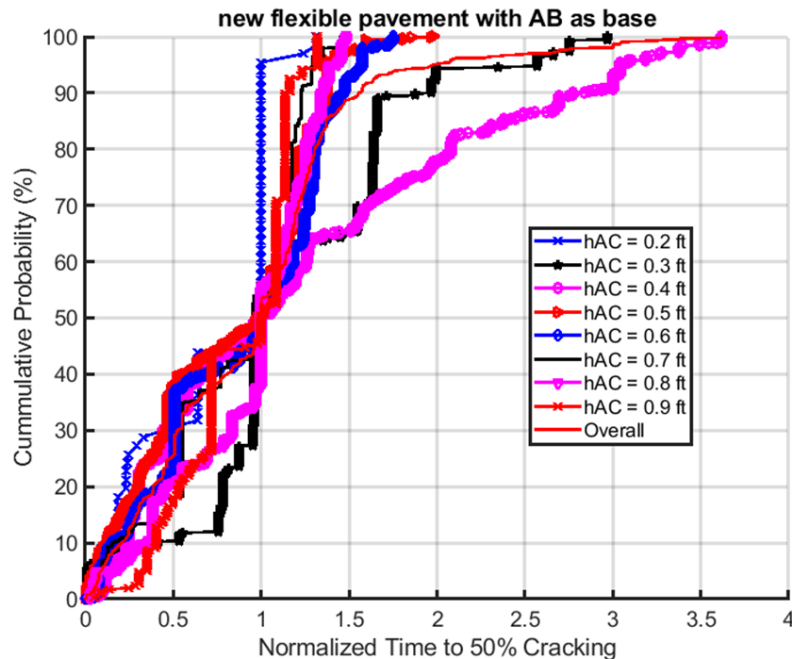


Figure 4.4: Distribution of relative performance factor for each asphalt concrete surface thickness.

Figure 4.4 shows that the CDF functions of RPF for different asphalt concrete surface thicknesses are generally similar. It is therefore believed that the overall CDF function can be used to account for the between-project variability (BPV). As shown in the figure, the CDF function is roughly a straight line between (0,0) and (1.0, 50%). Based on this observation, various performance multipliers were determined to account for BPV with the desired level of design reliability. They are listed in Table 4.8. Note that these multipliers are applied to the t_{50} predicted by *CalME* using design NMI to arrive at the design life for the given reliability level.

Table 4.8: Performance Multipliers for Different Design Reliability Levels

No.	Design Reliability (%)	Cumulative Probability for Relative Performance Factor (%)	Performance Multiplier
1	95	5	0.10
2	90	10	0.20
3	85	15	0.30
4	50	50	1.0

4.4 Calibration of Existing Transfer Functions for Existing Pavement Types

The transfer functions of the following types of pavements were calibrated following the same approach discussed previously:

- R-FP: Rehabilitation of Flexible Pavements with Asphalt Concrete Overlay
- R-RP: Rehabilitation of Rigid Pavements with Asphalt Concrete Overlay

For these sub-networks, the surface cracking observed is the result of fatigue cracking and reflective cracking combined. There is no way to separate these two types of cracks from each other in the PMS data, so they are treated as the same in the field calibration. The *CalME* model predicts the amount of cracking combined by default.

4.5 Damage Models and Calibration of Cracking Transfer Functions for In-Place Recycling

Damage models and transfer functions for full-depth recycling and partial-depth recycling (PDR) were added to *CalME* 3.0. The damage models of the newly introduced materials are briefly described here. A separate report will document the details of the development of the damage models for FDR-C and FDR-FA based on accelerated pavement testing with the Heavy Vehicle Simulator (HVS).

The transfer functions for FDR and PDR were calibrated using the same approach discussed earlier for flexible pavements. The following PDR and FDR field sections were sampled and tested and had condition surveys performed on them in the summer and fall of 2020. The data from these sections were used to develop estimated statewide median stiffnesses, and the performance data were used to augment the limited amount of data for FDR-C and PDR-FA, which have not been widely used on the Caltrans network to date. A summary of the field sections is shown in Table 4.9.

Table 4.9: Summary of PDR and FDR Field Sections Tested in Summer and Fall of 2020

Field Project	Project Type	Year Constructed	Direction	PM Start	PM End	Dates Sampled	HMA Layer Thickness (ft)	IPR Layer Thickness (ft)	Old HMA Thickness (ft)
UCPRC Test Track	CCPR-FA CCPR-EA	2019	N/A	N/A	N/A	8/31/2020, 9/25/2020	0.20	0.38	-
YOL99	FDR-FA	2008	NB	2.5	3.5	9/3/2020	0.29	0.90	-
MOD139	FDR-FA	2016	SB	20.5	19.5	8/26/2020	0.37	0.65	0.20
COL20	FDR-FA	2002	EB	14.0	15.0	9/9/2020	0.44	0.60	-
MNO270	FDR-FA	2011	EB	6.0	7.0	9/15/2020	0.25	0.63	-
SIE89	FDR-FA	2002	SB	27.0	26.0	9/22/2020	0.31	0.78	-
SB166	FDR-FA	2009	EB	55.0	56.0	9/23/2020	0.49	0.94	-
YOL32B	FDR-PC	2014	WB	1.6	0.0	7/21/2020	0.44	1.10	-
YOL31	FDR-PC	2010	SB	4.0	3.0	7/24/2020, 9/1/2020	0.42	1.29	-
PLU147	FDR-PC	2015	NB	7.5	8.9	8/24/2020	0.33	0.72	-
SIS161	FDR-PC	2016	EB	3.0	4.0	8/27/2020	0.29	0.82	-
PLU36	PDR-EA	2013	EB	6.5	7.4	8/25/2020	0.32	0.29	0.68
YOL84	PDR-EA	2017	SB	13.0	12.0	9/10/2020	0.18	0.28	0.20
YOL84	PDR-EA	2019	SB	6.0	5.0	9/11/2020	0.14	0.36	0.19
INY127	PDR-EA	2017	NB	7.5	8.5	9/14/2020	0.19	0.28	0.18
MNO395	PDR-EA	2018	SB	111.0	112.0	9/16/2020	0.22	0.32	1.10
STA132	PDR-EA	2011	EB	31.0	32.0	9/24/2020	0.20	0.27	0.20
LAK20	PDR-EA	2011	EB	34.0	34.6	9/28/2020	0.30	0.39	0.70
YOL22	PDR-FA	2019	WB	1.5	0.5	7/22/2020	0.16	0.32	0.31
Monterey Road, San Jose	PDR-FA	-	SB	Flintwell Way	3,805 ft South of Flintwell Way	9/2/2020	0.13	0.35	1.42
SON116	PDR-FA	2018	NB	32.2	31.8	9/18/2020	0.17	0.24	0.26

4.5.1 R-PDR-EA: Rehabilitation of Flexible Pavements with PDR-EA

As can be seen in Table 4.9, there were a reasonably large number of PDR-EA sections available for the estimation of stiffness. Review of available data indicated that cement contents on PDR-EA projects may generally be lower than those on PDR-FA projects. The fatigue damage models and transfer functions for PDR-EA have the same form as those for HMA because fatigue damage follows the same basic process. However, the fatigue damage performance is different. The damage model parameters were developed using laboratory flexural fatigue beam specimens taken from as-built pavements.

The permanent deformation damage model for PDR-EA has the same form as that of HMA and is based on repeated simple shear testing of field cores. Rutting is only considered if the layer is within 0.2 ft (60 mm) of the surface of the pavement.

Calibration of the transfer functions followed the same approach discussed previously.

4.5.2 R-PDR-FA: Rehabilitation of Flexible Pavements with PDR-FA

As can be seen in Table 4.9, there were few PDR-FA sections available for the estimation of stiffness. Residual asphalt contents on most California PDR-FA projects seem to be higher than on PDR-EA based on available information. The fatigue damage models for PDR-FA have the same form as those for HMA because fatigue damage is expected to generally follow the same basic process of loss of stiffness with repeated tensile strains. The statewide median stiffness for PDR-FA was also based on that of FDR-FA from both HVS data and the backcalculation of field sections, and the few PDR-FA projects shown in the table. FDR projects will typically have denser gradations than PDR projects because of somewhat higher fines contents. As more data are collected, particularly on PDR-FA projects, specific data from PDR-FA projects will be used to determine the median value for use in *CalME*.

Because of the lack of performance data in the pavement management system, the calibrated transfer function for fatigue cracking of PDR-FA is being used until more performance data become available.

The permanent deformation damage model for PDR-FA has the same form as that of HMA and was assumed to be the same as RHMA-G because no other information is currently available. Rutting is only considered if the layer is within 0.2 ft (60 mm) of the surface of the pavement.

4.5.3 *R-FDR-FA: Rehabilitation of Flexible Pavements with FDR-FA*

The fatigue models for FDR-FA have the same form as those for HMA because fatigue follows the same basic process. However, it has been observed on HVS test sections and in the field that the fatigue damage performance is different from HMA in that distinct cracks do not form at the bottom of the FDR-FA layer and then propagate upward. Instead, the discreet bonding points where droplets of foamed asphalt hold the particles together, essentially acting as “spot welds,” break under repeated tensile strains, and lead the FDR layer to behave like an unbound aggregate layer. The damage model parameters were developed using HVS test results from FDR-FA sections. The statewide median stiffness for FDR-FA was developed using HVS data and field section backcalculated stiffnesses.

Calibration of the fatigue transfer function followed the same approach discussed in previously.

The permanent deformation damage model for PDR-FA has the same form as that of HMA and was assumed to be the same as RHMA-G because no other information is currently available. Rutting is only considered if the layer is within 0.2 ft (60 mm) of the surface of the pavement.

4.5.4 *R-FDR-C: Rehabilitation of Flexible Pavements with FDR-C*

The fatigue models for FDR-C use a model developed for non-asphaltic materials described in a tech memo about the *CalME* standard materials library (6). The damage model parameters were developed using HVS test results from FDR-C sections. The statewide median stiffness for FDR-C was developed using HVS section and field section backcalculated stiffnesses; the field sections used for this are shown in Table 4.9.

Calibration of the fatigue cracking transfer function followed the same approach discussed previously and used the limited number of field sections shown in Table 4.9 and the few sections found in the Caltrans network data.

FDR-C does not have a permanent deformation damage function because it has not been observed to exhibit rutting.

4.5.5 *Cold Central Plant Recycled (CCPR) Materials*

The stiffnesses, damage functions and transfer functions for CCPR materials are assumed to be the same as those of the corresponding types of stabilized FDR and PDR materials.

4.6 Damage Models and Calibration of Transfer Functions for Pavements with Cemented Bases

4.6.1 N-CB: New Flexible Pavements with Cemented Base

The damage models for cemented base materials, CTB and LCB, were taken from research by Li et al. (25). These models replace the earlier models in *CalME* 2.0, which were developed from HVS information for materials with less cement stabilizer (14), as described in the standard materials library tech memo (6). See Section 4.6.3 for details of the updated models.

Calibration of the transfer functions followed the same approach discussed previously. Care was taken to consider the fact that Caltrans specifications for CTB have evolved over the years. The primary failure mechanism identified in the performance data for these materials was seen to be the reflection of shrinkage cracks from the cemented materials upward through the HMA, not fatigue damage of the cemented materials. It should be noted that the Caltrans PMS performance data does not clearly identify this type of cracking.

4.6.2 Cement-Stabilized Subgrade and Lime-Stabilized Subgrade

The fatigue models for cemented and lime-stabilized subgrade materials, CSS and LSS, were taken from the paper by Li et al. (25). These models replaced the earlier models in *CalME* 2.0, which had been developed from HVS information for materials with less cement stabilizer, as described in the standard materials library tech memo (6). These have the same model form as for cement-stabilized bases. These new models correct problems with unreasonably aggressive damage seen with the previous models. See Section 4.6.3 for details of the updated models.

The transfer functions for pavements with these materials are the same as those for other pavement types with unstabilized subgrades, with the increased stiffness of these materials affecting the strains in those pavements and therefore their performance. Performance data is not available for pavements with these types of subgrades.

4.6.3 Damage and Curing Models

Cemented materials are subjected to three mechanisms that affect layer stiffness: top-down crushing damage, bottom-up fatigue damage, and curing.

4.6.3.1 Bottom-up Fatigue Damage

Bottom-up fatigue damage is driven by the tensile stress at the bottom of the cement-stabilized layer. The model for fatigue life is:

$$\log_{10}(N_{ft}) = k_1 \cdot \left(\frac{k_3 \frac{\sigma_t}{MOR}}{k_2} \right) \quad (11)$$

where N_{ft} is the fatigue life, k_1 , k_2 , and k_3 are model parameters, σ_t is the tensile stress in the transverse direction, and MOR is the current modulus of rupture after accounting for curing. Once the fatigue life is determined for each axle load, the fatigue damage is accumulated following Miner's Law:

$$\omega_{ft} = \sum_i \frac{N_i}{N_{fti}} \quad (12)$$

where ω_{ft} is the fatigue damage, N_i is the number of passes for the i^{th} axle load, and N_{fti} is the crushing life corresponding the i^{th} axle load. The stiffness is then reduced by the following ratio:

$$SR_{fatigue} = 1 - \frac{m_2}{\ln(UCS_{28,psi})} \cdot \left(\frac{1}{2} - \frac{1}{1 + \exp[\sinh(n_2 \cdot \omega_{ft})]} \right) \quad (13)$$

where SR_c is the stiffness ratio due to crushing, m_2 and n_2 are model parameters that depend on the material type, $UCS_{28,psi}$ is the 28-day UCS in psi, and ω_{ft} is the crushing damage. Damage is updated after every set of loads following the incremental-recursive procedure in *CalME*.

4.6.3.2 Top-Down Crushing Damage

The top-down crushing damage in cement-stabilized materials is driven by vertical compressive stress. The model for the crushing life is:

$$\log_{10}(N_{fc}) = k_4 \cdot \log_{10} \frac{\rho}{wc_{opt}} \cdot \left(1 - \frac{\sigma_c}{k_5 \cdot UCS} \right) \quad (13)$$

where N_f is the crushing life, k_4 and k_5 are model parameters that depend on the material type, ρ is the maximum dry density of the material in lbs/ft^3 , wc_{opt} is the optimum moisture content in percent, and σ_c is the vertical compressive stress at the top of the layer. UCS is the current unconfined compressive stress after accounting for curing. Once the crushing life is determined for each axle load, the crushing damage ω_c is accumulated the same way as fatigue damage, following Miner's Law, but damage is updated after every set of loads following the incremental-recursive procedure in *CalME*. The stiffness is then reduced by a ratio $SR_{crushing}$, which is determined using the same equation as fatigue damage.

4.6.3.3 Curing

Curing in cement-stabilized materials only depends on time. At any given time of the service life, the material strength is increased from the 28-day value by a ratio determined by the following equation:

$$c_{strength} = p_1 \frac{1 - \frac{1}{1 + \frac{t-t_0}{p_2}}}{1} \quad (14)$$

where $c_{strength}$ is the curing factor for strength, p_1 and p_2 are model parameters, t is the current time in months, and t_0 is the initial time at which the strength (either UCS or MOR) was determined. This factor is used to calculate current UCS or MOR:

$$UCS = UCS_{28} \cdot c_{strength} \quad (15)$$

$$MOR = MOR_{28} \cdot c_{strength} \quad (16)$$

where UCS_{28} is the 28-day UCS and MOR_{28} is the 28-day MOR. Although not used in *CalME*, the layer stiffness of cement-stabilized material can be correlated to UCS through the following equation:

$$E_f = 15229 \times UCS^{0.35} \quad (17)$$

where E_f (psi) is the flexural stiffness. Accordingly, the curing factor for stiffness can be determined using the following equation:

$$c_{stiffness} = c_{strength}^{0.35} \quad (18)$$

4.6.4 Combining Damage and Curing Models

At any given time during the service life, the curing factors are first determined based on the current time. The stiffness is updated using the following equation:

$$E = E_{28} \cdot c_{stiffness} \cdot SR_{fatigue} \cdot SR_{crushing} \quad (19)$$

In the meantime, both UCS and MOR are updated using Equations (15) and (16) respectively. The vertical stress needed to drive crushing damage and the tensile stress needed to drive fatigue damage are then calculated for each axle load. The fatigue life and crushing life are then calculated using the updated UCS and MOR.

4.7 Summary of the Calibration Results

A summary of the field calibration results is listed in Table 4.10. The within-project variability for all sub-networks are the same as those listed in Table 4.7.

Table 4.10: Summary of Calibration Results for Different Sub-Networks

Abbreviation	Critical Damage ω_{50}	Shape Parameter β	Performance Modifier for 95% Reliability
N-AB	0.06	-30.0	0.10
N-CB	$0.0007 \cdot e^{0.0188 \cdot hAC_mm}$ minimum 0.01, maximum 0.10	-90.0	0.23
R-FP	0.11	-90.0	0.20
R-RP	0.03	-90.0	0.20
R-PDR-EA	0.03	-30.0	0.10
R-FDR-FA	0.06	-30.0	0.32
R-FDR-C	0.03	-90.0	0.20

5 DESIGN WITH NEW FIELD CALIBRATION

5.1 Design Inputs

To use the field calibrated models to do pavement design, a different set of statewide network median inputs (NMI) is needed to represent the condition of the pavements under design. The underlying assumptions for using the field-calibrated models are that the transfer functions, and the between-project and within-project variabilities remain the same.

The design NMIs were determined by reviewing testing results from current Caltrans specifications and practices and they should be revisited regularly to keep them up to date. Among the *CalME* inputs, traffic and climate are predetermined by the project location. The layer types are selected by the user and then thicknesses are determined by trial and error or by an optimization algorithm. The properties of the materials used in the structural layers are the NMI, which come from the standard materials library (SML) embedded in *CalME*.

5.1.1 Hot Mix Asphalt Materials

The new hot mix asphalt materials available for design are divided into several sub-groups based mainly on the binder type performance grade, as listed in Table 5.1. The properties of these materials were determined by reviewing all the available test data at the UCPRC for mixes in each sub-group and selecting the one that exhibited the median performance in *CalME* simulations within each sub-group. Some minor adjustments were made to the fatigue resistance properties to align the cracking performance of these mixes with what has been observed with experience.

For old asphalt concrete, only one material is used to represent the statewide median. This is the same as the one used for field calibration (see Table 4.2). The material is named “2020 Standard Old HMA.”

Table 5.1: Statewide Median New Asphalt Concrete Materials for Design

No.	Mix Type	Binder Type	RAP Content	Material Name
1	HMA Type A	PG 64-XX	No more than 15%	2020 Standard HMA Type A Mix with PG 64-XX Binder and up to 15% RAP for non-PRS ¹ Projects
2	HMA Type A	PG 70-XX	No more than 25%	2020 Standard HMA Type A Mix with PG 70-XX Binder and up to 15% RAP for non-PRS Projects
3	HMA Type A	Polymer modified	Not specified	2020 Standard HMA Type A mix with polymer-modified binder for non-PRS Projects ²
4	HMA Type A	Not specified	Between 15 and 25%	2020 Standard HMA Type A Mix with 25% RAP for non-PRS Projects ³
5	HMA Rich Bottom	Not specified	Not specified	2020 Standard Rich Bottom Mix for non-PRS Projects ⁴
6	RHMA-G	Rubberized asphalt	Not specified	2020 Standard RHMA-G for non-PRS Projects

Notes:

¹ PRS = performance-related specifications

² All mixes in the database were PG 64-28PM.

³ Primarily PG 64-16 mixes in the database; there were not enough mixes to divide into PG types.

⁴ Primarily PG 64-10 and PG 64-16 mixes in the database; there were not enough mixes to divide into PG types.

5.1.2 In-Place Recycled Materials

There are three groups of in-place recycled (IPR) materials: full-depth recycled (FDR), partial-depth recycled (PDR), and cold central plant recycled (CCPR). There are rules in *CalME* for the use of each of these types of materials in different types of structures. The materials available for design are listed in Table 5.2. As indicated there, the materials used for design are the same as the ones used for calibration, for those that were present in the historical network, except they are slightly stiffer. This was decided based on expected improvements in the construction quality of these IPR materials compared with the test sections used for calibration. The variabilities of the stiffness for the materials are represented by the standard deviation factors (SDF) shown in Table 5.2, which were estimated from measurements taken on the field test sections shown in Table 4.8.

Table 5.2: Statewide Median In-Place Recycled Materials for Design

No.	Material Type	Reference Stiffness (MPa/ksi) and SDF*	Material Name	Notes
1	FDR-N	310/45 (1.2)	2020 Standard FDR-N	Same as AB Class 2
2	FDR-FA	3,000/435 (1.7)	2020 Standard FDR-FA	Same as the material for calibration except slightly stiffer
3	FDR-C	10,000/1,450 (1.5)	2020 Standard FDR-C	Same as the material for calibration except slightly stiffer
4	PDR-EA	1,800/261 (1.3)	2020 Standard PDR-EA	Same as the material for calibration except slightly stiffer
5	PDR-FA	1,800/261 (1.3)	2020 Standard PDR-FA	Same as PDR-EA
6	PDR/CCPR-EA	1,800/261 (1.3)	2020 Standard PDR/CCPR-EA	Same as PDR-EA
7	PDR/CCPR-FA	1,800/261 (1.3)	2020 Standard PDR/CCPR-FA	Same as PDR-EA
8	CCPR-EA	1,800/261 (1.3)	2020 Standard CCPR-EA	Same as PDR-EA
9	CCPR-FA	1,800/261 (1.3)	2020 Standard CCPR-FA	Same as PDR-EA
10	CCPR-C	10,000/1,450 (1.3)	2020 Standard CCPR-C	Same as FDR-C in stiffness but with the same variability as other PDR layers

* SDF = standard deviation factor of variable x is calculated as $e^{cov(\ln x)}$, where cov is the coefficient of variation; SDF is used with lognormal distributed variable, and is similar to the standard deviation for normally distributed variables.

5.1.3 Cement-Stabilized Materials

Cemented materials include CTB (Class A and B), LCB, CTPB, LSS (lime-stabilized soil), and CSS (cement-stabilized soil), which are referred to in the software as treated subgrade (TS). The NMI for these materials are listed in Table 5.3. Note that the LSS and CSS have significantly higher variation in stiffness than other materials based on limited field observations.

Table 5.3: Statewide Median Cement-Stabilized Materials for Design

No.	Material Type	Reference Stiffness (ksi) and SDF*	Material Name
1	CTB-Class A	Same as LCB	2020 Standard CTB-Class A (Same as LCB)
2	CTB-Class B	$57\sqrt{UCS(psi)}$ (1.2)	2020 Standard CTB-Class B (designer inputs UCS)
3	LCB	1,313 (1.2)	2020 Standard LCB
4	LSS	$0.124 \cdot UCS(psi) + 10.0$ (2.5)	2020 Standard LSS (designer inputs UCS)
5	CSS	$1.20 \cdot UCS(psi)$ (2.5)	2020 Standard CSS (designer inputs UCS)

* SDF = standard deviation factor of variable x is calculated as $e^{cov(\ln x)}$, where cov is the coefficient of variation; SDF is used with lognormal distributed variable, and is similar to the standard deviation for normally distributed variables

5.1.4 Other Materials

The statewide medians for other materials are the same as those listed in the standard materials library report (6).

5.1.5 Updated Default Subgrade Soil Stiffnesses and Methods for Estimating

The default stiffnesses (resilient modulus) for subgrade soils based on Unified Soil Classification (USCS) were updated based on an extensive literature review and included in the standard materials library used by *CalME*. The default stiffnesses are shown in Table 5.4. All the available results found in the literature review were also used to develop regression equations relating the following test methods to triaxial or backcalculated subgrade stiffnesses:

- California Bearing Ratio (unsoaked)
- California Bearing Ratio (soaked)
- Dynamic Cone Penetrometer (DCP)
- R-value

The R-value test had the least amount of information available to correlate with subgrade resilient modulus.

5.1.6 Minimum Required Aggregate Base Thicknesses

The *CalME* subgrade rutting models have not been calibrated for pavement structures consisting of full-depth HMA placed directly on subgrade, and most of the subgrade rutting calibration data was for flexible pavements with aggregate base (AB) or AB and aggregate subbase (ASB) layers between the HMA and the subgrade. To reflect the need for adequate construction platforms for placement and compaction of HMA, and to also reflect the limited amount of subgrade rutting data used for the calibration, a study was conducted to determine minimum thickness requirements for AB based on subgrade soil classification. The resulting minimum base thicknesses are shown in Table 5.4. A warning has been included in *CalME 3.0* when minimum thicknesses are not included in the design.

Table 5.4: Default Subgrade Stiffnesses and Minimum Aggregate Base Thicknesses Based on USCS Soil Classification Included in CalME

USCS Soil Class	Default Stiffness		Minimum Thickness for AB Class 2 (Stiffness = 28 ksi or 193 MPa)		
	M _r (ksi)	M _r (MPa)	t (ft)	t (mm)	t (inch)
GW	38	262	0	0	0
GP	29	200	0	0	0
GM	30	207	0	0	0
GC	20	138	0.35	105	4
SW	21	145	0.35	105	4
SP	17	117	0.35	105	4
SM	21	145	0.35	105	4
SC	14	97	0.35	105	4
ML	11	76	0.50	150	6
CL	9	62	0.50	150	6
MH¹	6	41	0.75	225	9
CH^{1,2}	4	28	1.00	300	12

Notes:

¹ An alternative platform can be designed using aggregate subbase (ASB) with known stiffness combined with a minimum 0.35 ft (105 mm, 4 inch) lift of AB Class 2 on top of it as described in the Appendix; alternatively, subgrade stabilization should be considered.

^{1,2} The engineer should perform a soils expansion analysis based on laboratory testing of the subgrade soil.

5.2 Design Procedure

Pavement design using *CalME* 3.0 is a trial-and-error process. The designer comes up with a structure (layer materials and thicknesses) and *CalME* will predict whether it will reach the failure threshold within the design life. *CalME* looks up the proper field calibration parameters for the given pavement design and applies them automatically. The following are some important notes to keep in mind:

- *CalME* has a built-in design reliability of 95%, which was determined by Caltrans.
- Only the Monte Carlo simulations account for the within-project variability.
- The between-project variability is accounted for by amplifying the traffic intensity. For example, if the design traffic index for an FDR-FA project that should last 20 years is 13.0, *CalME* determines that the performance modifier for 95% design reliability in this case is 0.32 (see Table 4.10). *CalME* then amplifies the traffic intensity by a ratio of $1/0.32 = 3.125$. This equates to an internal design 20-year TI of $13 \cdot 3.125^{0.129} = 15.0$. In other words, the pavement needs to be able to sustain a 20-year TI of 15.0 to have a 95% probability of surviving the 20-year design life with a TI of 13.0.

With the new approach for field calibration, *CalME* 3.0 can accommodate the use of performance-related specifications (PRS) for asphalt concrete mixes. This is achieved by increasing the performance modifier to account for the smaller variability in the performance of the as-built mixes. It should be noted that the BPV cannot be completely removed even with PRS.

5.3 Comparison with Empirical Design Results

As a first order check of reasonableness, the pavement designs produced by the calibrated *CalME* 3.0 were compared with the corresponding empirical designs.

Based on the performance data (see for example Figure 3.8), the HMA thicknesses in new flexible pavements with aggregate base in the Caltrans network tend to have been under-designed, and the aggregate base layers tend to have been over-designed. It is therefore generally expected that calibrated *CalME* designs should produce thicker HMA and thinner AB than the R-value method. For new flexible pavements, Caltrans uses the R-value method for empirical design that is implemented in the software *CalFP*, which can be accessed through *CalME*. A comparison between designs from the two methods is shown in Figure 5.1 for a subgrade with R-value of 23, which is typical for soils classified as SC according to the USCS. The pavements have three layers with HMA, aggregate base (AB), and subgrade. The AB thickness is determined by *CalFP* for both methods. Thicker AB layers typically do not have much effect on asphalt fatigue life once a threshold thickness is reached, and the threshold is usually thinner than the AB thickness design using *CalFP*.

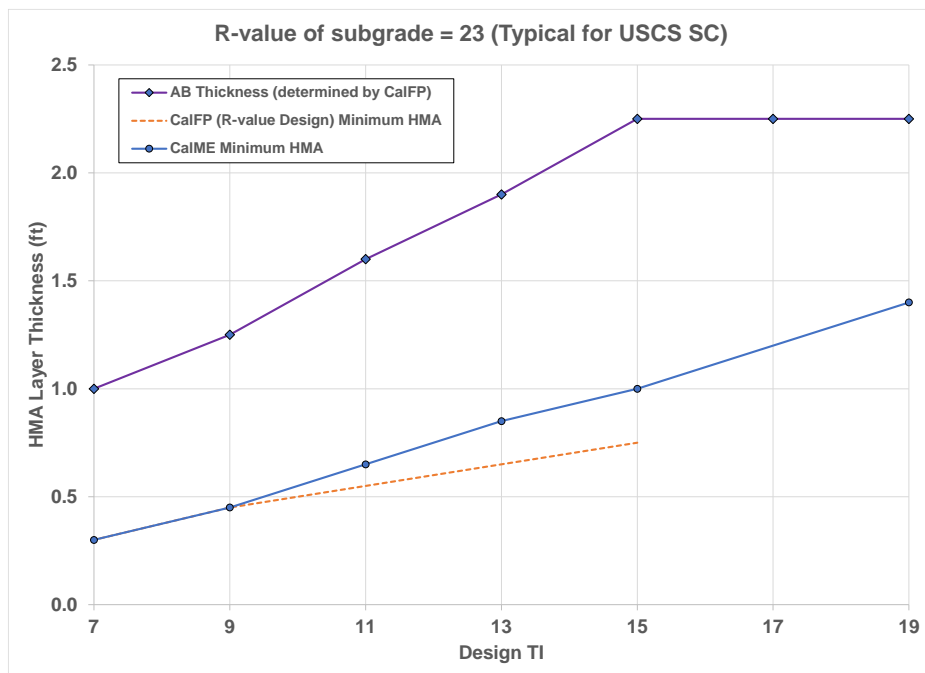


Figure 5.1: Comparison between HMA thickness designs produced by calibrated *CalME* (assuming same base thickness as the R-value method) and R-value method using *CalFP*.

As shown in Figure 5.1, the two methods produced the same HMA thickness design when the design traffic volume is no higher than a TI of 9 (i.e., 1.0 million ESALs). When the design traffic volume is greater than a TI of 9, *CalME* HMA thickness designs are thicker than the empirical design. The difference increases as the design traffic volume increases. For example, *CalME* requires 1.0 ft (300 mm) of HMA for a design TI of 15 (73 million ESALs), compared to 0.75 ft (225 mm) required by the empirical method.

6 SUMMARY AND RECOMMENDATIONS

6.1 Summary

The *CalME* flexible-surface pavement simulation and design software has been completely recoded as a web-based application called *CalME 3.0*. *CalME 3.0* retains the same incremental-recursive damage approach and the same forms for damage models and transfer functions as *CalME 2.0*, which were validated previously using accelerated pavement testing data from Heavy Vehicle Simulator test sections and the WesTrack full-scale traffic closed-circuit track experiment.

Fatigue cracking transfer functions for HMA on aggregate base, cement-stabilized bases, and portland cement concrete have been recalibrated using a new approach for the calibration of mechanistic-empirical pavement design methods. The method explicitly and separately considers between-project and within-project variability. Between-project variability is the variability of different materials that may be brought to a project by different contractors, and must be considered in design because the designer does not know which contractor and which materials will be used for construction at the time of the design in a design-bid-build (low-bid) project delivery environment. Within-project variability is the variability of construction and site conditions within a single project with the same contractor and same materials used throughout the project. The new approach in *CalME 3.0* permits use of “big data” from pavement management systems by assuming median properties for materials, and calibrating for different structures, material types, traffic levels, and climates. This approach offers better integration with pavement management systems and performance-related specifications. *CalME 3.0* assumes statewide median materials properties, although regional median materials can be characterized in the future.

New damage models and transfer functions have been introduced for in-place recycling materials, including full-depth recycling (FDR) with foamed asphalt plus cement and cement stabilization, and partial-depth recycling (PDR) with emulsified asphalt and foamed asphalt plus cement. The program now has been given the ability to model PDR using cold central plant recycled (CCPR) materials. New damage models have been introduced for cement-stabilized bases and cement-stabilized and lime-stabilized subgrade materials to correct problems with the models in *CalME 2.0*.

The calibration of the fatigue cracking transfer functions, using tens to hundreds of times more data than are used in conventional calibration methods, was successful. A limitation for the calibration was the scarcity of field sections for some materials, primarily full-depth recycling with cement stabilization (FDR-C), partial-depth recycling with foamed asphalt plus cement (PDR-FA), different types of cold central plant recycling (CCPR), and cement-stabilized and lime-stabilized subgrades. There were also some concerns regarding unexpected trends in

cracking performance versus estimated lane-based traffic in the performance data from the PMS, which is thought to be attributable to problems with lane distribution factors for truck traffic.

Minimum aggregate base thicknesses were developed for use in *CalME* 3.0 based on calculations of permanent deformation under construction traffic. Simplified methods were developed for estimating subgrade stiffnesses (resilient modulus) based on dynamic cone penetrometer (DCP) tests, California bearing ratio (CBR) tests, and R-value tests based on an extensive literature review and regression of relationships found in the literature. These methods are intended to supplement measurements of resilient modulus as part of site materials characterization.

6.2 Recommendations

The following recommendations address gaps and challenges identified in the calibration of *CalME* 3.0 and in the addition of new materials and models.

- The calibration should be updated with new data approximately every 3 to 5 years with a focus on new materials that had limited performance data in previous calibrations.
- Because they have implications for future designs, traffic estimates made by earlier methods should be examined in a review of Caltrans traffic data.
- An investigation should be conducted into the use of the Caltrans DIME database for calibrations since the database has the capability to capture as-built construction data that can provide better information regarding materials types, thicknesses, and, potentially, performance-related test results.

REFERENCES

1. Caltrans 2019: California Department of Transportation. 2019. State of the Pavement Report. Division of Maintenance, Pavement Program. dot.ca.gov/-/media/dot-media/programs/maintenance/documents/office-of-pavement-management/sop/2019_sop_report-v2_20200928_adacompliant.pdf
2. Basheer, I., Harvey, J., Hogan, R., Signore, J., Jones, D. and Holland, J. 2010. Transition to Mechanistic Empirical Pavement Design in California. 11th International Conference on Asphalt Pavements, Nagoya, Japan, 81-90.
3. Ullidtz, P., J. Harvey, I. Basheer, D. Jones, R. Z. Wu, J. Lea, Q. Lu. 2010. CalME, a Mechanistic-Empirical Program to Analyze and Design Flexible Pavement Rehabilitation. Transportation Research Record 2153, 143-152.
4. Wu, R. and Harvey, J. 2012. Calibration of Asphalt Concrete Cracking Models for California Mechanistic-Empirical Design (CalME). 7th International Conference on Cracking in Pavements, RILEM, Delft, Netherlands. 20-22 June, pp 537-547.
5. Harvey, J., Lu, Q., Lea, J. D., Ullidtz, P., Wu, R. Z., Basheer, I. 2010 Features of Mechanistic Empirical Asphalt Pavement Models for New Design and Rehabilitation in California. 11th International Conference on Asphalt Pavements, Nagoya, Japan, 91-100.
6. Wu, R., J. Zhou, J. Harvey. 2018. Development of the CalME Standard Materials Library. UCPRC-TM-2014-08. www.ucprc.ucdavis.edu/PDF/UCPRC-TM-2014-08.pdf
7. Ullidtz, P., J.T. Harvey, B.-W. Tsai, and C.L. Monismith. 2006. Calibration of Incremental-Recursive Flexible Damage Models in CalME Using HVS Experiments., in Report prepared for the California Department of Transportation (Caltrans) Division of Research and Innovation, UCPRC-RR-2005-06. 2006, University of California Pavement Research Center, Davis and Berkeley.
8. Jones, D., Harvey, J., and Monismith, C. "Reflective cracking study: Summary report." Davis & Berkeley, CA: University of California Pavement Research Center. UCPRC-SR-2007-01, 2007a.
9. Jones, D., Tsai, B., Ullidtz, P., Wu, R., Harvey, J. and Monismith, C. "Reflective Cracking Study: Second-Level Analysis Report." Davis & Berkeley, CA: University of California Pavement Research Center. UCPRC-SR-2007-09, 2007b.
10. Wu, R-Z. "Finite Element Analyses of Reflective Cracking in Asphalt Concrete Overlays". Doctoral dissertation. Department of Civil and Environmental Engineering, University of California, Berkeley, 2005.
11. Wu, R. Z., J. Harvey and C. Monismith, "A Mechanistic Model for Reflective Cracking in AC Overlays," Journal of the Association of Asphalt Paving Technologists, 2006, pp. 491-534.

12. Ullidtz, P., J. Harvey, B.-W. Tsai, and C. Monismith. 2007. Calibration of CalME models using WesTrack Performance Data, UCPRC-RR-2006-14. California Department of Transportation Division of Research and Innovation Office of Roadway Research.
13. Epps, J., A. Hand, S. Seeds, T. Schulz, S. Alavi, C. Ashmore, C. Monismith, J. Deacon, J. Harvey, R. Leahy. 2002. Recommended Performance-Related Specification for Hot-Mix Asphalt Construction: Results of the WesTrack Project. National Cooperative Highway Research Program Report 455. National Academy of Science, Transportation Research Board, Washington, DC.
14. Thoegersen, F., Busch, C. and Henrichsen, A. "Mechanistic design of semi-rigid pavements - An incremental approach." Fløng, Denmark: Danish Road Institute. (Report 138). 2004.
15. Wu, R. 2008. Calibration of the CalME Rutting Model Using 2000 NCAT Data. UCPRC-TM-2008-04. www.ucprc.ucdavis.edu/PDF/UCPRC-TM-2008-04.pdf
16. Tsai, B. and R. Wu. 2009. Mn/ROAD Case Study Using CalBack and CalME. UCPRC-TM-2008-16. www.ucprc.ucdavis.edu/PDF/UCPRC-TM-2008-16.pdf
17. Ullidtz, P., Mateos, A., Ayuso, J., Harvey, J., Basheer, I. 2010. Simulation of Full Scale Accelerated Pavement Test from CEDEX Using the Californian Predictive Pavement Design System (CalME). 11th International Conference on Asphalt Pavements, Nagoya, Japan, 284-294.
18. Khazanovich, L. D. Tompkins, P. Saxena, R. Wu, E. Coleri, J. Harvey. 2013. Use of the Mechanistic-Empirical Pavement Design Guide and CalME to Mitigate Rutting in Asphalt Overlays of Concrete Pavements. Transportation Research Record: Journal of the Transportation Research Board 2368, pp 36-44.
19. Khazanovich, L., D. Tompkins, R. Wu, J. Harvey. 2013. Investigation and Modification of Available Mechanistic-Empirical Procedures for Reflective Cracking in Asphalt Overlays of Concrete Pavements. Transportation Research Record: Journal of the Transportation Research Board 2368, pp 126-132. DOI: 10.3141/2368-12.
20. Harvey, J., J. Signore, R. Wu, I. Basheer, S. Holikatti, P. Vacura, T. J. Holland. 2014. Integration of Mechanistic-Empirical Design and Performance Based Specifications: California Experience to Date. Proceedings, 12th ISAP Conference on Asphalt Pavements. Raleigh, North Carolina. 1-5 June, 2014. Also published as TRB Circular E-C 189: Application of Asphalt Mix Performance-Based Specifications, At onlinepubs.trb.org/onlinepubs/circulars/ec189.pdf, Volume: Circular E-C 189.
21. Tsai, B.W., J. Signore, C. Monismith. Development of Hot Mix Asphalt Pavement Performance Properties for Long-life Pavement Designs: Caltrans District 2, Interstate-5 Red Bluff and Weed, CA, Summary Report UCPRC-SR-2012-01, UC Pavement Research Center, Davis and Berkeley, CA. 2013. www.ucprc.ucdavis.edu/PDF/UCPRC-TM-2014-04.pdf
22. ARA Inc., ERES Consultants Division. 2004. Guide for Mechanistic-Empirical Design of New and Rehabilitated Pavement Structures; Part 3. Design Analysis; Chapter 3. Design of New and Reconstructed

Flexible Pavements. Final Report, National Cooperative Highway Research Project 1-37A, National Cooperative Highway Research Program, Transportation Research Board, Washington, DC, March. onlinepubs.trb.org/onlinepubs/archive/mepdg/Part3_Chapter3_FlexibleDesign.pdf

23. Lu, Q., J. Harvey. 2008. Investigation of Conditions for Moisture Damage in Asphalt Concrete and Appropriate Laboratory Test Methods. UCPRC-RR-2005-15. www.ucprc.ucdavis.edu/PDF/UCPRC-RR-2005-15.pdf
24. Harvey, J., A. Liu, J. Zhou, J.M. Signore, E. Coleri, and Y. He. 2014. Superpave Implementation Phase II: Comparison of Performance-related Test Results. UCPRC-RR-2015-01. www.ucprc.ucdavis.edu/PDF/UCPRC-RR-2015-01.pdf
25. Li, X., J. Wang, H. Wen, B. Muhunthan. 2019. Field Calibration of Fatigue Models of Cementitious Stabilized Pavement Materials for Use in the Mechanistic-Empirical Pavement Design Guide. Transportation Research Record, Volume 2673, issue: 2, pp: 427-435. journals.sagepub.com/doi/abs/10.1177/0361198118821924

APPENDIX A: PROJECTS USED TO EVALUATE THICKNESS VARIABILITY

Project ID	Length (mi)	HMA Thickness			Project		Base Layer Thickness				Project	
		Average (mm)	Std	CoV (%)	Thickness (mm)	Comments	Material	Average (mm)	Std	CoV (%)	Thickness (mm)	Comments
CAL-4-E-33939-37433(2009)	2.2	198.6	22.7	11.4	152.4	-	-	-	-	-	-	-
CAL-26-E-42530-44344(2005)	1.1	141.5	30.8	21.8	152.4	-	-	-	-	-	-	-
KER-166-E-26443-27014(2010)	1.9	246.0	25.7	10.4	225.6	-	AB	301.3	127.1	42.2	466.3	AB-Class 2
ORA-55-N-20271-20839(2002)	0.3	366.3	12.3	3.3	374.9	(HMA+ATPB)	CTB	84.1	9.5	11.4	149.4	AB-Class 2
ORA-55-N-20839-21317(2002)	0.3	394.3	27.7	7.0	374.9	(HMA+ATPB)	AB	175.2	23.5	13.4	149.4	AB-Class 2
SCL-87-S-2169-6911(2007)	2.5	221.5	20.7	9.4	240.8	(HMA+ATPB)	CTB	186.7	15.5	8.3	137.2	CTB-Class A
SCL-680-S-14162-15884(2010)	1.1	235.6	32.9	13.9	289.6	(HMA+HMA)	CTB	105.3	15.2	14.5	152.4	LTB
SHA-44-E-29010-33326(2007)	2.7	155.5	16.5	10.6	149.4	-	AB	329.0	45.9	13.9	329.2	AB-Class 2
SHA-44-E-43410-45992(2005)	1.6	176.6	27.0	15.3	155.4	-	AB	364.0	39.4	10.8	353.6	AB-Class 2
SHA-89-N-47160-69757(2008)	14.2	136.4	13.3	9.8	152.4	-	AB	187.3	60.5	32.3	213.4	AB-Class 2
SON-12-W-32510-32768(2004)	0.2	170.3	14.9	8.7	249.9	-	CTB	181.6	18.4	10.1	106.7	AS-Class 4
SON-12-W-35343-36067(2010)	0.5	178.5	12.5	7.0	487.7	-	CTB	238.0	18.1	7.6	256.0	AS-Class 3
TRI-299-E-76589-78230(2003)	1.6	223.1	40.8	18.3	179.8	-	-	-	-	-	-	-
TUO-108-E-33648-38233(2007)	2.9	175.2	16.9	9.6	228.6	(HMA+ATPB)	-	-	-	-	-	-
Total Length (mi)	33.0	Median CoV (%)	10.1				Median CoV (%)	12.4				

APPENDIX B: DEVELOPMENT OF DEFAULT SUBGRADE STIFFNESSES AND METHODS OF TESTING TO ESTIMATE SUBGRADE STIFFNESS

B.1 Subgrade Stiffness Estimation

An oft neglected part of pavement design is the subgrade and subbase layers. Not only are these important for the long-term performance of the road, but also for the constructability of the upper layers. Without adequate support the upper layers cannot be compacted to the required density, and construction traffic may damage the supporting layers before the pavement is completed. While *CalME* includes models to handle the long-term performance of the lower layers of the pavement, especially to limit rutting, a simpler approach is needed to ensure an adequate construction platform. This only applies to new construction, not to pavements with existing surface layers. This appendix presents a proposed approach based on the DCP-DN design method. The Dynamic Cone Penetrometer (DCP) has been used worldwide since the 1950s as a tool for determining the strength of the top ~3ft of the unbound granular layers in pavements. The DCP is a very simple tool, involving using a hammer with a known weight and drop height, to drive a cone through the soil, while measuring the depth of penetration after each blow. The penetration rate (abbreviated DN for “DCP Number” in South African literature, hence the DCP-DN method) can be used to determine a strength profile with depth, and is reasonably well correlated with the field California Bearing Ratio (CBR), resilient modulus, unconfined compressive strength, and shear strength of the materials. In the US, this penetration rate is typically abbreviated as DCP Penetration Index or DPI, but it is still reported in mm/blow.

The DCP-DN design method originated in South Africa, where the DCP is widely used, and was based on DCP analysis combined with Heavy Vehicle Simulator (HVS) tests to determine the structural capacity of the pavements. The method was later validated with extensive field observations and is currently used widely within Africa for low-volume road design. The DCP-DN method builds on the long tradition of “cover” based designs, including the Caltrans R-value design, the AASHTO structural number concept and the USACE CBR cover curves, and probably all other empirical design methods. What these methods all have in common is that a certain subgrade requires a certain amount of “cover” to adequately handle the traffic loads, and that better quality materials (e.g., aggregate base compared to imported borrow) contribute more “cover” per unit thickness.

The DCP-DN design method has two differences from other empirical design methods, which are both beneficial if only the design of the lower unbound granular layers in a pavement is considered. The first is that the DCP-DN method uses the overall strength of the unbound layers rather than just a single subgrade measurement, and the second is that the method explicitly relies an additional concept of pavement “balance.” Balance has two components—a type of structure and how well the pavement fits that structure: A deeply balanced pavement is one that has successively stronger/stiffer layers on top of weaker/softer ones, in such a way that the ratio of

stiffnesses between successive layers is not too high. A pavement with shallow balance has a high ratio between the stiffnesses of the respective layers, meaning that the bottom of each layer tends to be in tension, and an inverted structure has weaker layers on stiffer layers. A well-balanced pavement is one that follows the stiffness profile closely (so that the modular ratio remains relatively constant with depth), while average and poorly balanced pavements have progressively different modular ratios with depth.

Balance is important for a construction platform because strength and stiffness are a function of density, and density is a function of compaction energy. Without a good construction platform to act as an “anvil” one cannot impart this energy into the layer being compacted. This implies that the construction platform can only be built using a deeply balanced design from bottom to top. Shallow and inverted designs can generally only be achieved in construction using mechanical stabilization. In addition, it is desired that the structure be well balanced, otherwise some of these concepts are difficult to apply and the calibration of the DCP-DN design method relies on average on well-balanced deep pavement structures. There is also some evidence that the balance number of the pavement influences the exponent in the ESAL calculation with a balance number 40 corresponding to a power of about 4.2 (as traditionally used by Caltrans)—although this is not that important for construction traffic.

The DCP-DN design method correlates performance (in terms of allowable ESALs) to the DSN_{800} number from the DCP test, which is the number of blows to reach a depth of 800 mm. A correction is applied for different moisture in the pavement (wet, moist, optimum, or dry). To be conservative, it is assumed that the construction platform is wet. It is also assumed that construction traffic loading is equal to approximately 1,000 ESALs ($TI=4$), which will be conservative for most projects. A balance number of 38, which is near the top end of the deeply balanced range, is appropriate for granular layer construction, since it builds the layers as thin as possible while still maintaining adequate cover. Based on these assumptions, the subgrade requires a DSN_{800} of 31 (31 blows to reach 800 mm, or about one blow per inch). The curve shown in Figure B.1 was derived using the balance number and a correlation between penetration rate and stiffness.

This curve describes a subgrade that has a DSN_{800} of 31 and a balance number of 38. Any measured stiffness profile that falls to the right of this curve will have at least a DSN_{800} of 31 but will likely have a different balance number. If there is some method of establishing the existing profile at a site, both the depth of cover and the required stiffness of the cover can be determined. However, unlike the R-value design, the DCP-DN based design specifies the minimum required stiffness at the surface, so it is not sufficient to cover a weak subgrade with a thick layer of better, but still not strong, material (like an imported borrow).

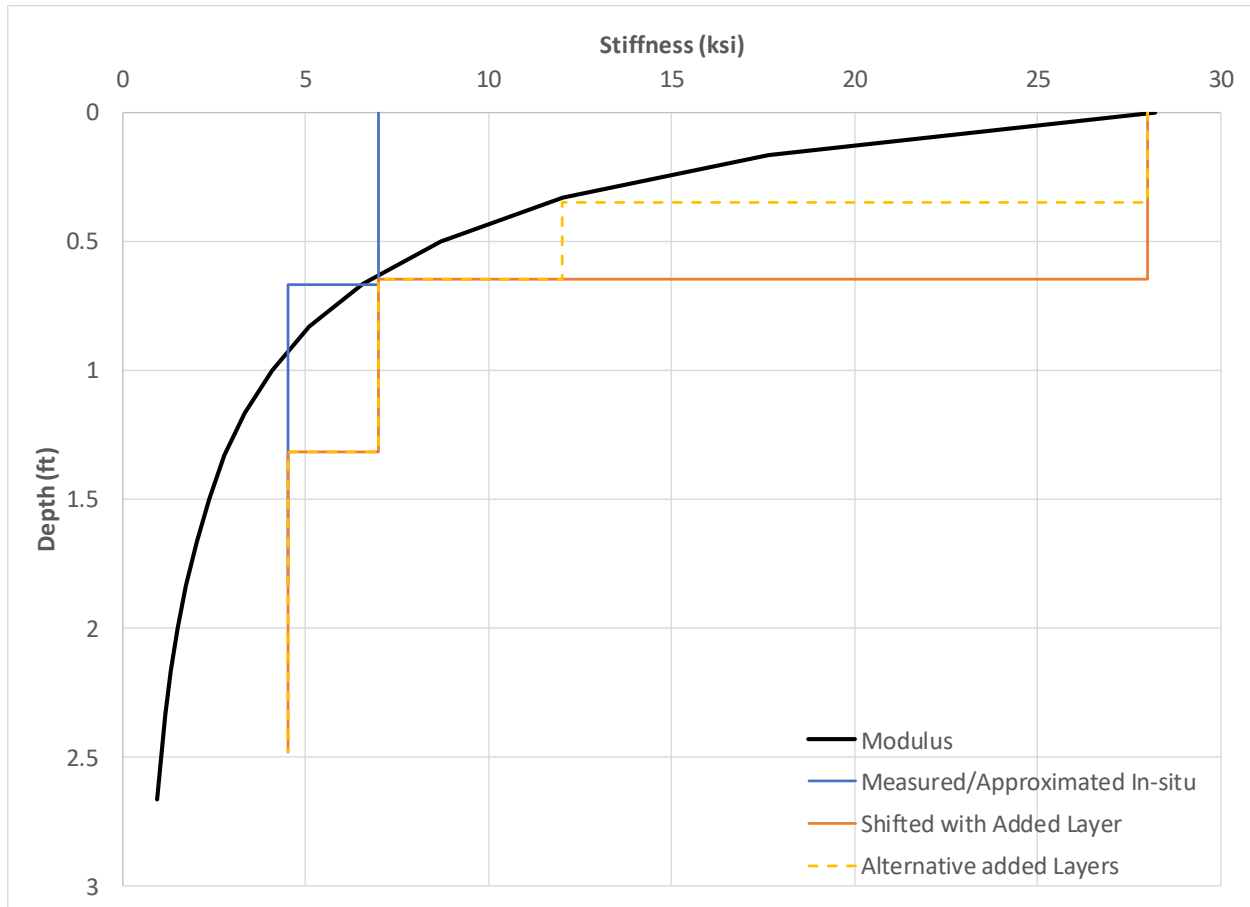


Figure B.1: Required minimum modulus with depth.

The best method for establishing an existing stiffness profile with depth at a site is through DCP testing, because this provides a field measurement at various depths. Not only is this relatively quick and easy, it allows multiple tests to be run at different locations, and the cover thickness adjusted based on the measurements. However, if a full profile with depth is not possible, then using a single value to characterize the subgrade is acceptable, as long as it can be established that the sample represents the weakest layer. If the in-situ condition has a stiffer layer on a weak layer (for example from an existing imported layer), then a depth profile should be developed. Table B.1 or Figure B.1, can be used, with caution, to estimate the elastic modulus of the material from other tests, including Caltrans R-value. The correlation equations used to develop the figure and table are based on a meta-analysis of a large number of published correlations from the literature and estimated to be internally consistent with one another, which is discussed in Section B.3. In the future, this method can also be adjusted to account for chemical stabilization of the existing subgrade, or other improvements (such as ripping and recompacting the surface). This would currently require additional design or approvals.

Table B.1: Representative Modulus for Various Materials

	M_r (MPa)			M_r (ksi)		
	Min	Max	Default	Min	Max	Default
AASHTO Soil Class						
A-1-a	207	290		30	42	
A-1-b	163	241		24	35	
A-2-4	108	179		16	26	
A-2-5	92	186		13	27	
A-2-6	65	127		9	18	
A-2-7	74	108		11	16	
A-3	87	163		13	24	
A-4	65	108		9	16	
A-5	55	92		8	13	
A-6	39	87		6	13	
A-7-5	21	55		3	8	
A-7-6	17	39		3	6	
USCS Soil Class						
GW	179	290	262	26	42	38
GP	127	241	200	18	35	29
GM	108	290	207	16	42	30
GC	87	179	138	13	26	20
GW-GM	167	275		24	40	
GP-GM	132	259		19	37	
GW-GC	113	259		16	37	
GP-GC	113	240		16	35	
SW	108	211	145	16	31	21
SP	65	179	117	9	26	17
SM	65	179	145	9	26	21
SC	39	108	97	6	16	14
SW-SM	92	186		13	27	
SP-SM	92	186		13	27	
SW-SC	74	170		11	25	
SP-SC	74	170		11	25	
ML	39	92	76	6	13	11
CL	39	87	62	6	13	9
OL	33	39		5	6	
MH	22	65	41	3	9	6
CH	17	87	28	3	13	4
OH	27	31		4	4	

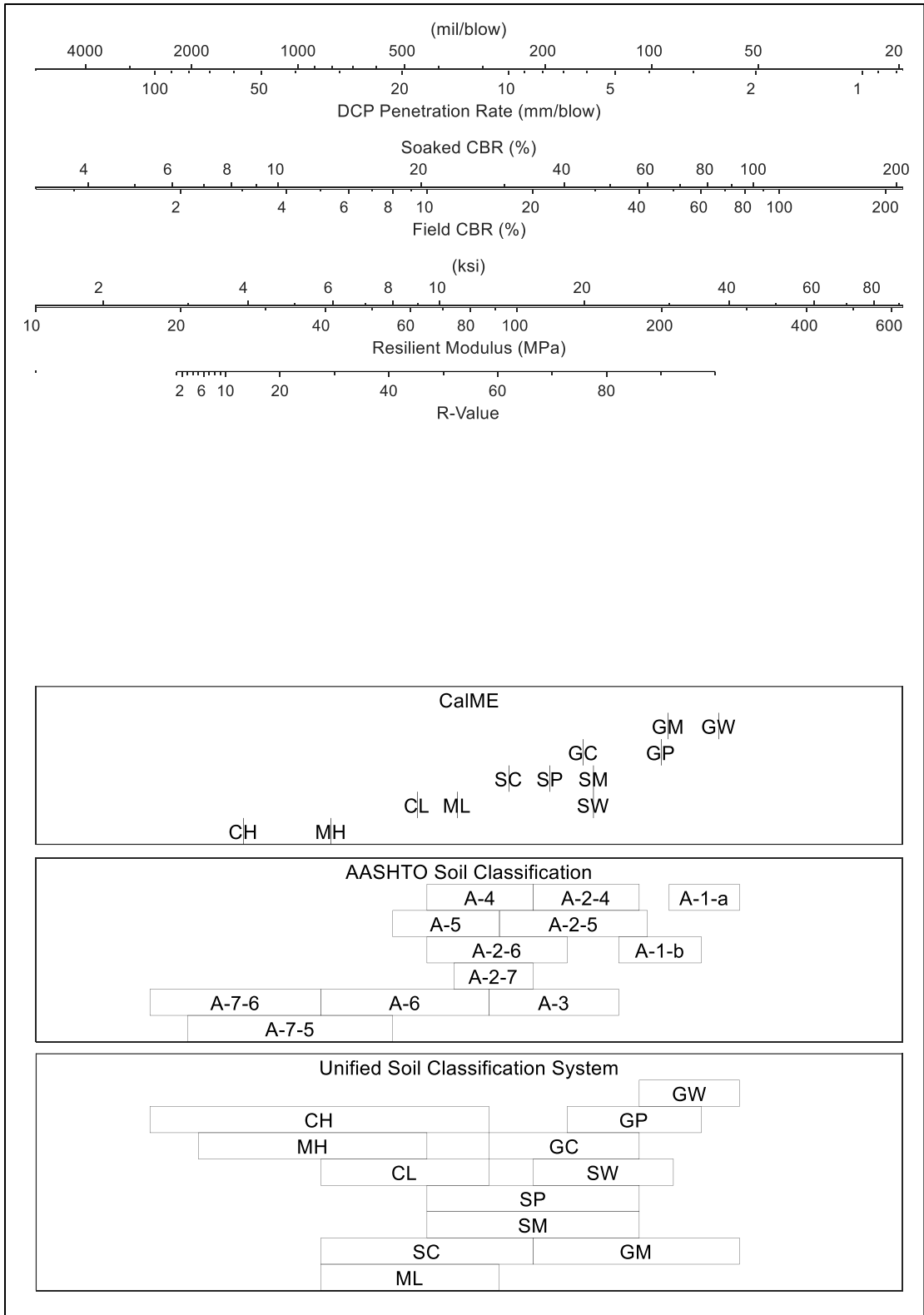


Figure B.2: Nomograph for estimating soil stiffness from various test methods.

B.2 Minimum Base Thickness in CalME Design

Table B.2 illustrates the minimum thickness for Aggregate Base (AB) Class 2 laid on subgrade consisting of different soil types. By assuming a stiffness 28 ksi (193 MPa) for AB Class 2, its minimum thickness was obtained through Figure B.2 based on default stiffness of each type of subgrade listed in Table B.2.

Table B.2: Minimum Thickness for Aggregate Base Course from the Chart

UCSC Soil Class	Default Stiffness		Minimum Thickness for AB Class 2 (Stiffness = 28 ksi or 193 MPa)		
	M _r (ksi)	M _r (MPa)	t (ft)	t (mm)	t (inch)
GW	38	262	0	0	0
GP	29	200	0	0	0
GM	30	207	0	0	0
GC	20	138	0.13	38	1.5
SW	21	145	0.13	38	1.5
SP	17	117	0.21	64	2.5
SM	21	145	0.13	38	1.5
SC	14	97	0.25	76	3
ML	11	76	0.42	127	5
CL	9	62	0.50	152	6
MH	6	41	0.75	229	9
CH	4	28	1.00	305	12

Table B.3: Minimum Thickness for Aggregate Base Course from the Chart Rounded for Constructability and to the Nearest 0.05 ft

UCSC Soil Class	Default Stiffness		Minimum Thickness for AB Class 2 (Stiffness = 28 ksi or 193 MPa)		
	M _r (ksi)	M _r (MPa)	t (ft)	t (mm)	t (inch)
GW	38	262	0	0	0
GP	29	200	0	0	0
GM	30	207	0	0	0
GC	20	138	0.35	105	4
SW	21	145	0.35	105	4
SP	17	117	0.35	105	4
SM	21	145	0.35	105	4
SC	14	97	0.35	105	4
ML	11	76	0.50	150	6
CL	9	62	0.50	150	6
MH ¹	6	41	0.75	225	9
CH ^{1,2}	4	28	1.00	300	12

Notes:

¹ An alternative platform can be designed using Fig. 1 using ASB with known stiffness combined with a minimum 0.35 ft (105 mm, 4 inch) lift of AB Class 2 on top of it; alternatively, subgrade stabilization should be considered.

² The engineer should perform a soils expansion analysis based on laboratory testing of the subgrade soil.

B.3 Meta-Analysis to Correlate Empirical Tests with Resilient Modulus

CalME relies on having representative modulus values for the foundation layers in the pavement structure. In an existing pavement these can be determined from deflection testing, but in new construction they need to be sampled and tested in the laboratory using the resilient modulus test. Caltrans has traditionally used R-value to characterize subgrade materials but (like triaxial tests) these tests require field sampling and laboratory testing, which makes the tests more expensive than some simpler field tests and means that it is difficult to obtain a large number of samples, which is particularly important for determining variability within a project, and sub-sections where subgrade properties are most critical. The simpler field tests, such as the dynamic cone penetrometer (DCP) and deflection tests, should be used to characterize stiffness over the entire project length, to measure variability, and to identify critical locations for sampling for resilient modulus testing.

As noted previously, the DCP is a tool for determining the strength of the top ~3ft of the unbound granular layers in pavements. The DCP is a remarkably simple tool, involving using a hammer with a known weight and drop height, to drive a cone through the soil, while measuring the depth of penetration after each blow. The penetration rate can be used to determine a strength profile with depth and is reasonably correlated with the field CBR, resilient modulus, unconfined compressive strength, and shear strength of the materials. In the US, penetration rate is typically abbreviated as DCP Penetration Index or DPI, but it is still reported in mm/blow.

Caltrans has records of historical R-value tests on the same alignments as current highways. However, because R-value is not used extensively outside California and the DCP has not been widely used within California, there are no correlation studies between R-value and DPI. However, R-value has also been correlated to modulus in several studies and, in any case, for *CalME* the modulus value is what is required. Many other pavement-building organizations around the world use the California Bearing Ratio (CBR) test as an empirical soil strength test as Caltrans has used the R-value, such as the US Army Corps of Engineers and the South African national roads agency. These and other organizations have correlated DCP with resilient modulus.

It is possible to use published correlations between various properties to establish approximate estimated modulus values for use in *CalME*, if one of these other properties (DCP, R-value, CBR) is available. However, there are many such published correlations from materials all over the world, and it is not clear which is best for California. As a result, a meta-analysis of these correlations was undertaken. In a meta-analysis the equations (which represent the median result for each study) are used as if they represent data, and a best fit can be obtained through all the published relationships. In addition, because there are five different properties that are commonly correlated (M_r , unsoaked and soaked CBR, R-value and DPI) the meta-analysis can simultaneously fit all published pairs of

correlations, which is more robust than chaining conversions (e.g., from DPI to CBR and then to M_r). Since M_r is the desired variable the equations are expressed as conversions from another test to the modulus in units of ksi.

$$\log_{10}(M_r) = 1.105 + 0.726 \log_{10}(CBR_u)$$

$$\log_{10}(M_r) = 1.081 + 0.861 \log_{10}(CBR_s)$$

$$M_r = 7.7 + 3.8R$$

$$\log_{10}(M_r) = 2.722 - 0.730 \log_{10}(DPI)$$

The meta-analysis is based on 90 published correlation equations from the bibliography included in Section B.4 and five tables of representative values for soils with different classifications (both AASHTO and USCS) based on the correlation equations. Only the M_r to R-value equation was fixed to the equation traditionally used in *CalME*, to preserve continuity with past practice. The format of the other correlations was chosen to match the most popular models in literature. The published models are shown on the following plots, along with the median value among the published models and the best fit equation following the models above.

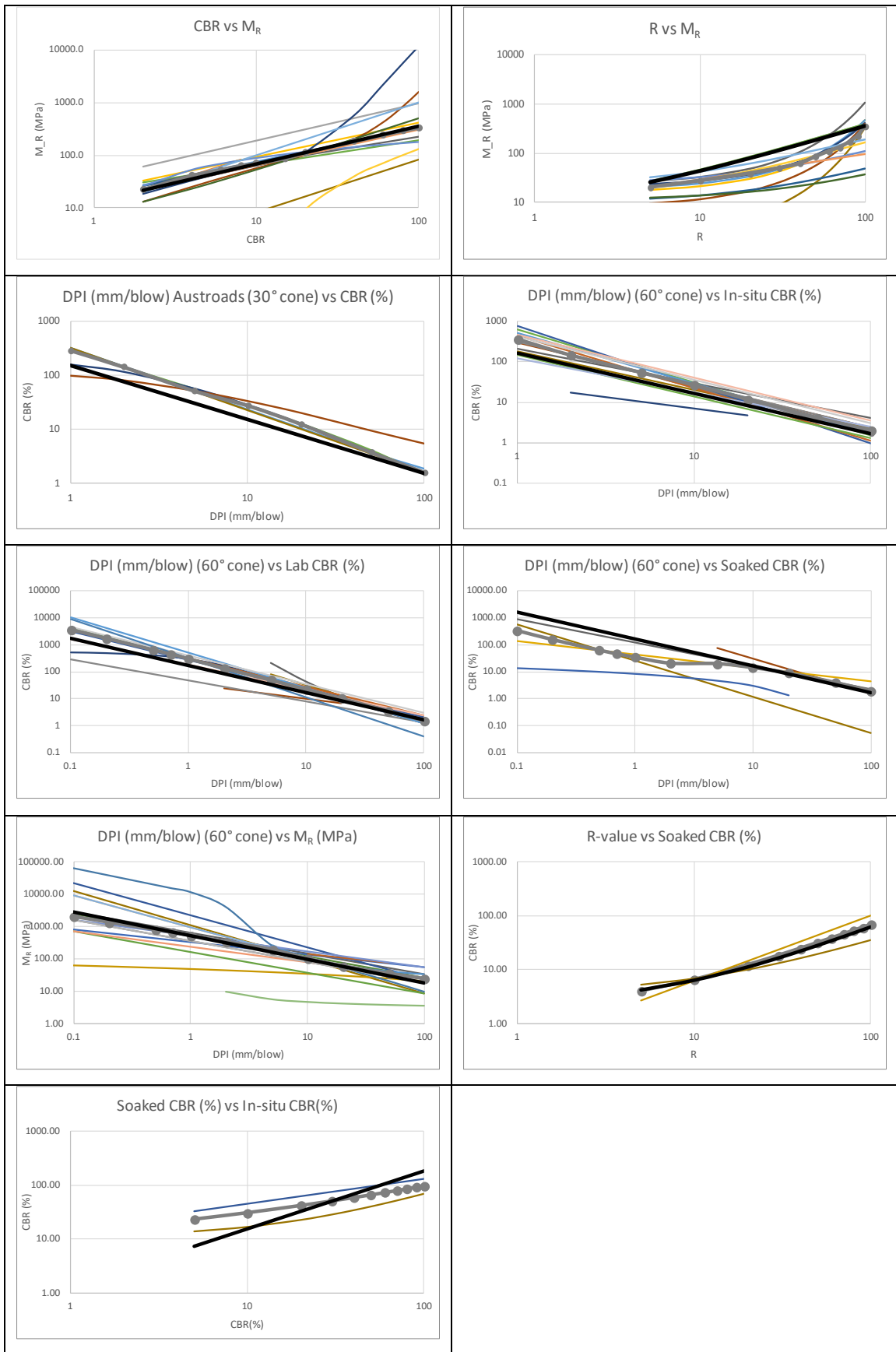


Figure B.3: Plots showing published models, median value among the published models (thick gray line), and best fit equation (thick black line).

B.4 References for Development of Subgrade Stiffness Estimation Equations

- Black, W. P. (1962). A method of estimating the California bearing ratio of cohesive soils from plasticity data. *Geotechnique*, 12, 271–282.
- Chai, G., & Roslie, N. (1998). The structural response and behaviour prediction of subgrade soils using the falling weight deflectometer in pavement construction. *3RD INTERNATIONAL CONFERENCE ON ROAD & AIRFIELD PAVEMENT TECHNOLOGY, PROCEEDINGS VOLUME 2*.
- Chai, K. M., & Tenison, J. (1987). Explaining the Dynamic cone penetrometer Test: Relating Resilient modulus and DCPI and CBR values. *Journal of Testing and Evaluation*.
- Chen, D.-H., Lin, D.-F., Liao, P.-H., & Bilyeu, J. (2005). A correlation between dynamic cone penetrometer values and pavement layer moduli. *Geotechnical Testing Journal*, 28, 42–49.
- Chen, J., Hossain, M., & Latorella, T. M. (1999). Use of falling weight deflectometer and dynamic cone penetrometer in pavement evaluation. *Transportation Research Record*, 1655, 145–151.
- Danistan, J., & Vipulanandan, C. (2009). Relationship between CBR values (un-soaked) and undrained shear strength of artificial CH soils. *CIGMAT-2009 Conference*.
- Dawson, A. R., Cheung, L. W., Brown, S. F., Rogers, C. D., & Fleming, P. R. (1990). Requirements of laboratory design and field assessment tests for pavement foundations. *Transport Research Laboratory, Crowthorne*.
- De Beer, M. (1991). Use of the Dynamic Cone Penetrometer (DCP) in the design of road structures. *Geotechnics in the African environment. Regional conference for Africa on soil mechanics and foundation engineering*, (pp. 167–176).
- Gebrehiwot, N. G. (2014). *Evaluation of Dynamic Cone Penetrometer (DCP) for Purpose of Soil Investigation for Low Volume and Inaccessible Road Design*. Ph.D. dissertation, Addis Ababa University.
- George, K. P., Uddin, W., & others. (2000). *Subgrade characterization for highway pavement design*. Tech. rep., Mississippi. Dept. of Transportation.
- George, V., Rao, N. C., & Shivashankar, R. (2009). PFW, DCP and CBR correlations for evaluation of lateritic subgrades. *International Journal of Pavement Engineering*, 10, 189–199.
- Hassan, A. (1996). *Effects of Material Parameters on Dynamic Cone Penetrometer Results for Fine-grained Soils and Granular Materials*. Ph.D. dissertation, Oklahoma State University.
- Herath, A., Mohammad, L. N., Gaspard, K., Gudishala, R., & Abu-Farsakh, M. Y. (2005). The use of dynamic cone penetrometer to predict resilient modulus of subgrade soils. In *Advances in pavement engineering* (pp. 1–16).
- Kaur, P., Gill, K. S., & Walia, B. S. (2012). Correlation between soaked CBR value and CBR value obtained with dynamic cone Penetrometer. *IJREAS Volume2*.
- Konrad, J.-M., & Lachance, D. (2001). Use of in situ penetration tests in pavement evaluation. *Canadian geotechnical journal*, 38, 924–935.
- Kumar, R. S., Ajmi, A. S., & Valkati, B. (2015). Comparative Study of Subgrade Soil Strength Estimation Models Developed Based on CBR, DCP and FWD Test Results. *International Advanced Research Journal in Science, Engineering and Technology*, 2, 92–102.
- Lee, C., Kim, K.-S., Woo, W., & Lee, W. (2014). Soil Stiffness Gauge (SSG) and Dynamic Cone Penetrometer (DCP) tests for estimating engineering properties of weathered sandy soils in Korea. *Engineering geology*, 169, 91–99.
- Livneh, M., & Ishai, I. (1988). The relationship between in-situ CBR test and various penetration tests. *International Symposium on penetration testing; ISOPT-1. 1*, (pp. 445–452).
- Monteiro, F. F., de Oliveira, F. H., Zitllau, O., de Aguiar, M. F., & de Carvalho, L. M. (2016). CBR Value Estimation Using Dynamic Cone Penetrometer—A Case Study of Brazil’s Midwest Federal Highway.
- Mukabi, J. N., & Wekesa, S. F. (2014). Performance Based Value Engineering Design of Airport Runways Employing the TACH-MD Design Methodology—Geotechnical Investigations. *E-Publication on academia. edu website*.
- Packard, R. G. (1973). *Design of concrete airport pavement*. Tech. rep.
- Pandey, B. B. (2003). Recent trends on design of bituminous mix design. *Seminar on Design of Bituminous Mixes*, (pp. 45–50).

- Patel, M. A., & Patel, H. S. (2012). Experimental Study to Correlate the Test Results of PBT, UCS, and CBR with DCP on Various soils in soaked condition. *International Journal of Engineering (IJE)*, 6, 244.
- Schmertmann, J. H. (1970). Static cone to compute static settlement over sand. *Journal of Soil Mechanics & Foundations Div.*
- Thornton, S. I. (1983). Correlation of Subgrade Reaction with CBR, Hveem Stabilometer, or Resilient Modulus.
- Tulebekov, K., & Brill, D. R. (2014). Correlation between subgrade reaction modulus and CBR for airport pavement subgrades. *T&DI Congress 2014: Planes, Trains, and Automobiles*, (pp. 813–822).
- White, D. J., Vennapusa, P. K., Gieselman, H. H., Douglas, S. C., Zhang, J., & Wayne, M. H. (2011). In-ground dynamic stress measurements for geosynthetic reinforced subgrade/s